Graduate School ETD Form 9
(Revised 12/07)

PURDUE UNIVERSITY
GRADUATE SCHOOL
Thesis/Dissertation Acceptance

This is to certify that the thesis/dissertation prepared

By Michael Zane King

Entitled
Evaluating NOx Sources And Oxidation Pathways Impacting Aerosol Production On The Southern Ute Indian Reservation And Navajo Nation Using Geochemical Isotopic Analysis

For the degree of Master of Science

Is approved by the final examining committee:

Dr. Harshvardhan
Chair

Dr. Greg Michalski

Dr. Jon Harbor

To the best of my knowledge and as understood by the student in the *Research Integrity and Copyright Disclaimer (Graduate School Form 20)*, this thesis/dissertation adheres to the provisions of Purdue University's "Policy on Integrity in Research" and the use of copyrighted material.

Approved by Major Professor(s): Dr, Greg Michalski

Approved by: Dr, Jeff Trapp 07/12/2013
Head of the Graduate Program Date

EVALUATING NO_X SOURCES AND OXIDATION PATHWAYS IMPACTING AEROSOL PRODUCTION ON THE SOUTHERN UTE INDIAN RESERVATION AND NAVAJO NATION USING GEOCHEMICAL ISOTOPIC ANALYSIS

A Thesis

Submitted to the Faculty

of

Purdue University

by

Michael Z. King

In Partial Fulfillment of the

Requirements for the Degree

of

Master of Science

August 2013

Purdue University

West Lafayette, Indiana

ProQuest LLC.
789 East Eisenhower Parkway
P.O. Box 1346
Ann Arbor, MI 48106 - 1346

To my family and friends:

Thank you for all your support.

ACKNOWLEDGEMENTS

I would like to thank the Southern Ute Indian Tribe, Navajo Nation, Tribal Air Monitoring Support Center, United States Environmental Protection Agency, and the Sloan Indigenous Graduate Partnership for assisting in making this thesis project possible. I would like to thank the Honorable Chairman Jimmy Newton, Jr. and the Southern Ute Indian Tribal Council for all your support and encouragement. I would like to thank the Southern Ute Indian Tribe Environmental Programs Division – Air Quality Program and the Navajo Nation – Air Quality Control Program for their collaborative work in the collection of tribal particulate matter samples and ambient air monitoring data. I would like to thank the Tribal Air Monitoring Support Center for gravimetric analysis of tribal PM filters and their continual efforts in providing technical air quality training and support for American Indian tribes. I would like to thank my major advisor, Greg Michalski, for his guidance in helping me understand stable isotope theory, atmospheric and surface interactions and overall assistance with making this thesis project successful. I would also like to thank my graduate committee members: Dr. Harshvardhan, Dr. Jon Harbor, and Dr. Kenneth Ridgway for their thoughtful insight and discussion in shaping this project. Lastly, I like to thank the US EPA Science to Achieve Results Program (EPA-F2011-STAR-B1) and the Sloan Indigenous Graduate Partnership Scholarship for funding

the work presented in this thesis. I am very grateful and it is with great accomplishment to present this research herein to the Southern Ute Indian Tribe and Navajo Nation as they continue to lead Indian Country in the development of policies and regional planning efforts to improve air quality and protect human health.

"This thesis was developed under STAR Fellowship Assistance Agreement no. 91729101-0 awarded by the U.S. Environmental Protection Agency (EPA). It has not been formally reviewed by EPA. The views expressed in this thesis are solely those of Michael Z. King, and EPA does not endorse any products or commercial services mentioned in this thesis."

TABLE OF CONTENTS

Page

LIST OF TABLES

LIST OF FIGURES

Figure Page

Figure Page

Figure Page

Appendix Figure

ABSTRACT

King, Michael Z. M.S., Purdue University, August 2013. Evaluating NO_x Sources and Oxidation Pathways Impacting Aerosol Production on the Southern Ute Indian Reservation and Navajo Nation Using Geochemical Isotopic Analysis. Major Professor: Greg Michalski.

Increased emissions of nitrogen oxides (NO_x = NO + NO_2) as a result of the development of oil, gas and coal resources in the Four Corners region of the United States have caused concern for area American Indian tribes that levels of ozone, acid rain, and aerosols or particulate matter (PM) may increase on reservation lands. NO_x in the atmosphere plays an important role in the formation of these pollutants and high levels are indicators of poor air quality and exposure to them has been linked to a host of human health effects and environmental problems facing today's society. Nitrogen oxides are eventually oxidized in the atmosphere to form nitrate and nitric acid which falls to earth's surface by way of dry or wet deposition. In the end, it is the removal of NO_x from the atmosphere by chemical conversion to nitrate that halts this production of oxidants, acids, and aerosols. Despite the importance of understanding atmospheric nitrate (NO_3^- = $HNO_{3(g)}^-$, $NO_{3(aq)}^-$, $NO_{3(s)}^-$) production there remains major deficiencies in estimating the significant key reactions that transform NO_x into atmospheric nitrate.

Stable isotope techniques have shown that variations in oxygen (^{16}O, ^{17}O, ^{18}O) and nitrogen (^{14}N, ^{15}N) isotope abundances in atmospheric nitrate provide significant insight to the sources and oxidation pathways that transform NO_x. Therefore, this project applied this resolution using high pressure liquid chromatography and isotope ratio mass spectrometry to determine the chemical and isotopic composition of particulate nitrate ($PM_{2.5}$ and PM_{10}), collected on the Southern Ute Indian Reservation and Navajo Nation. It was determined that the observed particulate nitrate concentrations on tribal lands were likely linked to seasonal changes in boundary layer height (BLH), local sources, meteorology, photochemistry and increases in windblown crustal material. The Southern Ute Indian Reservation indicated higher $\delta^{15}N$ values in comparison to the Navajo Nation study site. The offset accounted for a 9.7‰ mean difference and was likely associated with higher NO_x inputs from anthropogenic sources. It was determined both sources and NO_x chemistry attribute to $\delta^{15}N$ seasonal variations in coarse particulate nitrate (PM_{10}). The observed $\delta^{18}O$ values and $\Delta^{17}O$ values measured in PM_{10} nitrate on both tribal lands exhibited a seasonal trend similar to observed values in particulate nitrate collected at mid-latitudes (Michalski et al., 2003). Elevated values were observed during winter compared to summer, reflecting changes in NO_x oxidation pathways. This thesis project provides insight into the sources of NO_x and the oxidation pathways that convert NO_x into nitrate on these tribal lands.

CHAPTER 1. INTRODUCTION

The Four Corners region is home to four federally recognized American Indian tribes: Navajo (UT, AZ, NM), Southern Ute (CO), Ute Mountain Ute (CO), and the Jicarilla Apache (NM). These Reservation lands lay atop some of the United States largest deposits of coal, uranium, and natural gas (BIA, 1955; Baars, 1995; Baars, 2000). Within the past decade, these lands have seen a rapid industrialization and an increase in emissions of primary air pollutants as a result of the development of oil, gas, and coal resources in the region (FCAQTF, 2007). Both the Navajo Nation and Southern Ute Indian Reservation are home to numerous minor sources and several major sources of air pollution in the Four Corners region.

The Southern Ute Indian Tribe and Navajo Nation emission inventories both indicate that nitrogen oxides or NO_x emissions contribute largely to total inventory emissions. Recent studies (Michalski, 2003; Elliot et al., 2007; Freyer, 1990) have shown that variations in nitrogen and oxygen isotope abundances in aerosol nitrate reflect changes in atmospheric NO_x oxidation pathways and provide insight into source contributions versus transport in the NO_x budget. This thesis aims to utilize this resolution to supplement Tribal Air Quality Programs (AQP) and assist with their

continual development of policies and regional planning efforts to improve air quality by assessing how expected increases in NO_x emissions on reservation lands might impact local tribal air quality, specifically ozone and particulate concentrations.

Table 1 2005 Navajo Nation Emissions Inventory

Category	CO (tons/yr)	NH_3 (tons/yr)	NO_x (tons/yr)	$PM_{2.5}$ (tons/yr)	PM_{10} (tons/yr)	SO_2 (tons/yr)	VOC (tons/yr)
Point Sources	7,525.5	301.9	80,918.4	7,157.3	12,367.5	16,610.4	906.9
Area Sources	117,537.5	1,476.9	5,444.5	21,512.9	109,905	623	54,279
Total Emissions	125,063	1,778.8	86,362.9	28,670.2	122,272.5	17,233.4	55,185

A detailed description of each source sector is available in Appendix A

Table 2 2005 Southern Ute Indian Tribe Emissions Inventory*

Category	CO (tons/yr)	NO_x (tons/yr)	VOC (tons/yr)	PM_{10} (tons/yr)	SO_x (tons/yr)	HAP (tons/yr)
Point Sources	6,114.6	4,860.7	2,087.8	44.4	9.0	413.6
Area Sources	12,529.8	7,158.5	35,287.9	4.0	1.3	243.4
Mobile Sources	5,842.9	618.2	515.5	33.2	20.8	
Biogenic Sources		66.7	4,417.6			
Total Emissions	24,487.3	12,704.3	42,309.0	81.7	31.1	657.0

*Preliminary SUIT 2005 EI

To determine source contributions and chemical formation pathways of nitrate, archival aerosol filters collected by tribal dry deposition air samplers were examined for chemical and isotopic composition. The release of archival tribal aerosol filters to the Purdue Stable Isotopes laboratory was accomplish through collaborative work with the Navajo Nation Environmental Protection Agency-Air Quality Control Program, Southern Ute Indian Tribe Environmental Programs Division-Air Quality Program, Southern Ute

Tribal Council, Inter-Mountain Lab, Inc., Tribal Air Monitoring Support Center and United States Environmental Protection Agency. Depending on aerosol diameter (coarse or fine), each aerosol filter was placed inside its own 50 mL or 15 mL centrifuge tube, labeled with filter ID number and filled with ultrapure millipore water. Aerosol solutions were then centrifuged for 30 minutes and sonicated for 30 minutes, respectively. Each aerosol solution was then filtered at 0.22 microns (μm) and the entire sample solution pumped through a chromatographic column in which the absorbed anions were then eluted using a carbonate mobile phase. Ion-exchange chromatography separates chloride, nitrate, nitrite, and sulfate, which were detected by conductivity, and the nitrate peak collected for isotopic analysis using a fraction collector. This ion chromatography has a detection limit of ±0.014 μg/mL or 5 nanomoles (nMol) of nitrate.

The total isotopic composition of nitrate from tribal aerosols from the Four Corners region was carried out using the "denitrifier technique" (Kaiser et al., 2007) Nitrate in the filter extraction solution was purified and concentrated using preparative ion chromatography (IC). The nitrate was then added to a solution containing a unique strain of denitrifying bacteria that convert NO_3^- into gaseous N_2O (Casciotti et al., 2002). The N_2O was collected using a headspace extraction device and gas chromatograph before being passed over a gold reaction tube where the N_2O was quantitatively converted into N_2 and O_2. Isotopic analysis on the product N_2 and O_2 was done using a continuous flow isotope ratio mass spectrometer (IRMS) to determine the $\delta^{15}N$, $\delta^{18}O$, and $\Delta^{17}O$ values of the original nitrate with precision of ±0.7, 0.4, and 0.6 ‰ respectively.

All isotope measurements of nitrate extracted from tribal aerosols was carried out at the Purdue Stable Isotopes Laboratory under the direction of Professor Greg Michalski.

The following sections in this chapter are intended to provide background information to better understand tribal air quality control in the Four Corners region and the sources and chemical formation pathways of nitrate from its precursor, NO_x. In chapter 3 this background knowledge will then be supplemented with isotopic observations in particulate nitrate to qualitatively estimate sources and chemical formation pathways leading to nitrate and reduce uncertainties regarding the NO_x budget and impacts on atmospheric processes that control air quality over tribal lands.

1.1 Implementation of Clean Air Act by American Indian Tribes

The 1990 Clean Air Act (CAA) amendments authorized the United States Environmental Protection Agency (EPA) to "treat Indian tribes as states," allowing American Indian tribes to develop and implement CAA programs in a similar manner as states within tribal jurisdiction (42 USC §7601, 2006). On February 12, 1998, EPA issued a final rule, also known as the Tribal Authority Rule (TAR), which specifies provisions of the CAA which are applicable to tribes, and therefore appropriate to treat eligible Indian tribes in a similar manner as states (40 CFR §49.1, 2010). Since tribes are not mandated by the CAA statue to implement CAA programs, EPA determined that it is not appropriate to treat Indian tribes in a similar manner as states for the purposes of program submittals and implementation deadlines (Martineau, Jr. and Novello, 2004). Instead, EPA set forth a "modular approach" providing Indian tribes the flexibility to

address important air quality issues as EPA is aware that Indian tribes often have limited resources with which to address their environmental concerns (Martineau, Jr. and Novello, 2004).

In order for an Indian tribe to be eligible, under TAR, for "treatment as state" (TAS) status, EPA must complete a review of the Tribe's pending authority to regulate air pollution sources located within the exterior boundaries of the Reservation (42 USC §7601, 2006). This means the tribe must demonstrate that: (1) It is a "federally-recognized tribe;" (2) it has a "governing body carrying out substantial governmental duties and powers;" (3) the functions to be exercised by the tribe "pertain to the management and protection of air resources within the exterior boundaries of the reservation or areas within the tribe's jurisdiction;" and (4) it can "reasonably be expected to be capable, in the judgment of the (EPA) Administer, of carrying out the functions" for which it seeks approval, consistent with the CAA and applicable regulations (42 USC §7601, 2006). If EPA finds that a tribe meets these four criteria then the tribe is granted TAS approval for administering the CAA program for which the tribe has made a TAS application. Of the four tribes in the Four Corners region, the Navajo Nation and Southern Ute Indian Tribe (SUIT) have established AQPs under the TAR and have "Treatment as State" status which allows tribes to develop what is called a Tribal Implementation Plan (TIP), in which federally enforceable tribal air quality regulations can be used to reduce air pollution on Reservation lands (Martineau, Jr. and Novello, 2004).

A misconception is “reservation lands” only include Tribal Trust and allotments; rather all land within the exterior boundaries of a reservation, regardless of ownership is referred to as "Indian Country." The term “Indian Country” is used to determine tribal and federal jurisdiction for purposes of federal Indian law and is important to determining the relative jurisdiction of the United States, the State, and Tribe over activities conducted on those lands (18 USC §1151, 2006). Therefore, the implementation of CAA programs in Indian Country is voluntarily accomplished by Indian tribes, in cooperation with state air pollution control agencies, industry and EPA. Tribal jurisdiction and authority to implement CAA programs is a process subject to controversy and litigation. EPA currently administers air permits for most major sources of air pollution in Indian Country, while hundreds of minor sources often go unregulated.

The Navajo Nation is the largest Indian reservation in the United States and it encompasses 27,425 square miles to include parts of northern Arizona, New Mexico, and southeastern Utah (Navajo Nation, 2011). The Navajo Nation is composed of Tribal Trust, Tribal Fee, Public, Bureau of Land Management (BLM), Private, State, and Bureau of Indian Affairs (BIA) Indian allotment lands. The Hopi Indian reservation is also located within the Navajo Nation in northern Arizona and consists of 2,532 square miles. The Southern Ute Indian Reservation is located in southwestern Colorado and expands over 680,000 acres which also includes Tribal Trust, Tribal Fee, Public, BLM, National Forest and allotment lands (SUIT, 2013).

Both the Navajo Nation and Southern Ute Indian Reservation are home to numerous minor sources and several major stationary sources of air pollution. Minor

sources are predominantly area sources and mobile sources with the potential to emit less than 100 tons per year of any criteria pollutant. Major stationary sources or Title V facilities are those that have the potential to emit over 100 tons per year and must adhere to strict emission regulations and compliance inspections, monitoring and record keeping. EPA sets pollution limits for six criteria pollutants: carbon monoxide (CO), nitrogen dioxide (NO_2), sulfur dioxide (SO_2), ozone (O_3), lead (Pb), and particulate matter (PM) as well as 187 hazardous air pollutants to protect human health and the environment. The delegation of authority from EPA to the Navajo Nation and SUIT to implement CAA operating permit programs and regulations within the exterior boundaries of reservation lands are first of its kind in Indian Country.

In 2004 and 2006, the Navajo Nation Air Quality Control Program (NNAQCP) received delegation approval to administer a Part 71 Operating Permit Program (OPP) to promulgate Navajo Nation Operating Permit Program Regulations and Navajo Nation Acid Rain Deposition Control Regulations, respectively, to reduce air pollution from 14 Title V facilities. The NNAQCP also monitors for several criteria pollutants and meteorology at five monitoring locations. The Nazlini monitoring site, located near Nazlini, AZ (35.881974 °N, -109.434003 °W) was selected for the purpose of this thesis project. The Nazlini monitoring site collects filter based PM and meteorological parameters: wind speed (WS), wind direction (WD), relative humidity (RH), solar radiation (SOL RAD), precipitation (PRECEP) and ambient temperature (TEMP).

The SUIT AQP received delegation approval to administer a Part 70 Operating Permit Program in 2012. The SUIT/State of Colorado Environmental Commission is

authorized to develop air quality rules and regulations and coordinates with EPA and Tribal AQP staff in administering the Part 70 OPP. The implementation of the Part 70 OPP is first of its kind in Indian Country, in which air quality regulations more stringent than those mandated by EPA can be applied to reduce air pollution. Essentially, the SUIT Part 70 OPP has allowed the tribe to gain local regulation over local sources, capturing air emissions from 45 Title V facilities on the reservation. In addition, the SUIT AQP monitors for several criteria pollutants and meteorology at two air monitoring stations known as Ute 1, located in Ignacio, CO (37.136705 °N, -107.628768 °W) and Ute 3, located in Bondad, CO (37.102627°N, -107.870148°W). Both Ute 1 and Ute 3 monitoring stations were selected for the purpose of this thesis project. Ute 1 and Ute 3 collect filter based PM along with the following gaseous and meteorological monitoring parameters: O_3, NO_x, CO, RH, TEMP, SOL RAD, PRECEP, SOL RAD, WS, WD, and visibility.

Both the Navajo Nation and SUIR monitoring sites adhere to EPA citing criteria and guidelines for monitoring, including 40CFR50, 40CFR53, and 40CFR58. The EPA criteria and guidelines allow monitoring data to be regionally representative of concentrations of ambient air pollutants in order to assess trends over time and space. Each tribal AQP implements what is known as a Quality Assurance Project Plan (QAAP) to ensure monitoring data meets specific data completeness, capture, quality assurance and quality control requirements. Tribal air monitoring staff follow a structured and documented management system describing the policies, objectives, principles, standard operating procedures, organizational authority, responsibilities, and accountability to ensure monitor data comparability and representativeness (USEPA,

2008). In addition, tribal AQP staff submit tribal air monitoring data to the EPA air quality systems database and raw data can be publicly accessed via EPA datamart or EPA AirNow websites.

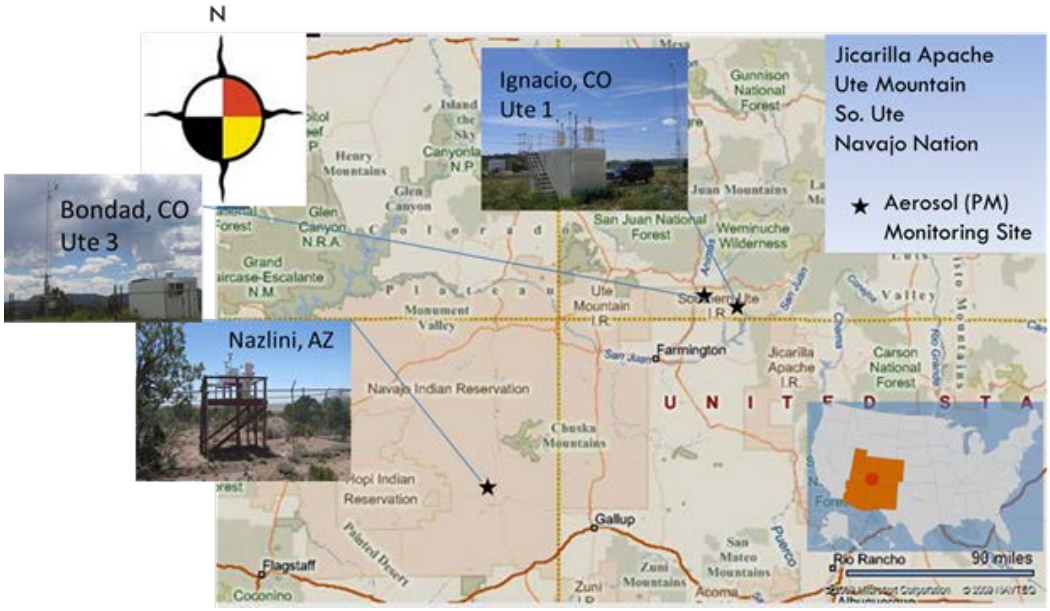

Figure 1 Filter based aerosol (PM) monitoring on tribal lands in the Four Corners Region: Ute1, Ute3, and Nazlini.

1.2 Tribal Air Quality Concerns in the Four Corners

Ambient air quality measurements in the Four Corner region are indicating ozone levels approaching “nonattainment” with existing EPA National Ambient Air Quality Standards (NAAQS). Ground level ozone can cause harmful human health effects because it is an extremely strong oxidant even at low concentrations of 60 parts per billion (ppb) (WHO, 2007). The current EPA ozone NAAQS is set at 75 parts per billion, assessed as the 4th highest monitored ozone concentration value over a running average 8-hour period, over 3 continuous years (Figure 3). In 2007, EPA proposed to

lower the level of the 8-hour primary standard between 60 to 70 ppb to provide increased human protection. This proposed draft rule which has been reconsidered for further review would have put much of the Four Corners region out of attainment. Increases in NO_x emissions are known to increase O_3 levels. In turn, O_3 production is also linked to the formation of PM in the atmosphere. Tribes are concerned over the visual and health impacts of airborne PM. Furthermore, high concentrations of O_3 and PM smaller than 2.5 microns ($PM_{2.5}$) in diameter are indicators of poor air quality and have been linked to an array of adverse health effects. These include decreased lung function, resulting in increased hospital emergency room visits and hospital admissions for respiratory complications during periods of poor air quality (Hwang, 2002). Other possible health effects include cardiovascular and cardiopulmonary mortality in children, the elderly, and people with respiratory ailments and chronic heart disease (Lippmann, 2007; Kampa and Castanas, 2008).

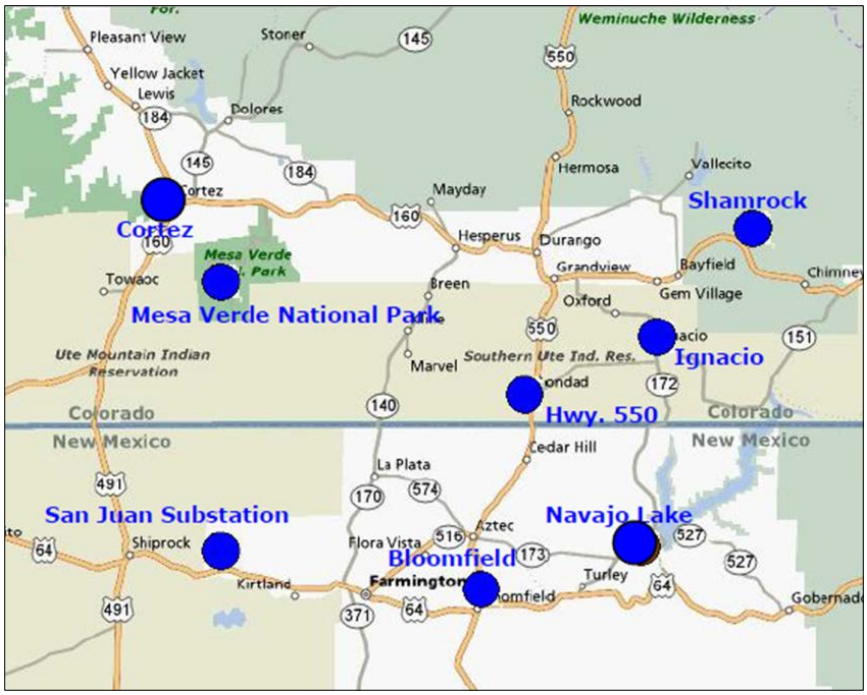

Figure 2 Ozone monitoring locations in the Four Corners Region (Nydick, 2009).

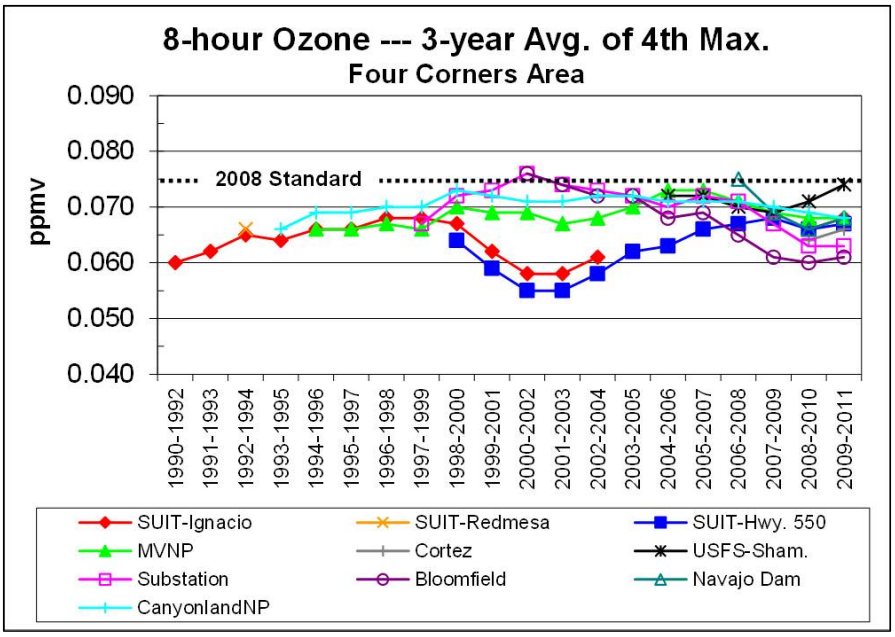

Figure 3 Four Corners annual 4th daily maximum 8-hour ozone concentration averaged over 3 years compared to NAAQS.

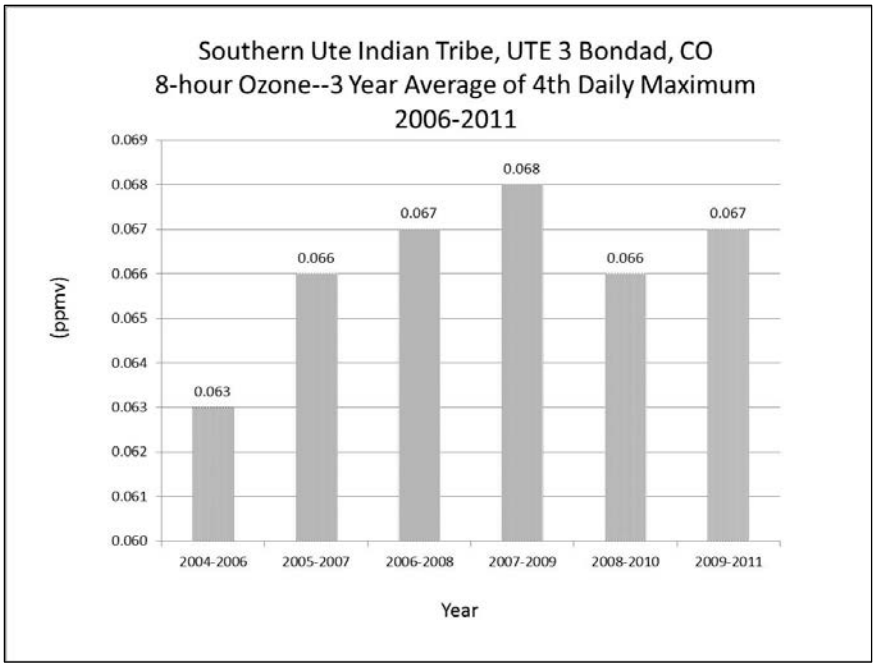

Figure 4 SUIT annual 4th daily maximum 8-hour ozone concentration averaged over 3 years, 2006-2011.

The development of oil, gas, and coal resources in the Four Corners region have led to concerns that levels of O_3, nitrates (formed from oxides of nitrogen) and PM may increase. The Four Corners Air Quality Task Force (FCAQTF, currently Four Corners Air Quality Working Group), a group of regulatory agencies, tribes and interested parties focusing on air quality issues in the Four Corners region reported that while regulation efforts have led to decreases in SO_2 across the west, nitrogen oxides or NO_x emissions are estimated to increase with population growth and energy demand (FCAQTF, 2007). NO_x (nitric oxide (NO) and nitrogen dioxide (NO_2)) emissions are predominantly emitted into the troposphere from anthropogenic sources and are highly reactive forms of nitrogen (Jaegle et al., 2005). The conversion of this NO_x into particulate nitrate ($NO_3^-{}_{(s)}$) may lead to even greater visual impairment in sensitive areas such as Mesa Verde

National Park and Wiminuche Wilderness Area in Colorado, which are routinely impaired by air pollution (FCAQTF, 2007) even though they are protected by EPA's Regional Haze Rule.

The 1984 EPA Indian Policy for the Administration of Environmental Programs on Indian Reservations, stated that "in keeping with the federal trust responsibility," it would "assure that tribal concerns and interests are considered whenever EPA's actions and/or decisions may affect reservation environments (EPA, 1984)." In the Four Corners region, EPA action becomes important as it may designate the region as being "non-attainment" for ozone levels in the near future. However, transport of air pollution from other regions can lead to elevated ozone, yet trans-boundary pollution is poorly integrated into EPA non-attainment designations. While states are increasingly trying to resolve trans-boundary problems through regional planning organizations, most tribes do not have the staff and resources required to actively participate in them (Milford, 2004). This non-attainment status will have direct implications on tribal economic development, self-sufficiency, sovereignty, and human health.

1.3 Aerosols

Aerosols are tiny colloidal liquid or solid particles suspended in the atmosphere, in which common usage of the word "aerosol" refers mostly to the airborne particulate component known as particulate matter. Aerosols can be emitted directly as particles (primary aerosol) or formed in the atmosphere by way of gas-to-liquid or gas-to-particle conversion processes (secondary aerosol) (Whitby and Cantrell, 1976). Efflorescence

(process of aerosol droplets losing water and becoming solid particles) and deliquescence (process of aerosol particles taking up water and become aerosol droplets) are the two most important physiochemical processes of aerosol particles and are highly dependent on relative humidity (Brown, et al., 2006). Aerosols take part in many physiochemical processes and chemical species externally/internally mixed within aerosol structures, allows their surfaces to act as catalysts, determining the rates of chemical and photochemical reactions by way of heterogeneous chemical reactions (Brown, et al., 2006).

Coarse aerosol particles, those larger than 10 microns in diameter (PM_{10}), may arise from natural sources, such as volcanoes, windblown dust, and sea spray. Fine particles (<2.5 microns) or $PM_{2.5}$ are typically formed from anthropogenic activities, such as combustion of fossil fuels (McKenna, 2008). More than 40 trace elements are routinely found in PM (Seinfield and Pandis, 2006) where size and composition is determined by condensation of vapor species, evaporation, or by coagulation with other particles by chemical reactions or by acting as cloud condensation nuclei, playing an important role in the atmosphere's hydrological cycle (McKenna, 2008). $PM_{2.5}$ are efficient at scattering and absorbing sunlight causing visibility degradation and direct radiative forcing, impacting both regional air quality and global climate (Liao and Seinfield 2005; Hansen et al., 2005; Feng and Penner 2007; Bauer et al., 2007). Increased NO_x oxidation that forms aerosol nitrate has a "direct effect" by increasing planetary albedo (reflectivity), cooling the planet (Andreae and Crutzen, 1997; Chuang et al., 1997). On the other hand, black carbon aerosols can absorb solar radiation, heating the planet

(Haywood and Shine, 1995). Aerosols play a key role in the atmosphere's hydrological cycle and radiation budget with indirect feedback mechanisms that are not yet fully understood (Archer, 2010).

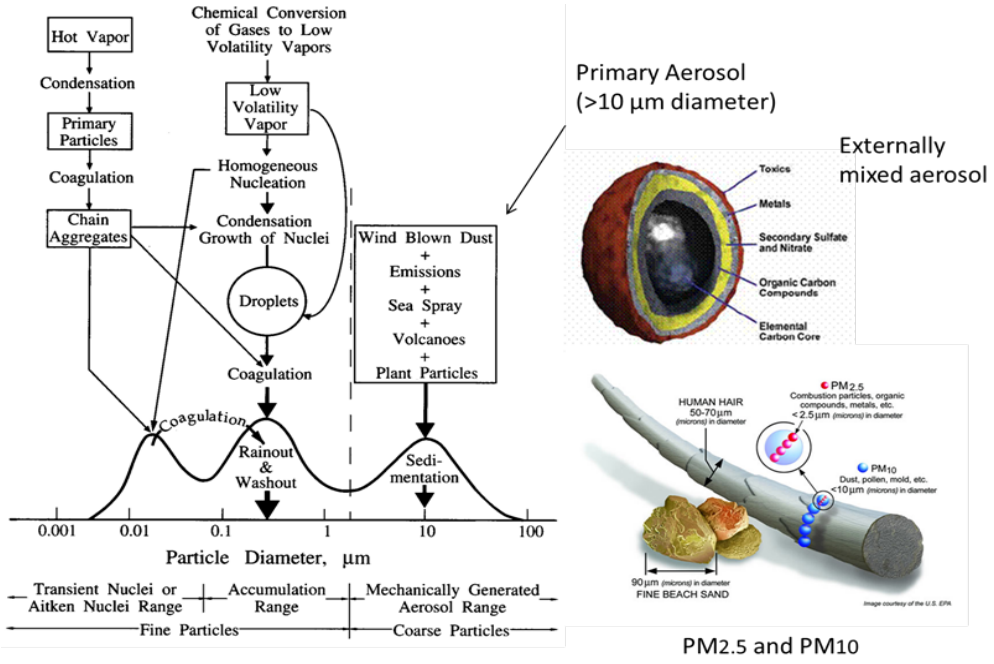

Figure 5 Aerosol size distribution (Whitby and Cantrell, 1976; USEPA, 2013).

1.4 Nitrogen Oxides

The combustion of fossil fuels, biofuels, biomass and lightning fix inert nitrogen (N_2) into a highly reactive form known as nitrogen dioxides (NO_x = NO + NO_2) (Alexander et al., 2009). Nitrogen dioxides can also be emitted from soils due to microbial processes (nitrification-denitrification) as well as transported into the troposphere from the stratosphere (Logan, 1983). Nitrogen oxides play a key role in atmospheric chemistry, producing acid rain and leading to the production of secondary oxidants, which lead to the production of secondary aerosols, such as nitrate, sulfate,

and organic aerosols (Galloway et al., 2004). Anthropogenic activities are the dominant source of NO_x in the troposphere (Jaegle et al., 2005) and these activities have influenced the global nitrogen budget over the past ~100 years as seen in increasing nitrate concentrations found in Greenland ice cores (Mayewski et al., 1990).

Nitrogen oxides are oxidized in the atmosphere to a soluble form known as atmospheric nitrate (NO_3^- = $HNO_3^-{}_{(g)}$, $NO_3^-{}_{(aq)}$, $NO_3^-{}_{(s)}$), and regionally deposited to Earth's surface. The lifetime of NO_x in the boundary layer varies from 1 day (in tropics and summer) to 3 days (during winter) before its converted to atmospheric nitrate (Levy et al., 1999). Nitrate is the main sink of NO_x and is a nutrient to many ecosystems (Galloway et al., 2008) and anthropogenic increases to deposition of nitrogen (N) has been linked to ecosystem disruption, shifts in biodiversity, and exacerbation of wildfires (Bobbink et al., 2010; Fenn et al., 2003; Galloway, 1995). Atmospheric deposition of nitric acid (HNO_3) can cause acidification of soils and increases in introduced N deposition leads to crop damage and deforestation (Likens et al., 1996; Fenn et al., 2003). Furthermore, overabundances of N deposition to water systems increase the growth of aquatic plants and algae leading to lacustrine and estuarine eutrophication and poor water quality (Paerl et al., 2002). It is the removal of NO_x from the atmosphere by chemical conversion to atmospheric nitrate that halts this production of oxidants, acid, and aerosols. Therefore, the processes that transform NO_x into atmospheric nitrate are important for understanding atmospheric chemistry, climate, and health from a local to global status.

During the daytime, ultraviolet (UV) radiation dissociates the O_3 and NO_2 molecule (R1.1). The photolysis of the O_3 and NO_2 molecule creates either a ground-state oxygen atom or an excited state oxygen atom, O (^{1}D). This single oxygen atom reacts back 97% of the time with O_2 molecules and 3% with water (H_2O) in the atmosphere to produce ozone (R1.2) and the hydroxyl radical (OH), respectively (Pandis and Sienfeld, 2006). The highly reactive hydroxyl radical, the most important reactive species in the atmosphere, reacts with VOCs (extracting a hydrogen atom from organic compounds) to produce organic radicals (R•) that react with O_2 to form peroxy (hydroperoxy (HO_2) and organic peroxy (RO_2)) radicals (R1.4) (Sienfield and Pandis, 2006). The lifetime of OH in the atmosphere is less than a second and depends highly on water vapor, giving it a low concentration in the atmosphere of about $8x10^5$ molecules/cm^3 (Seinfeld and Pandis, 2006). Peroxy radicals allow NO_2 to be regenerated without destroying O_3; therefore, allowing O_3 to build up in the atmosphere (Seinfeld and Pandis, 2006). In mid-latitudes, the NO_2 that is generated undergoes photolysis every 3 minutes (Seinfeld and Pandis, 2006), allowing the photochemical cycling of NO_x and O_3 to restart with continual exchange of oxygen atoms between the two species.

$NO_2 + hv \rightarrow NO + O$ (λ<420 nm) R1.1

$O + O_2 \rightarrow O_3$ R1.2

$NO + O_3 \rightarrow NO_2 + O_2$ R1.3

H (or R•) + $O_2 \rightarrow HO_2$ (or VOC--OO•) R1.4

NO + HO_2 (or VOC-OO•) $\rightarrow$ NO_2 + OH (or RO•) R1.5

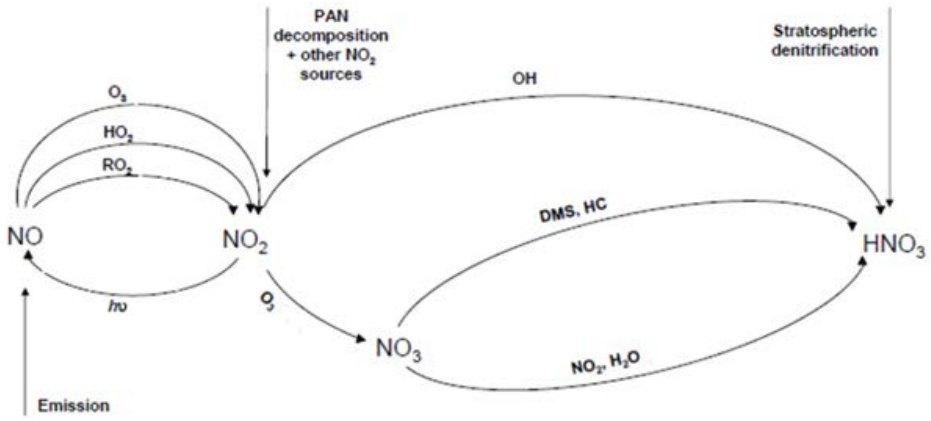

Figure 6 Atmospheric Nitrogen Cycle (from Alexandar et. al., 2009).

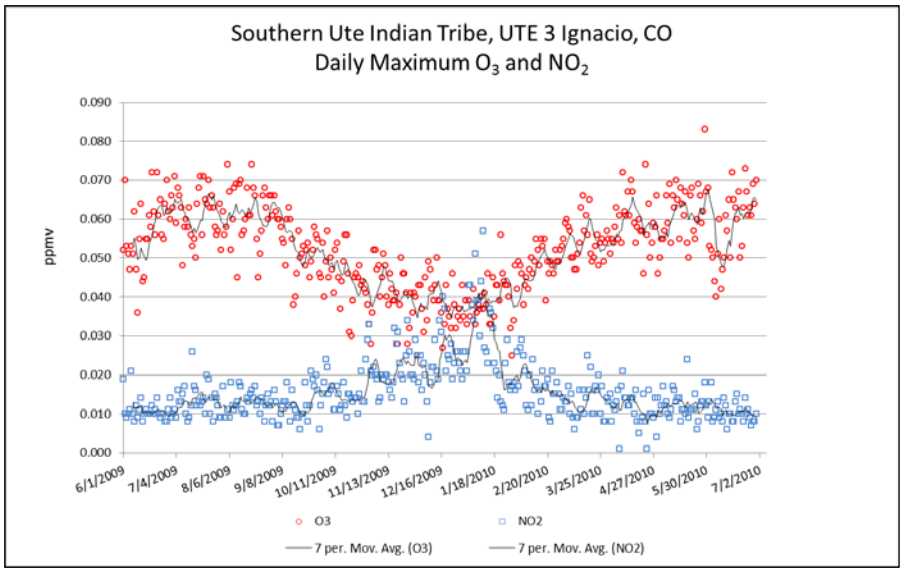

Figure 7 SUIT NO_2 and O_3 photochemistry. The daily maximum 1-hour O_3 ppmv increase during the summer months and decrease during the winter months.

The three most important oxidizing species in the atmosphere are the hydroxyl radical, nitrate radical, and ozone molecule. Once air pollutants or chemical compounds are emitted into the atmosphere these oxidizing agents act as detergents, oxidizing

them to a less volatile, water soluble form, by which they can be removed by precipitation which is known as wet deposition. Without the aid of precipitation, gases and dry aerosols can also be removed by dry deposition and it is the dominant form of N deposition in arid climates, such as the western United States (Fenn et al.2003). Oxidation is the loss of electrons, however in the atmosphere oxidation often involves the reaction of a chemical species with an oxygen containing compound. In the daytime NO_2 is oxidized by OH to form nitric acid (HNO_3) which partitions between gas and aerosol phase to form the nitrate aerosol.

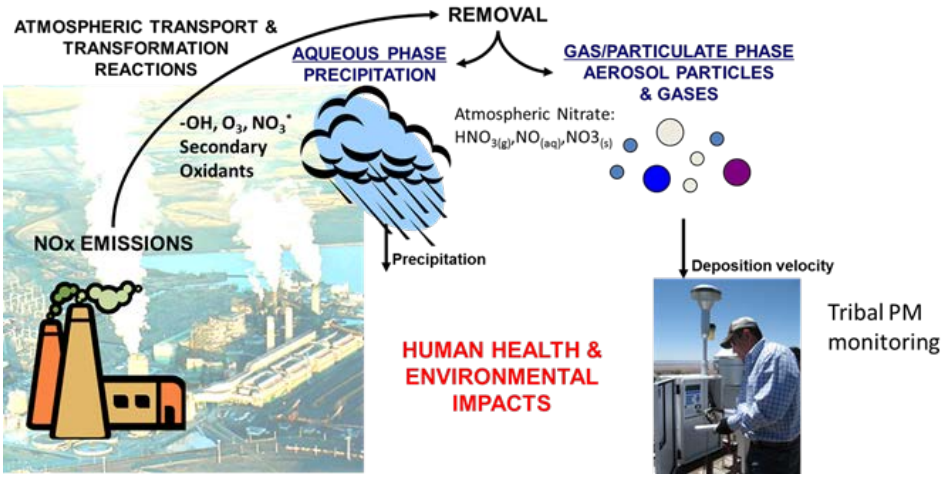

Figure 8 Atmospheric dry/wet deposition of nitrogen dioxides (NO_x).

At night time, NO_2 is oxidized by O_3 to form the nitrate radical (R1.6). The nitrate radical leads to HNO_3 through reactions with VOCs (H abstraction), but this pathway to nitrate is relatively minor. However, during the night time, nitrate radicals can react with NO_2 to form dinitrogen pentoxide (N_2O_5) which then reacts on an aerosol surfaces

via heterogeneous hydrolysis to form nitric acid (HNO_3) and is a major pathway to forming particulate nitrate. The nighttime removal of NO_x counteracts the daytime photochemical production of O_3 by depleting the two main ingredients (NO_x and VOCs) required for photochemical O_3 production while consuming, rather than producing O_3 (Brown et al., 2006).

Both the daytime and night time NO_x removal pathways form HNO_3 which is followed by deposition on the surface of an existing aerosol. Aerosols rather serve as sinks, in which reactions of NO_2, NO_3, and HO_2 on aerosol surfaces can reduce HNO_3, by reducing NO_x and HO_x (HO_x=OH+HO_2+RO_2) concentrations (Liao and Seinfeld, 2005). Furthermore, absorption of hydroperoxy (HO_2) radicals by aerosols reduces OH from $HO_2 + O_3 \rightarrow OH+2O_2$ and $HO_2 + NO \rightarrow NO_2 + OH$. Also, the absorption of NO_x by aerosols reduces O_3 concentrations, leading to lower OH concentrations by reducing O_3 photolysis ($O_3 + hv \rightarrow O_2 + O$) which would otherwise produce OH from $O + H_2O \rightarrow 2OH$ (Liao and Seinfeld, 2005). Heterogeneous gas-aerosol reactions play an important role in the concentrations of O_3, sulfate, nitrate, black carbon, primary and secondary organic aerosols (Liao and Seinfeld, 2005; Feng and Penner 2007; Bauer et al., 2007).

1.5 Heterogeneous Reaction of N_2O_5 on Aerosols

The link between high ozone levels, NO_x, and organic emissions is well established in atmospheric chemistry (Sienfeld and Pandis, 2006), but recent studies have highlighted that heterogeneous NO_x removal mechanisms, which shuts down O_3 production, are poorly understood (Brown, et al., 2006). The heterogeneous hydrolysis

of dinitrogen pentoxide (N_2O_5) plays a key step in removal of NO_x from the atmosphere at night which has a direct effect on the formation of oxidants (O_3, OH, NO_3,) and PM (Russell and Cass 1986).

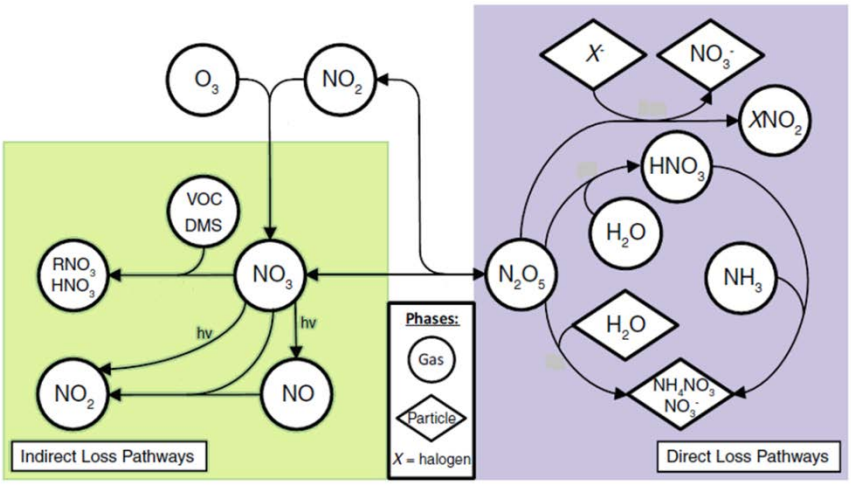

Figure 9 Indirect and direct N_2O_5 loss pathways (Chang et. al., 2011).

N_2O_5 has long been understood as a storage or sink for NO_x through its reaction with water (either in gas or particulate phase). During the night, N_2O_5 is in rapid equilibrium with the nitrate radical, a strong nocturnal oxidant in the atmosphere.

$NO_2 + O_3 \rightarrow NO_3 + O_2$ R1.6

$NO_3 + NO_2 \rightarrow N_2O_5$ R1.7a

$N_2O_5 \rightarrow NO_3 + NO_2$ R1.7b

N_2O_5 is thermally unstable, so it dissociates back to NO_3 and NO_2, and the equilibrium constant between NO_2, NO_3, and N_2O_5 shifts, favoring N_2O_5 during cool weather and large NO_2 concentrations (R1.7a,b) (Brown et. al, 2006; Chang et. al., 2011). The equilibrium between NO_2, NO_3, and N_2O_5 is given by:

$$[N_2O_5] = K_{eq} [NO_2] [NO_3] \quad \text{Eq. 1.1}$$

where, K_{eq} is the temperature-dependent equilibrium constant (cm^3/molecule). The gas-phase reaction of N_2O_5 with H_2O is slow and relatively constant, while the heterogeneous reaction is more variable and can be quite rapid on aerosol surfaces that contain water to produce nitric acid (HNO_3) (Detener and Crutzen, 1993).

$$N_2O_{5\,(g)} + H_2O_{\,(aerosol)} \rightarrow 2HNO_{3\,(aq)} \quad \text{R1.8}$$

The hydrolysis of N_2O_5 on and within aerosol particles, fog, or cloud droplets has been found to be much faster under tropospheric conditions and is believed to be the dominant pathway of N_2O_5 removal (Russell et al., 1985; Dentener and Crutzen, 1993; Hanway and Tao, 1998). Furthermore, the N_2O_5 hydrolysis product, HNO_3, partitions to the aerosol phase at low temperatures or when excess ammonia is present, therefore N_2O_5 directly influences the tropospheric aerosol budget (Stelson and Seinfield 1982; Russell and Cass 1986). The tropospheric N_2O_5 chemistry is not well known and the rate of N_2O_5 uptake by aerosols remains very uncertain and is determined by aerosol composition and meteorological conditions (relative humidity and temperature) (Brown et al., 2006; Bertram et al., 2009). The N_2O_5 heterogeneous hydrolysis reaction can be modeled as a pseudo-first order process (Heikes and Thompson, 1983; Chang et al. 1987):

$$\frac{d[N_2O_5]}{dt} = -K_{N2O5} [N_2O_5] \quad \text{Eq. 1.2}$$

In which *dt* denotes an incremental change in time and K_{N2O5} is the reaction rate constant for the heterogeneous gas to surface reaction. The rate constant, based on the

probability of the number of molecules striking a unit area per unit of time and simplified using an N_2O_5 reaction uptake coefficient (< 0.1), is expressed by (Riemer et al., 2003):

$$K_{N2O5} = \frac{1}{4} * C_{N2O5} * \gamma_{N2O5} \qquad \text{Eq. 1.3}$$

Where C_{N2O5} is the mean molecular velocity of N_2O_5, S is the aerosol surface area density and γ_{N2O5} is the uptake coefficient or reaction probability. The uptake coefficient or reaction probability (gamma, γ) is the ratio of collisions between N_2O_5 and aerosol surfaces that result in N_2O_5 being up taken on aerosol particles to form HNO_3.

$$\gamma = \frac{(\#\ of\ reactions\ forming\ HNO_3)}{(\#\ of\ theoretical\ collisions\ (N_2O_5 + H_2O))} \qquad \text{Eq. 1.4}$$

Three dimensional transport modeling has shown that the global concentrations of NO_x, OH radicals, and O_3 is affected by NO_x removal via tropospheric aerosol chemistry (Crutzen and Dentener, 1993). The model suggests that heterogeneous reaction of N_2O_5 on aerosols in the northern hemisphere can cause a reduction in NO_x and O_3 concentrations by as much as 50% and 25%, respectively (Crutzen and Dentener, 1993). The modeled N_2O_5 heterogeneous reaction rates were based on laboratory determined N_2O_5 uptake coefficients and it was concluded that sulfate aerosols from SO_2 emissions would have minimal influence on O_3 concentrations because the heterogeneous hydrolysis of N_2O_5 would be saturated and go to completion on any reasonable aerosol surface area (Crutzen and Dentener, 1993).

On the other hand, measurements of N_2O_5 uptake coefficients, based on N_2O_5 lifetimes, in the eastern U.S., were shown to be highly variable and are influenced by

relative humidity, aerosol acidity, and aerosol composition, such as sulfate mass or sulfate to organic ratio (Brown, et al., 2006). They suggested that "emissions of SO_2, followed by its conversion to particulate sulfate, can indeed decrease the lifetime of NO_x and therefore influence photochemical ozone production" (Brown, et al., 2006). If true, this would mean the decreases in SO_2 emissions in the Four Corners region and increases in NO_x emissions could lead to elevated ozone levels. The N_2O_5 uptake variability has regional scale effects on both NO_x and volatile organic compound (VOC) oxidation, which then impacts the photochemical formation of ozone and atmospheric nitrate formation rates (Brown, et al., 2006).

Furthermore, discrepancies between simulated and observed atmospheric nitrate concentrations in the EPA air quality model CMAQ (Community Multiscale Air Quality model) are currently attributed to "uncertainties associated with HNO_3 production via heterogeneous pathways and its effects on simulated airborne total nitrate" (Mathur et al., 2005). Widely different NO_3^- loading is predicted by global chemical transport models (Bauer et al., 2004; Dentener and Crutzen, 1993; Feng and Penner, 2007) depending on how heterogeneous chemistry of N_2O_5 is parameterized.

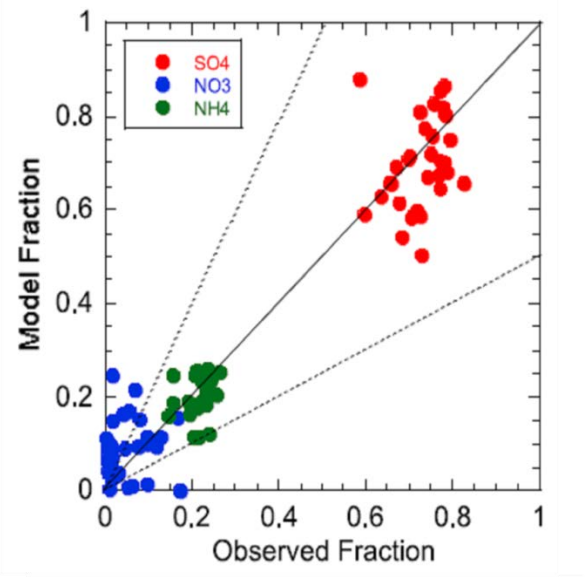

Figure 10 Poor agreements between observed summer NO_3^- and CMAQ predictions (Mather et al., 2005).

Therefore, understanding aerosol nitrate formation pathways and NO_x removal mechanisms by N_2O_5 is important for understanding O_3 production and ultimately the atmosphere's oxidation capacity. This capacity in turn controls the production of secondary aerosols and dictates a region's over all air quality. In order to improve our understanding of these chemical mechanisms and use this knowledge to help mediate air pollution over tribal lands, I posed three important research questions and a guiding hypothesis that has been the template for my graduate research:

1) How can we better constrain NO_x sources and assess the relative importance of NO_x removal by N_2O_5 to better understand the link between NO_x emissions and ozone and particulate formation in the Four Corners region?

2) Can this new knowledge of NO_x removal mechanisms by N_2O_5 be combined with regional air quality monitoring and modeling simulations to assist with regional ozone mitigation strategies?
3) How can we use these results to assist tribal authorities in the Four Corners region to develop polices and regional planning that will improve air quality, and ultimately protect the health and welfare of tribal members and residents?

1.5.1 Hypothesis

In order to address these questions we utilize the stable isotopes ^{14}N, ^{15}N, ^{16}O, ^{17}O, and ^{18}O in aerosol nitrate to provide insight into the sources of NO_x and the oxidation pathways that convert NO_x into atmospheric nitrate. The chemical and isotopic analysis of nitrate in particulate matter filters ($PM_{2.5}$ and PM_{10}) collected from the Navajo Nation and Southern Ute Indian Reservation in the Four Corners region coupled with photochemical box model simulations can help resolve uncertainties regarding the N_2O_5 production pathway. This resolution may help in assessing how expected NO_x emissions from power plants and increases in oil and gas exploration on reservation lands might impact local tribal air quality, specifically ozone and particulate concentrations.

1.6 Isotope Theory

For any chemical element (X), the atomic number (A) refers to the total number of protons in the nucleus and the atomic mass number (Z) refers to the total number of protons and neutrons in the nucleus (Criss, 1999).

$_{A}^{Z}X$ (example: $_{7}^{14}N$ or nitrogen-14)

An element that has the same number of electrons to balance the number of charged protons in its nucleus is known as a neutral element. Even though the number of protons may stay consistent within the nucleus, the atomic mass of an atom can vary with the number of neutrons. Atoms that remain stable despite their varying number of neutrons are known as stable isotopes. Stable isotopes are defined as atoms of the same element with the same atomic number, but differing numbers of neutrons. For geochemical research purposes it is common to drop the unchanging atomic number for stable isotopes (e.g., ^{14}N, ^{15}N).

Isotope abundances can vary within a given compound and this change is quantified in terms of a delta value (δ) in parts per thousand ("per mil," ‰).

$$\delta = \left[\frac{(R\ sample)}{(R\ standard)} - 1\right] * 1000 \qquad \text{Eq. 1.5}$$

Isotope abundances are measured based on the ratio of heavy to light isotopes in a sample (*R sample*) relative to the same ratio of heavy to light isotopes in a standard reference (*R standard*). For nitrogen, this value is a change in $^{15}N/^{14}N$ ratio in a sample relative to the same ratio in a standard reference (N_2 in atmospheric air, $^{15}N/^{14}N$ = 0.0036765). For oxygen, this value is a change in $^{17}O/^{16}O$ and $^{18}O/^{16}O$ in a sample

relative to Vienna Standard Mean Ocean Water (VSMOW, $^{17}O/^{16}O = 0.0003799$, $^{18}O/^{16}O = 0.0020052$) (Coplen, 1994). The isotope delta value for any isotope standard is 0‰, so a sample with a $\delta^{18}O$ value of -21.1‰, means the sample is depleted in the heavier isotope by 21.1 parts per thousand relative to the VSMOW standard. The -21.1‰ value can also be interpreted as the sample having 2.1% less ^{18}O than the reference material VSMOW. The natural isotopic abundances for ^{14}N and ^{15}N is O.996337 and 0.003663, respectively. The natural isotopic abundances for ^{16}O, ^{17}O, and ^{18}O are 0.99757, 0.00038, and 0.00205, respectively (Coplen, 2002). Therefore, for most stable isotopes, the ratio for each minor isotope is close to its isotope natural abundance (e.g. $^{18}O/^{16}O = 0.00205/0.99757 = 0.00205499 \approx 0.00205/1$).

Biogeochemical processes involving compounds of light elements such as hydrogen (H), carbon (C), nitrogen (N), oxygen (O) and sulfur (S), undergo kinetic and equilibrium isotope fractionation effects (Freyer, 1990). Isotopic fractionation is the separation of light isotopes from heavy isotopes during physical or chemical reactions (Criss, 1999). Isotopic fractionation changes the isotope ratio causing variations in the isotopic abundances of light elements and these variations can be used as indicators of environmental change in natural systems (Criss, 1999). Therefore measuring stable isotope ratios in compounds can be used to identify sources and sinks and provide insight to better understand the physical and chemical reactions behind biogeochemical processes.

Molecules with the same chemical formula but differ only in their isotopic composition are known as isotopologues and these differences in masses influence their

thermodynamic properties. The reaction rates of isotopologues are dependent upon molecular velocities in which lighter isotopes move faster subsequently reacting faster. Lighter isotopes have a higher molecular vibrational frequency forming weaker bonds and breakage of these bonds leads to fractionation. The differences in bond strength affect the kinetics of reactions and molecules with the lighter isotope react faster and are concentrated in the products. The heavier isotopes then become enriched in the reactants while the products are depleted, yielding a lower delta value.

Substituting an isotope near an atom where bonds are breaking or rehybridizing can lead to a change in the rate of the reaction. This kinetic isotope effect can be measured and is expressed as a ratio of rate constants (k_2/K_1): the rate constant for the reaction with the heavy isotope over the rate constant for the reaction with the light isotope.

Reactant → Product (k_1 = reaction rate constant of light isotope)

Reactant → Product (k_2 = reaction rate constant of heavy isotope)

$$\alpha = k_{2\,(heavy)}/k_{1\,(light)} \qquad \text{Eq. 1.6}$$

Isotope fractionation is then based on the ratio of the rate constants expressed as alpha (α), and is also known as the fractionation factor.

Isotopologues involved in biological (enzyme reactions) or physical processes (diffusion, evaporation, freezing) are subject to kinetic isotope effects, where lighter molecules will diffuse faster and evaporate faster. Isotope fractionation due to mass differences in unidirectional kinetic reactions (e.g. open systems where products escape) can be expressed using the following fractionation factor:

$$\alpha_{P\text{-}S} = R_p/R_s \qquad \text{Eq. 1.7}$$

Where R is the isotope ratio, P is the product and S is the reactant and $\alpha_{P\text{-}S}$ is the fractionation factor of product relative to the reactant.

Isotope fractionation can also occur under chemical equilibrium reactions in which molecules exchange isotopes of the same element in equilibrium such as the exchange of ^{18}O between nitrate and water. During equilibrium reactions the species with the highest oxidation state tends to become enriched in the heavy isotope.

$$OONO_{(aq)} + H_2{}^{18}O_{(g)} \leftrightarrow OON^{18}O_{(aq)} + H_2O_{(g)}$$

The species with the lower oxidation state then becomes depleted in the heavy isotope. Equilibrium isotopic fractionation can be expressed as a fractionation factor ($\alpha_{A\text{-}B}$), which is equivalent to the equilibrium constant (K): where A and B are different phases such as gas and liquid.

$$\alpha_{A\text{-}B} = R_A/R_B \qquad \text{Eq. 1.8}$$

Therefore, the isotopic fractionation factor ($\alpha_{NO3\text{-}H2O}$) for ^{18}O exchange between nitrate and water is written as:

$$\alpha_{NO3\text{-}H2O} = (OON^{18}O/OONO)/(H_2{}^{18}O/H_2O)$$

If the NO_3^- and H_2O did not discriminate between ^{16}O and ^{18}O, then α would be equal to unity (α = 1.00). However, if α > 1, this implies that NO_3 prefers ^{18}O and H_2O prefers ^{16}O. For both kinetic and equilibrium reactions, α is typically around one (1.00) and can be expressed in permill as the isotopic enrichment factor, ε:

$$\varepsilon_{A\text{-}B}\ (‰) = (\alpha\text{-}1)*1000 \qquad \text{Eq. 1.9}$$

The enrichment factor $\varepsilon_{A\text{-}B}$ is the enrichment of A relative to B for equilibrium reactions and the enrichment factor $\varepsilon_{P\text{-}S}$ is the enrichment of product relative to reactant for kinetic unidirectional reactions.

1.7 Nitrogen Isotope Variations in Atmospheric Nitrate

Variations of nitrogen isotopes (^{14}N, ^{15}N) in atmospheric nitrate may determine which emission sources (mobile, stationary, and natural) are contributing to the formation of nitrate aerosols or infer shifts in seasonal NO_x oxidation pathways (Freyer, 1991; Elliot et al., 2007; Elliot et al., 2009). Atmospheric nitrate encompasses particulate nitrate and nitric acid vapor (both commonly referred to as dry deposition) and nitrate in precipitation (wet deposition) with seasonal trends of $\delta^{15}N$ values ranging from -19 to +14‰, -14 to +10.8‰, and -8.1 to +3.2‰, respectively (Elliot et al., 2007; Elliot et al., 2009). Recent studies have suggested that the variations in the $\delta^{15}N$ values in nitrate aerosols are "fingerprints" of different NO_x sources (Elliot et al., 2007; Elliot et al. 2009, Felix et al., 2012). For example, $\delta^{15}N$ values of NO_x emitted from power plants range from +6 to +13‰, whereas vehicle NO_x has a much lower $\delta^{15}N$ value of +3.7 to +5.7‰ (Moore, 1977; Pearson et al., 2000; Ammann et al., 1999), with reports as low as -13 to -2‰ (Heaton, 1990).

Table 3 $\delta^{15}N$ of NO_x Sources

NO_x Source	δ15N (‰)	Citation
Coal Fired Power Plants	+6 to +13	Heaton, 1990
Vehicle Exhaust	+3.7 to +5.7	Ammann et al., 1999; Moore, 1977; Pearson et al., 2000; Middlecamp and Elliot, 2009
Vehicle Exhaust	-13 to -2	Heaton, 1990
Simulated Lightening	0 to +2	Hoering, 1957
Biogenic	-49 to -20	Middlecamp and Elliot, 2011; Li and Wang, 2008
Biomass Burning	+14	Hastings et al., 2009

Measurements of natural sources of NO_x are limited, but Moore (1977) have found NO_2 in pristine air to have a $\delta^{15}N$ value of -9.3 ± 3.5‰ and laboratory simulation of nitrogen fixation by lightning show a range from 0 to +2‰ (Hoering, 1957). In addition, studies have shown enrichment of $\delta^{15}N$ in polluted air with depletion occurring during the summer and spring months (Elliot et al., 2007; Elliot et al., 2009; Hastings et al., 2003). NO emitted from soils as an intermediate to the nitrification-denitrification process show a $\delta^{15}N$ range from -49 to -20‰ (Middlecamp and Elliot, 2009). Large kinetic isotope effects have been observed in both the nitrification-denitrification reactions; contributing to the depletion of $\delta^{15}N$ in NO emitted from soils in summer months (Freyer, 1978; Medina and Schmidit, 1982; Mariotti, et. al., 1981). These comparisons suggest that natural and anthropogenic NO_x sources could potentially attribute to observed seasonal variations in $\delta^{15}N$ of atmospheric nitrate.

On the other hand, Freyer (1991) observed $\delta^{15}N$ in aerosol nitrate (collected via wet and dry deposition monitors in Germany and France) and suggests $\delta^{15}N$ variations likely reflect seasonal shifts in NO_x oxidation pathways that form aerosol nitrate rather than differences in emission sources. Freyer (1991) suggests kinetic and equilibrium

nitrogen isotope fractionation effects occur during chemical formation mechanisms, therefore impacting observed $\delta^{15}N$ values in aerosol nitrate. The two main pathways to form aerosol nitrate is the absorption of nitric acid (HNO_3) into a water droplet (R1.9) and the nighttime heterogeneous reaction of N_2O_5 on a wet aerosol surface (R1.10). Both pathways form HNO_3 which can react with ammonia to form ammonium nitrate (NH_4NO_3), a form of fine particulate nitrate. Ammonium nitrate is in dynamic equilibrium with ammonia and nitric acid and is thermally unstable but formation favors high RH and low temperature (R1.11).

$$HNO_{3\,(vapor)} \leftrightarrow NO_{3\ (aerosol)} + H+ \qquad \text{R1.9}$$

$$N_2O_5 + H_2O_{\ (aerosol)} \rightarrow 2HNO_3 \rightarrow 2NO_{3\,(aerosol)} + 2H+ \qquad \text{R1.10}$$

$$NH_3 + HNO_3 \leftrightarrow NH_4NO_3 \qquad \text{R1.11}$$

Ammonium nitrate can be found in regions where sulfate levels are low and ammonia and nitrogen oxide emissions are high (e.g., southern California and the Mountain West) (NOAA, 2000). The nighttime exchange reaction between NO_2, NO_3, and N_2O_5 are in thermal equilibrium (R1.7a, b) and subject to equilibrium isotope fractionation and this leads to the enrichment of ^{15}N in the more oxidized species. The nighttime formation mechanisms (R1.7a, b, R1.10) dominate the formation of winter aerosol nitrate, due to low temperatures and decreased sunlight. Therefore, Freyer (1991) suggests the enrichment of $\delta^{15}N$ values in aerosol nitrate would shift $\delta^{15}N$ values higher in the winter.

The daytime oxidation of NO_2 by OH radicals is the main photochemical reaction to nitric acid (HNO_3) formation. Based on reduced masses, Freyer (1991) estimated a

kinetic isotope fractionation of 0.9971 for the NO_2 + OH reaction to yield a $\delta^{15}N$ value of -3‰ for HNO_3, which compared reasonably to the observed value of -(2-3‰) with no seasonal trend reported. Freyer (1991) suggested the dissociation equilibrium of NH_4NO_3 during summer months would prefer the lighter ^{14}N in HNO_3, therefore masking any seasonal trend because the residual NH_4NO_3 would be enriched in ^{15}N. Assuming no isotopic fractionation effects occurring in R1.9, the depleted $\delta^{15}N$ signature in HNO_3 would then be carried on to the formation of aerosol nitrate. Therefore, the depleted $\delta^{15}N$ values in aerosol nitrate as a result of the NO_2 + OH reaction occur largely during the summer months, due to higher solar radiation and higher OH concentrations (Calvert et al., 1985).

Both Elliot et al. (2007) and Freyer (1991) concluded that variable anthropogenic and natural NO_x sources could contribute to seasonal variations in $\delta^{15}N$ in atmospheric nitrate. Elliot et al. (2007) reported $\delta^{15}N$ (NO_x) values emitted from stationary sources and found no significant chemical contributions to ^{15}N variations. Therefore, a mixing model can be applied to $\delta^{15}N$ isotope distributions reported for NO_x sources supplemented with emission inventory data to estimate contributions from individual NO_x sources to atmospheric nitrate (Felix et al., 2012). The $\delta^{15}N$ reported for NO_x maybe a new tool for assessing the relative effectiveness of NO_x reduction technologies and strategies as well as transport and fate of emissions across regions (Felix et al., 2012).

Contrasting Elliot et al., Freyer (1990) suggests: 1) the temperature-dependent isotopic exchange equilibria between atmospheric nitrogen species and 2) seasonal

changes in NO_x oxidation pathways forming aerosol nitrate should also be considered when assessing $\delta^{15}N$ seasonal variations. Both Elliot et al. (2007) and Freyer (1991) agree more observations and analyses of $\delta^{15}N$ values of NO_x oxidation products and NO_x sources are needed to better interpret and understand the chemical and source apportionment relationship to seasonal variations.

Major influences to variations in observed seasonal $\delta^{15}N$ values in atmospheric nitrate include equilibrium and kinetic isotope fractionation effects occurring during formation mechanisms, varying NO_x source emissions, control technologies and operating conditions (Freyer, 1991; Elliot et al., 2007; Felix et al., 2012). Therefore, examining changes in the $\delta^{15}N$ of nitrate aerosols collected in the Four Corners region over seasons may be an effective new tool for monitoring regulatory NO_x emission reductions from stationary sources as well as determining the relative importance of source versus transport in the NO_x budget over tribal lands.

1.8 Oxygen Isotope Variation in Atmospheric Nitrate

While $\delta^{15}N$ values in atmospheric nitrate may be useful for tracing NO_x sources, the oxygen isotope (^{16}O, ^{17}O, ^{18}O) composition of aerosol nitrate has been shown to be effective for elucidating NO_x oxidation pathways (Michalski, et al., 2003). For most stable isotopes participating in biogeochemical processes, nuclear mass differences cause kinetic and equilibrium isotopic fractionations that alter the isotopic composition of compounds. The $\delta^{18}O$ values of a compound usually have a mass-dependent

relationship (terrestrial fractionation line-TFL) with the $\delta^{17}O$ that is quantitatively defined using the equation (Matsuhisa et al., 1978; Miller, 2002):

$$\delta^{17}O = 0.52 \times \delta^{18}O \qquad \text{Eq. 1.10}$$

The 0.52 defines the slope of the TFL and may range from 0.50 to 0.529 depending on the molecular mass of the oxygen-bearing molecule and fractionation caused by temperature and thermodynamics of reactions. Most oxygenated compounds in the terrestrial environment lie on the TFL and include: surface and atmospheric water, air O_2, igneous and sedimentary rocks (Patris et al., 2007).

However, photochemically produced ozone has $\delta^{17}O$ values that do not obey this mass dependent rule; and instead it has a large "^{17}O anomaly". This difference between the observed $\delta^{17}O$ value and that expected based on $\delta^{18}O$ values is known as a mass independent fractionation (MIF) (Thiemens et al., 2001; Thiemens and Heidenreich, III, 1983) and is quantified by the "cap delta" notation (Miller, 2002):

$$\Delta^{17}O = \delta^{17}O - 0.52 \times \delta^{18}O \qquad \text{Eq. 1.11}$$

Ozone has high $\delta^{18}O$ and $\Delta^{17}O$ values (Morton et al., 1990; Thiemens and Jackson, 1990) and these enrichments are transferred from O_3 to NO_2 and NO_3 via oxidation reactions. MIF occurs because of the differences in molecular symmetry and zero point energies of O_3 which lead to the stabilization of the asymmetric ($^{17,18}O$, ^{16}O, ^{16}O) isotopomers over the symmetric (^{16}O, ^{16}O, ^{16}O) during formation, regardless of the substituted ^{17}O or ^{18}O (Gao and Marcus, 2011). As a result, ozone has a near equal enrichment of ^{17}O and ^{18}O in spite of the 0.52 mass-dependent relationship.

The $\Delta^{17}O$ signal has become an important new tool for accessing how NO_x is oxidized in situ and then removed from the atmosphere (Michalski, et al., 2003; Morin et al.,2008; Alexander et al., 2009). Nitrogen oxides are very important in the formation and loss of tropospheric ozone. During the daytime, NO_x react with VOCs in the presence of sunlight to form ground-level ozone (R1.1-R1.5). NO is oxidized by O_3 or peroxy radicals (HO_2 and RO_x) to produce NO_2 that can undergo photolysis (and form ozone) or react with an OH to from HNO_3 (R1.12). The formation of atmospheric nitrate, defined herein as gas-phase HNO_3 plus particulate nitrate are enriched with ^{17}O and ^{18}O and is removed by way of dry or wet deposition. The HNO_3 formed by this daytime pathway has a $\Delta^{17}O$ value of ~20‰ (Alexander et al., 2009; Michalski et al., 2003).

$$NO+O_3 \rightarrow NO_2 + OH \rightarrow HNO_{3\,(g)} \quad (\delta^{17}O \sim 20‰) \qquad \text{R1.12}$$

On the other hand, night time oxidation of NO_2 by ozone produces the nitrate radical that has a higher $\Delta^{17}O$ value of ~32‰ (Alexander et al., 2009; Michalski et al., 2003). The nitrate radical is quickly photolyzed during the daytime, but at night it leads to the production of HNO_3 through reactions with VOCs or dimethylsulfide (DMS); but this pathway to nitrate is relatively minor (R1.13). However, during the night time, nitrate radicals can react with NO_2 to form N_2O_5 which then reacts on an aerosol surfaces via heterogeneous hydrolysis to form HNO_3 (R1.14) and is a major pathway to forming particulate nitrate. The HNO_3 formed by this pathway is estimated to have a $\Delta^{17}O$ value of ~28‰ (Alexander et al., 2009; Michalski et al., 2003).

$$NO_2+O_3 \rightarrow NO_3+O_2 \rightarrow NO_3 + VOC \rightarrow HNO_3 \quad (\Delta^{17}O \text{ value of } \sim 32‰) \qquad \text{R1.13}$$

$$NO_2+NO_3 \rightarrow N_2O_5 + H_2O_{\,(aerosol)} \rightarrow 2HNO_3 \quad (\Delta^{17}O \text{ value of } \sim 28‰) \qquad \text{R1.14}$$

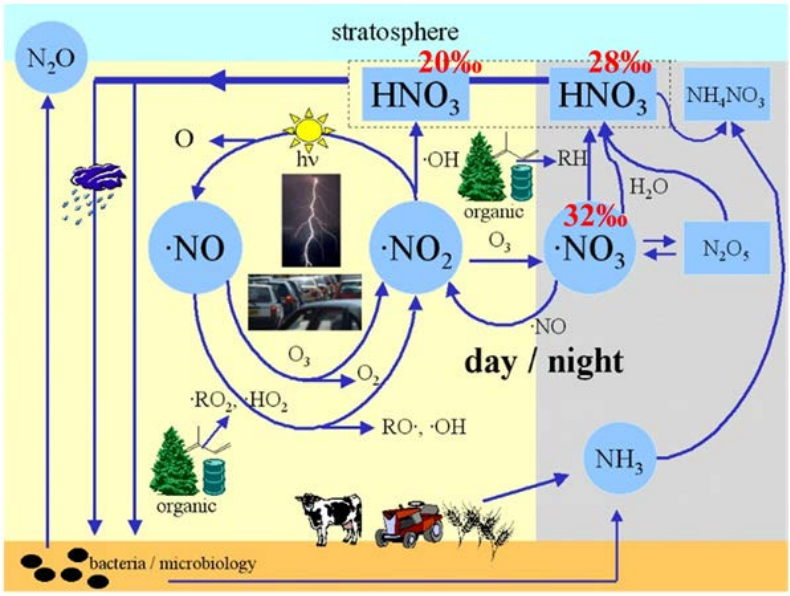

Figure 11 The $\Delta^{17}O$ values of atmospheric nitrate in the daytime and night time cycling and removal of NO_x in the atmosphere (MPIC, 2010).

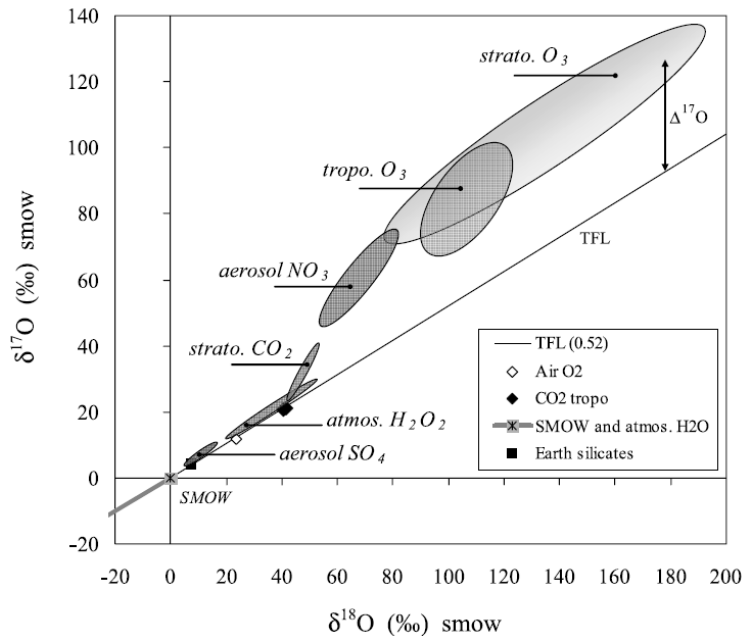

Figure 12 The terrestrial fractionation line (TLF) and observed $\Delta^{17}O$ ranges for a number of oxygenated species from Earth's surface and atmosphere (Michalski et al., 2003; Kaieser et al., 2007; Morin et al., 2009; Patris et al., 2007).

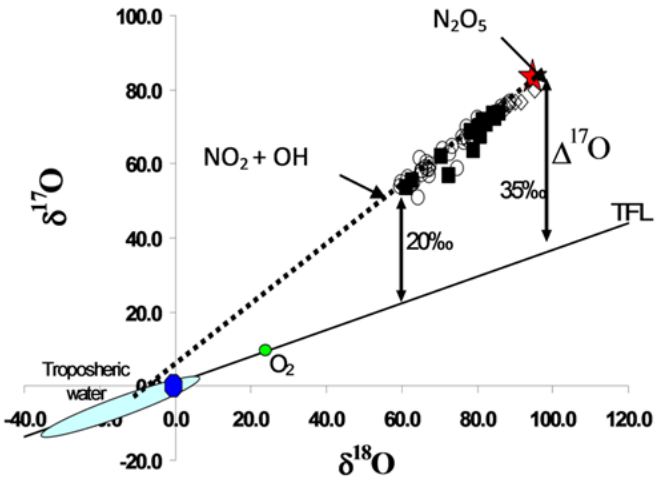

Figure 13 The terrestrial fractionation line (TLF) and observed $\Delta^{17}O$ values for mid-latitude atmospheric nitrate. The approximate triple oxygen isotope composition for tropospheric ozone (red star), water (blue oval), O_2 (green dot), and VSMOW (blue dot) are also indicated (Michalski et al., 2003; Kaieser et al., 2007; Morin et al., 2009).

Michalski et al. (2003) observed $\Delta^{17}O$ values for mid-latitude atmospheric nitrate ranging from 20-30‰ with seasonal trends showing maximum $\Delta^{17}O$ values occurring during midwinter. The observed $\Delta^{17}O$ seasonal trends were compared to a $\Delta^{17}O$ isotope fractionation model coupled with a photochemical box model, by which the shifts in NO_x oxidation pathways were found to be a result of temperature dependences, NO_x concentrations and hours of sunlight (Michalski et al., 2003). Therefore, qualitatively observed increases in particulate nitrate $\Delta^{17}O$ values would suggest an increase in N_2O_5 hydrolysis. The observed atmospheric nitrate $\Delta^{17}O$ values further supports the assumption that the O atoms found in atmospheric nitrate are a function of the $\Delta^{17}O$ anomaly found in ozone as this signature propagates into nitrate formation via NO_x oxidation pathways. By utilizing the difference in the transfer of $\Delta^{17}O$ from ozone to

HNO_3 during different NO_x oxidation reactions, isotopes of oxygen in particulate nitrate collected on tribal lands can be used to trace degree of N_2O_5 hydrolysis (Michalski et al., 2003).

Furthermore, measured nitrogen isotopes in fixed nitrogen (NH_3 and NO_3^-) species can be coupled with measured oxygen isotopes using the dual isotope technique to better constrain sources and chemical pathway formation of nitrate. An example of the dual isotope approach is seen in Figure 14. Since atmospheric nitrate is enriched in ^{18}O compared to other sources, it has gained acceptance as a tracer of atmospheric nitrate (Kendall et al., 2008). Anthropogenic activities are predicted to double the amount of naturally fixed nitrogen contributions by 2050 (Galloway, 2008), so it is important to be able to identify sources and understand the fates of nitrate in order to better understand the nitrogen cycle.

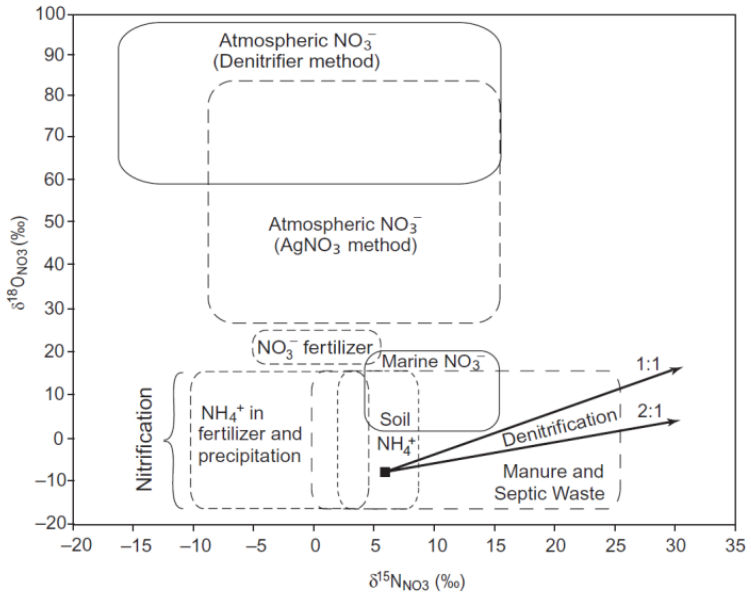

Figure 14 Dual isotope ^{18}O and ^{15}N plot for known nitrate sources (Kendall et al., 2008).

1.9 Modeling $\Delta^{17}O$ in Atmospheric Nitrate-

The cycling and oxidation pathways of NO_x to form HNO_3 play a key role in determining the $\Delta^{17}O$ values in atmospheric nitrate (Alexander et al., 2009; Michalski et al., 2003). Observations of $\Delta^{17}O$ values for atmospheric nitrate collected throughout the world range from ~10-40‰ (Kaiser et al., 2007; Kendall et al., 2008; McCabe et al., 2007; Michalski et al., 2003; Morin et al., 2007, 2008; Savarino et al.; 2007). The $\Delta^{17}O$ observed in atmospheric nitrate are attributed to the mass transfer of O atoms from tropospheric ozone to NO_2 during oxidation reactions (see Section 1.9). Modeling of the $\Delta^{17}O$ isotopic composition must incorporate any possible dilution of the ^{17}O anomaly by mass-dependent mechanisms such as the addition of isotopologues or isotopic exchange with different species.

In the summer, photochemistry increases the production of OH and thus enhancing peroxy radical oxidation (HO_2 and RO_2), consequently reducing the fraction of NO being oxidized into NO_2 by ozone (R1.1-R1.15) (Michalski et al., 2003; Patris et al., 2007). The NO_2 formed cycles rapidly between NO and NO_2 by way of photolysis. This NO_x photo-stationary state occurs much faster than NO_2 removal pathways (R1.12-1.14), so the oxygen atoms in NO_2 reach equilibrium with O_3 and HO_2 (RO_2) fairly quickly. Organic radicals (R•) typically obtain their O_2 from atmospheric O_2 ($\Delta^{17}O$ ~-0.3‰); for this reason the $\Delta^{17}O$ of HO_2 (RO_2) is estimated to be <1‰ (Rockmann et al., 2001), whereas tropospheric O_3 has been calculated to have a $\Delta^{17}O$ value of ~35‰ (Lyons, 2001; Morton et al.; 1990).

Therefore, the mass transfer of O atoms from ozone to NO_2 during oxidation can become diluted by peroxy radical (HO_2 and RO_2) oxidation; subsequently modifying the amount of ^{17}O excess found in atmospheric nitrate. As a result, the $\Delta^{17}O$ value for NO_2 ($^{\Delta}NO_2$) can be reduced into a two component mass balance isotope mixture expression:

$$^{\Delta}NO_2 = X * {}^{\Delta}O_3 + (1\text{-}X)\ {}^{\Delta}O_2 \qquad \text{Eq. 1.12}$$

Where X is the mole fraction of NO oxidized into NO_2 by O_3 and 1-X is the remaining mole fraction that is oxidized by peroxy radicals, represented here by atmospheric O_2. Since organic radicals typically obtain their O_2 from atmospheric O_2 ($\Delta^{17}O$ ~0‰), the expression is then simplified to (Michalski et al., 2003):

$$^{\Delta}NO_2 = \alpha * {}^{\Delta}O_3 \qquad \text{Eq. 1.13}$$

Where $^{\Delta}X$ can be read as the cap delta ($\Delta^{17}O$) of molecule X, in this case the $\Delta^{17}O$ of NO_2. The mole fraction (X) then becomes alpha (α) which is the proportion of NO oxidized into NO_2 by ozone and peroxy radicals (HO_2, RO_2), observed as:

$$\alpha = \frac{NO+O_3}{NO+HO_2\ (RO_2)} \qquad \text{Eq. 1.14}$$

The NO_2 produced is a common reactant for each of the nitrate formation pathways (R1.12-R1.14), transferring the ^{17}O anomaly from O_3 through reactive species during NO_x oxidation. Therefore, an isotope mass balance approach can be used to model NO_x oxidation and estimate the $\Delta^{17}O$ of the relative atmospheric nitrate formation pathways.

During the daytime NO_2+OH oxidation reactions forming HNO_3 are the major pathway to atmospheric nitrate formation. A mass balance calculation can be applied to determine the $^{\Delta}HNO_3$ value by substituting Eq. 1.13 for NO_2 as follows:

$NO + O_3 \rightarrow NO_2 + OH \rightarrow HNO_3$ *R1.12*

$^{\Delta}HNO_{3\,(R1.12)} = 2/3 * \alpha\, ^{\Delta}O_3 + 1/3 * ^{\Delta}OH$ Eq. 1.15

Where 2/3 of the oxygen atoms propagate from NO_2 and 1/3 from OH yielding a total of 3 oxygen atoms in the product HNO_3. The isotopic exchange between OH and water is rapid and eliminates any $\Delta^{17}O$ signature from photochemistry. For that reason, tropospheric water is estimated to have a $\Delta^{17}O$ of ~0‰, (Dubey et al., 1997; Lyons, 2001). Thus, the $^{\Delta}OH$ becomes zero and the mass balance can be simplified to:

$^{\Delta}HNO_{3\,(R1.12)} = 2/3 * \alpha\, ^{\Delta}O_3$ Eq. 1.16

The daytime NO_2 can also become oxidized by O_3 to form the nitrate radical (NO_3). The nitrate radical is rapidly photolyzed during the day but at night it can react with VOCs or dimethyl sulfide (DMS) to produce HNO_3. A mass balance calculation can be applied to determine $^{\Delta}HNO_3$ from this pathway by substituting Eq. 1.13 for NO_2 as follows:

$NO_2 + O_3 \rightarrow NO_3 + VOC \rightarrow HNO_3$ *R1.13*

$^{\Delta}HNO_{3\,(R1.13)} = 2/3 * \alpha\, ^{\Delta}O_3 + 1/3\, ^{\Delta}O_3$ Eq. 1.17

Since the NO_3+VOC reaction leads to H abstraction, it is assumed that VOCs are not responsible for any oxygen transfer; therefore the $^{\Delta}HNO_3$ is the same for $^{\Delta}NO_3$ (nitrate radical). Thus, 2/3 of the total oxygen atoms in the product HNO_3 propagate from NO_2 and 1/3 from ozone.

Although the nocturnal oxidation of VOCs by the nitrate radical leads to nitrate formation, this pathway is relatively minor. Instead, nitrate radicals react with NO_2 to form N_2O_5 which then leads to the second major pathway to nitrate formation, which is

the N_2O_5+H_2O heterogeneous hydrolysis reaction on an aerosol surface. A mass balance calculation can be applied to determine the $^{\Delta}HNO_3$ value by substituting E1.13 for NO_2 and E1.17 for NO_3 as follows:

$$NO_2+NO_3 \rightarrow N_2O_5 + H_2O_{(aerosol)} \rightarrow 2HNO_3 \qquad R1.14$$

$$^{\Delta}HNO_{3\,(R1.14)} = [2/6 * \alpha\, ^{\Delta}O_3 + 3/6\, (2/3 * \alpha\, ^{\Delta}O_3 + 1/3\, ^{\Delta}O_3)] + 1/6\, ^{\Delta}H_2O \qquad \text{Eq. 1.18}$$

Where, 2/6 of the oxygen atoms propagate from NO_2, 3/6 from NO_3 and 1/6 from H_2O yielding a total of 6 oxygen atoms in the product, $2HNO_3$. Recall earlier, tropospheric water has a $\Delta^{17}O$ of ~0‰, (Dubey et al., 1997; Lyons, 2001), therefore removing any possibility of isotopic exchange between water and N_2O_5 during the hydrolysis reaction. Thus, the $^{\Delta}H_2O$ becomes zero and the mass balance can be simplified to:

$$^{\Delta}HNO_{3\,(R1.14)} = 1/3 * \alpha\, ^{\Delta}O_3 + 1/2\, (2/3 * \alpha\, ^{\Delta}O_3 + 1/3\, ^{\Delta}O_3) \qquad \text{Eq. 1.19}$$

Where, 1/3 of the total oxygen atoms in the product $2HNO_3$ propagate from NO_2 and 1/2 from NO_3. Using the mass balance approach, dilution by peroxy radical oxidation can shift α and impact the $^{\Delta}HNO_3$ for each formation pathway. For example, assuming $\Delta^{17}O$ = 35‰ for O_3, and if 15% of the NO_2 is formed from peroxy oxidation, then α = 0.85. The calculated $\Delta^{17}O$ signatures for each HNO_3 formation pathway would then be the following: $\Delta^{17}O$ = 25.7‰ for N_2O_5 hydrolysis pathway, $\Delta^{17}O$ = 19.8‰ for NO_2+OH pathway and $\Delta^{17}O$ = 31.5 for NO_3+VOC/DMS pathway.

In order to better constrain formation pathways and interpret seasonal variations observed in $\Delta^{17}O$ in atmospheric nitrate, Purdue Stable Isotope laboratory has developed the “ISO-Regional Atmospheric Chemistry Mechanism” (ISO-RACM) model

(Michalski and Xu, in review). ISO-RACM is essentially a photochemical box model that incorporates the isotope mass balance mechanism to model the $\Delta^{17}O$ signature of the three main nitrate formation pathways in terms of α and $^{\Delta}O_3$ (Michalski et al., 2003):

$$^{\Delta}HNO_{3\ (R1.12)} = 2/3 * \alpha\ ^{\Delta}O_3 \qquad \textit{Eq. 1.16}$$

$$^{\Delta}HNO_{3\ (R1.13)} = 2/3 * \alpha\ ^{\Delta}O_3 + 1/3\ ^{\Delta}O_3 \qquad \textit{Eq. 1.17}$$

$$^{\Delta}HNO_{3\ (R1.14)} = 1/3 * \alpha\ ^{\Delta}O_3 + 1/2\ (2/3 * \alpha\ ^{\Delta}O_3 + 1/3\ ^{\Delta}O_3) \qquad \textit{Eq. 1.19}$$

The $^{\Delta}HNO_{3\ (Total)}$ for each day is then calculated by ISO-RACM by simplifying the mass balance mechanism and applying an atmospheric chemistry scheme to calculate the mole fractions of HNO_3 produced by each reaction pathway (Michalski and Xu, in review):

$$^{\Delta}HNO_{3\ (R1.12)} = {}^{\Delta}O_3 * (2\alpha/3) \qquad \text{(Beta, } \beta\text{)} \qquad \text{Eq. 1.20}$$

$$^{\Delta}HNO_{3\ (R1.13)} = {}^{\Delta}O_3 * [(2\alpha+1)/3] \qquad \text{(Eta, } \varepsilon\text{)} \qquad \text{Eq. 1.21}$$

$$^{\Delta}HNO_{3\ (R1.14)} = {}^{\Delta}O_3 * [(4\alpha+1)/6] \qquad \text{(Chi, } \chi\text{)} \qquad \text{Eq. 1.22}$$

$$^{\Delta}HNO_{3\ (Total)} = \beta * {}^{\Delta}HNO_{3\ (R1.12)} + \varepsilon * {}^{\Delta}HNO_{3\ (R1.13)} + \chi * {}^{\Delta}HNO_{3\ (R1.14)} \qquad \text{Eq. 1.23}$$

The Beta (β), Eta (ε), and Chi (χ) are the mole fractions of HNO_3 produced by the reaction pathways R1.12, R1.13, and R1.14 respectively. Each ISO-RACM simulation then yields $^{\Delta}HNO_{3\ (Total)}$ value for each day that reflects shifts in nitrate formation pathways (Eq. 1.23). In the winter, the N_2O_5 hydrolysis pathway becomes dominate due to limited photochemistry and cold temperatures, thus yielding a high $\Delta^{17}O$ signature in observed nitrate (Michalski et al., 2003). On the other hand, summer conditions limit the N_2O_5 hydrolysis pathway and the NO_2+OH pathway to nitrate formation becomes more relevant. The origin of the O atoms in atmospheric nitrate (i.e. O_3, H_2O, NO_x, HO_x, RO_x),

the α (proportion of NO oxidized into NO_2 by ozone and peroxy radicals), and $^{\Delta}O_3$ play an important role in modeling the $\Delta^{17}O$ value of nitrate formation pathways.

Experimentally derived $\Delta^{17}O$ values for tropospheric ozone on mid-latitude experimental temperatures and pressures yields a $^{\Delta}O_3$ range from 33-37‰ (Morton et al., 2007; Michalski and Bhattacharya, 2009). However, ISO-RACM is parameterized using the $\Delta^{17}O$ = 35‰ for ozone at 298 K to calculate the $\Delta^{17}O$ values for HNO_3 for each day based on experimental pressure and temperature dependent studies by Morton et al. (1990). According to Morton et al. (1990), typical surface pressures have a minor influence on $^{\Delta}O_3$, thus the $^{\Delta}O_3$ is dependent only on temperature (K). Therefore, ISO-RACM simulations are run at 101.5 kPa, in which $^{\Delta}O_3$ is parameterized using (Michalski et al., 2004):

$$\Delta^{17}O\ (‰) = 10*[(0.0243*T(K) + 3.7667) - .52*(0.035*T(K) + 4)] \qquad \text{Eq. 1.24}$$

which yields a $\Delta^{17}O$ value of 35‰ based on Morton et al. (1990).

The current ISO-RACM model is not a multidimensional model in that it does not include any fluxes (zero dimensional), so that only production pathways control the $\Delta^{17}O$ of atmospheric nitrate. Furthermore, the ISO-RACM model does not incorporate (dry/wet) deposition loss processes, explicit aerosol chemistry and chemical transport mechanisms. Despite the absence of these features, ISO-RACM can explore which reactions, conditions, and parameterizations that may have pronounced impacts on controlling $\Delta^{17}O$ values in atmospheric nitrate without large amounts of computation (Michalski and Xu, in review).

ISO-RACM is a second generation to the Regional Atmospheric Chemistry Mechanism (RACM) (Stockwell et al., 1997), originally developed as the Regional Acid Deposition Model (RACM1 and RACM2) (Stockwell et al., 1990). The ISOI-RACM model has 238 atmospheric reactions with the most recent rate constants and product outputs based on laboratory measurements verified against environmental chamber data. The model uses trace gas mixing ratios, meteorological data, and chemical boundary conditions to simulate the troposphere from the Earth's surface through the upper troposphere as well as simulating rural to urban conditions (Michalski and Xu, in review). ISO-RACM, like RACM has included biogenic compounds such as isoprene and anthropogenic hydrocarbons (alkane, alkene and aromatics) in its reaction schemes but most notably the difference is the incorporating of isotope mass balance mixing and the addition of heterogeneous N_2O_5 uptake by aerosols (Michalski and Xu, in review).

ISO-RACM is an effective photochemical modeling tool to provide insight into the importance of NO_x oxidation, HNO_3 formation, heterogeneous reactions, and trace gas chemistry. This becomes important as global 3-D chemical transport model (GEOS-CHEM) simulations have shown the global mean inorganic nitrate burden to be dominated by nitrate formation via NO_2+OH (76%), followed by N_2O_5 hydrolysis (18%) and NO_3+DMS/VOC (4%) (Alexander et al., 2009). Studies using the mass balance approach have shown that the ozone oxidation of NO_x to higher oxidation states produces positive $\Delta^{17}O$ values in atmospheric nitrate (Savarion et. al., 2008; Michalski et al., 2003; Lyons, 2001). Qualitatively, observed increases in observed $\Delta^{17}O$ values in tribal particulate nitrate would suggest an increase in N_2O_5 hydrolysis. Such increases

might be regressed against other atmospheric pollutant data to look for correlations. For example, heterogeneous uptake of N_2O_5 should be proportional to aerosol surface area, which is roughly proportional to PM mass, so there could be possible correlation between nitrate $\Delta^{17}O$ values and mass of PM. On the other hand, Brown et al. (2007) suggested that aerosol composition is more important than simply surface area. In this case, nitrate $\Delta^{17}O$ values may be inversely correlated with organic loading.

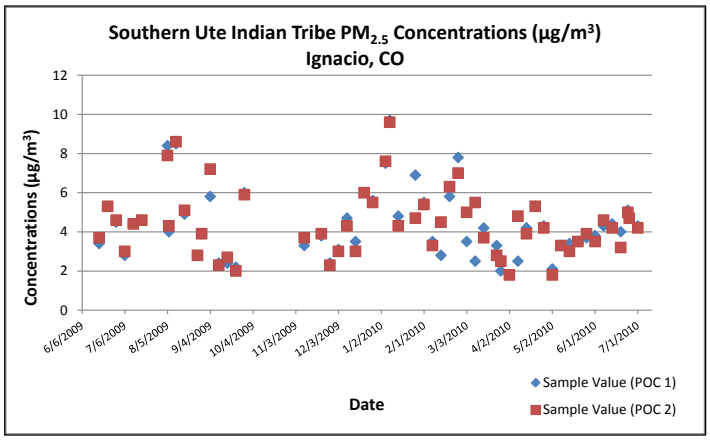

Figure 15 Southern Ute Indian Tribe $PM_{2.5}$ mass concentrations ($\mu g/m^3$), 2009-2010 (US EPA Data Mart, 2010).

ISO-RACM model simulations can be initialized using tribal meteorological data, aerosol mass concentrations, and trace gas mixing ratios. The photochemical and mass balance schemes can then determine seasonal changes in the branching ratios for each NO_x removal pathway as well as the corresponding $\Delta^{17}O$ value of the nitric acid product. The model derived $\Delta^{17}O$ values can then be adjusted to match observed $\Delta^{17}O$ values, therefore allowing for better parameterization of the N_2O_5 uptake coefficient and NO_x

removal pathways which then lead to accurate predictions of trace gas concentrations (Detener and Crutzen, 1993).

CHAPTER 2. ION CHROMOTOGRAPHY INSTRUMENTATION FOR TRIBAL NITRATE SEPERATION

2.1 Technical Note

This chapter details the procedures I have taken to request archival tribal aerosol filters and the analytical and preparative ion chromatography system that I developed to separate, measure and collect anions in aerosol samples.

2.2 Introduction

This project will examine the stable oxygen and nitrogen isotope composition of particulate nitrate collected on the Southern Ute Indian Reservation and Navajo Nation to provide insight into the sources of NO_x and the oxidation pathways that convert NO_x into nitrate on these reservation lands. Tribal Air Quality Programs (AQP) operate particulate matter ($PM_{2.5}$ and PM_{10}) monitoring networks as part of USEPA PM national monitoring network. Tribal AQPs monitor dry deposition particulates by collecting filter based PM using hi-volume flow and low-volume flow air samplers operating on 24hr sample durations every 1 in 6 days (EPA PM national monitoring schedule). Low-volume samplers collect $PM_{2.5}$ and hi-volume samplers collect PM_{10}. After sample exposure, tribal PM filters are retrieved and properly packaged and sent to gravimetric laboratories for determination of PM mass.

For this thesis, coarse particulates from both reservations were collected using the Anderson Instruments Graseby PM_{10} hi-volume air sampler (GMW 1200) with a flow rate of 1.13 m^3/min (1,130 L/min). The fine particulates on the Southern Ute Indian Reservation were collected using the $PM_{2.5}$ single filter Anderson Reference Ambient Air Sampler (RAAS2.5-100) with a flow rate of 16.7 L/min. The Navajo Nation fine particulates were collected using the $PM_{2.5}$ Thermo Electron Federal Reference Method air sampler (FRM 2000) at 16.7 liters/min.

Air samplers draw greater than 270° of unrestricted ambient air at a constant volumetric flow rate maintained by a mass flow controller coupled to a microprocessor. Ambient air is collected at ~3 m above ground and directed into specially designed inertial particle-size separators (i.e. cyclones or impactors) where the suspended particulate matter in the $PM_{2.5}$ or PM_{10} size ranges is separated for collection on filter media. Particulates are collected on non-reactive filter media which include: 46 mm diameter polytetrafluoroethylene (PTFE, Teflon) filter membrane disks (particle retention 0.3 µg) for $PM_{2.5}$ and 8”x11’’ quartz (SiO_2) fiber filters for PM_{10}.

a) b) c)

Figure 16 Tribal dry deposition air samplers. (a) Anderson Graseby PM_{10} air sampler, (b) Thermo Electron Partisol $PM_{2.5}$ air sampler, and (c) Anderson RAAS $PM_{2.5}$ air sampler.

Each dry deposition PM filter contains common anions: nitrate (NO_3^-), nitrite (NO_2^-), sulfate (SO_4^{2-}) and chloride (Cl^-). In order to measure the isotopic composition of nitrate, other anions must be separated and the nitrate isolated in order to prevent any possible interference in isotope measurements. For example, if NO_2^- and NO_3^- are both present in sample, the isotopic analysis of oxygen in NO_3^- using the "denitrifier technique" can produce inaccurate oxygen isotope values (Casciotti et al., 2007; Kaiser et al., 2007). In addition, the bulk of the $PM_{2.5}$ filters are estimated to contain nitrate below the 500 nanomole (nMol) requirement needed for IRMS analysis, therefore nitrate from each filter must be separated and those below the requirement are combined into a monthly nitrate composite. The following sections in this chapter discuss the procedures taken for the release for tribal PM filters, extraction processes to remove anions from filters, the analytical ion chromatography developed to measure

anion concentrations and the preparative ion chromatography system used to isolate the NO_3^- anion in order to provide adequate composites for isotope analysis.

2.3 Requesting the Release of Archival Tribal Aerosol Filters

Both the Southern Ute Indian Tribe Air Quality Program (SUIT AQP) and Navajo Nation Air Quality Control Program (NNAQCP) send exposed $PM_{2.5}$ filters to the Tribal Air Monitoring Support (TAMS) Center laboratory in Las Vegas, NV for gravimetric analysis. The SUIT AQP sends PM_{10} filters to the Inter-Mountain Lab, Inc. in Sheridan, WY for gravimetric analysis while the NNAQCP provided its own analysis in Fort Defiance, AZ. As part of the USEPA's quality assurance protocol, monitoring agencies are required to archive filters for a year following sampling after collection (USEPA, 1998). After which the national guidance becomes more flexible in which agencies quality assurance project plans more stringent than the national guidance will take priority. Most monitoring agencies discard filters that have exceeded archival requirements, but in this case, the TAMS Center and Inter-Mountain Lab, Inc. retains all archival filters for tribes unless tribes specifically request for their filters to be discarded or returned back to the tribe.

A graduate research proposal outlining my proposed work and methodology along with an official written request for the release of one (1) year of archival PM_{10} and $PM_{2.5}$ filters was respectfully sent to the SUIT AQP, Southern Ute Indian Tribal Council, NNAQCP, and TAMS Center. Both the Southern Ute Indian Tribe and Navajo Nation agreed to provide one (1) year of archival PM_{10} and $PM_{2.5}$ filters from their monitoring

sites for isotopic and chemical analysis. The chain of custody releasing archival tribal PM filters to the Purdue Stable Isotopes (PSI) laboratory was accomplish through collaborative work with the SUIT AQP, Southern Ute Tribal Council, NNAQCP, Inter-Mountain Lab, Inc., TAMS Center and USEPA.

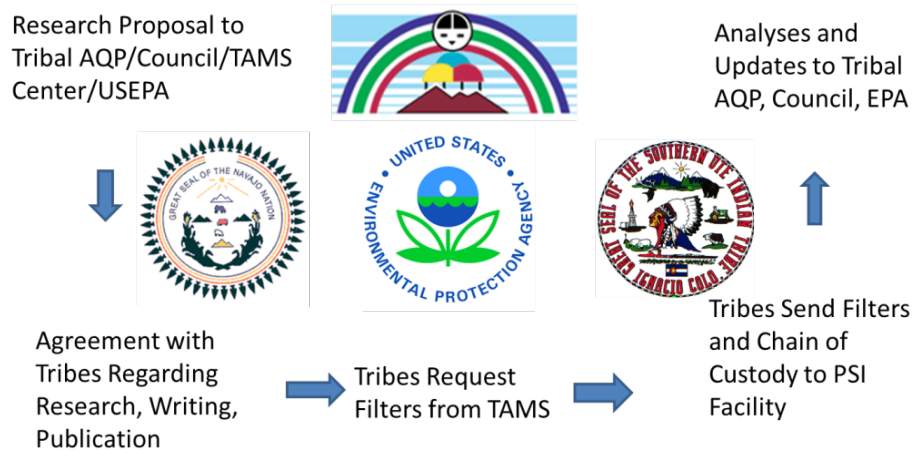

Figure 17 Flow chart of steps taken for the release of archival Tribal PM filters.

2.4 Extraction of Anions from Tribal Aerosol Filters

Upon arrival to PSI laboratory each $PM_{2.5}$ and PM_{10} filter was inspected and filter ID number and exposure date recorded. Field and trip blank filters were separated from sample filters and each sample filter was divided into three groups based on aerosol net weight and estimated nitrate composition: High, Medium, and Low. An aseptic technique was applied prior to the handling of the $PM_{2.5}$ filters, where latex powder free exam gloves (Microflex) were cleaned using lab detergent and ultrapure Millipore water (Synergy 185). Stainless steel tweezers were cleaned using ethanol and non-abrasive, low lint accu-wipes (Fort Howard). The $PM_{2.5}$ Teflon filters were then removed from

filter cassettes by tweezing support rings and each individual filter folded in half using latex gloves and placed inside sterile (VWR polypropylene) 15 mL centrifuge tubes.

Each centrifuge tube was then labeled with corresponding filter ID number, exposure date and filled with 15 mL of Millipore water using an air displacement pipette (Thermo Scientific Finnpippette® II, 2-10 mL). The centrifuge tubes containing the Teflon filter solutions were then placed into an ultrasonic sonicator bath (Branson 5210) for 30 minutes and centrifuged (International Equipment Co. IEC-HN-S) for 30 minutes at 2000 rpm, respectively to extract anions and separate supernate (Figure 18). While Teflon filters remained in the initial centrifuge tubes, each aerosol solution was then decanted into another sterile 15 mL centrifuge tube, properly labeled and weighed using an analytical balance (Sartorius Research R200D) in preparation for analytical and preparative mode ion chromatography (IC) analysis.

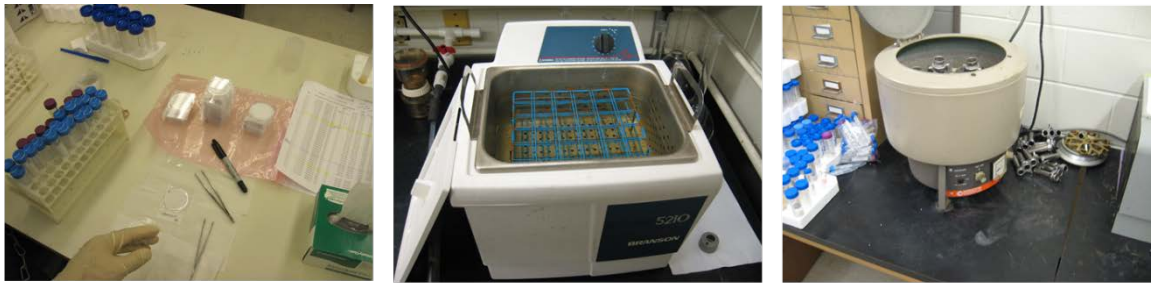

a) b) c)

Figure 18 $PM_{2.5}$ filter extraction process. a) $PM_{2.5}$ filter removal into aerosol solution, b) ultrasonic sonication bath and c) clinical centrifuge.

Similarly, the PM_{10} quartz filters were removed from filter sheet protectors using clean latex powder free gloves and placed inside individual (128 oz., 1 gal) Ziploc bags and labeled with corresponding filter ID number and exposure date. Sterile (VWR,

polypropylene) 50 mL centrifuge tubes were then filled with 50 mL of Millipore water, properly labeled and decanted into each corresponding Ziploc bag. The Ziploc bag technique directs Millipore water onto PM_{10} filter media, saturating the filter, and allowing for anion extraction without contaminating the filter by lightly compressing the Ziploc bag. The aerosol solution is then decanted back into its corresponding 50 mL centrifuge tube and into a filtration system to remove any suspended organic particulate matter.

A sterile, single use Steriflip (50 mL centrifuge tube) filter system (Steriflip® Millipore Filter Systems) was used to filter aerosol solutions. The 50 mL centrifuge tube containing the aerosol solution is attached to the threaded insert on the Steriflip, which then creates a system of two 50 mL centrifuge tubes that are connected by a sterile plastic housing containing a 0.22 µm filter and a side port (Figure 19, b). When in use, a pump is attached to the side port to create a vacuum and forces the sample through the filter while collecting the filtrate in the second centrifuge tube.

An alternative filtration system was also utilized similarly to the Steriflip, but instead (polypropylene) containers connected by O-ring fittings to a 0.22 µm filter housing, replaced the 50 mL centrifuge tubes (Figure 19, c). Each container was cleaned using lab detergent and triple rinsed using Millipore water after each use. After filtration, each PM_{10} aerosol solution was then stored in a deep freezer until IC analysis.

a) b) c)

Figure 19 PM_{10} aerosol extraction process. a) PM_{10} filter removal into aerosol solution, b) steriflip filter system, and c) vacuum filtration system.

A series of PM filters were extracted twice to determine the efficiency of the extraction procedure using analytical ion chromatography (Alltech Associates Inc.). This ion chromatography has a detection limit of 5 nMol of nitrate and it was determined that the secondary extraction concentrations were below the detection limit of the IC indicating that our procedure is effectively 100% efficient, within the uncertainty of the IC. Field filter blanks were also extracted and were determined to be below the detection limit of the IC as well. Before each aerosol sample solution undergoes IC analysis, an estimate of the nitrate composition in PM mass must be determined in order to mix standard solutions of NO_3^-, SO_4^{2-}, and Cl^- to concentrations that will bracket each aerosol solution to determine anion concentrations, specifically nitrate.

The PM mass concentration over tribal air sheds is computed as the total mass of collected particles in the $PM_{2.5}$ or the PM_{10} size ranges divided by the actual volume of air sampled, and is expressed in $\mu g/m^3$ at local temperature and pressure (LTP). Therefore, the estimated amount of nitrate in PM filters was accomplished by first

determining the actual sample volume (if not already known) using the following expression:

$$V_a = Q_{avg} \times T \qquad \text{Eq. 2.1}$$

Where V_a is the actual sample volume (m^3), Q_{avg} is the average sample flow rate (m^3/min) and T is the sample duration time (min), which yielded air sampling volumes of ~24 m^3 and ~1627 m^3 for $PM_{2.5}$ and PM_{10}, respectfully.

The sampling volume and mass concentration was then use to determine the net aerosol weight for each filter using the following expression:

$$N = M \times V_a \qquad \text{Eq. 2.2}$$

where N is the net aerosol weight (µg) and M is the mass concentration (µg/m^3). The net aerosol weight was then compared to Colorado Plateau aerosol composition measurements which yielded ~5% nitrate composition (NARSTO, 2004). Five percent of net aerosol weight was then used to estimate nitrate composition for each filter using the following expression.

$$\mu g\ NO_3^- = N \times 5\% \qquad \text{Eq. 2.3}$$

The molecular weight of NO_3^- (62.0049 g/mol) was then used to convert µg into nMol NO_3^- giving an estimated NO_3^- composition for each individual PM filter. The calculation (Eq. 2.1-2.3) yielded estimated NO_3^- averages of ~85 nMol for $PM_{2.5}$ and ~13,385 nMol for PM_{10} collected on the Southern Ute Indian Reservation. And ~69 nMol for $PM_{2.5}$ and ~19,565 nMol for PM_{10} collected on the Navajo Nation. Each individual nMol amount of nitrate in PM filters was then used to divide filters into groups based on (High, Medium, and Low) nitrate composition. This becomes important

in preparation for analytical anion measurements by ion chromatography. Determining standard solutions of NO_3^-, SO_4^{2-}, and Cl^- at known concentrations are needed in order to bracket each group of aerosol solution to determine anion concentrations.

2.5 Ion Chromatography

Ion chromatography (IC) is the separation of ions or polar molecules in a solution based on their size and charge. Each entire aerosol sample solution is pumped through an ion-exchange analytical column where the anions are absorbed onto the column based on ionic interactions with the column resin. The anions are then eluted off the column and back into solution using a carbonate mobile phase. The anions do not desorb back into solution all at the same time, rather each anion has a specific elution time as the mobile phase passes through the column, changing the solution conductivity. The change in conductivity is then measured using a conductivity detector. The time interval between the sample injection into the column and the detection of the anion is known as the retention time. Each anion retention time is then correlated with conductivity detection to determine specific anions.

The IC instrumentation in the PSI laboratory was altered to separate chloride, nitrate, and sulfate in each aerosol solution using a single analytical column. The anions were then collected and the nitrate isolated for isotopic analysis using a fraction collector. The IC instrumentation was altered to operate simultaneously in two modes: analytical and preparative. The analytical mode measures the concentrations of each anion by pumping a measured volume of aerosol sample solution onto the analytical

column and referencing sample conductivity to those of standards mixed to known concentrations. The analytical mode can send the sample volume to waste or direct the solution into the preparative mode. The preparative mode utilizes a fraction collector based on anion retention time to collect and then isolates the anions fractions from each aerosol sample solution.

2.5.1 $PM_{2.5}$ Ion Chromatography Instrumentation

The Ion chromatography process in the PSI lab utilizes two high pressure pumps (sample pump and mobile phase pump) to employ the High Pressure Liquid Chromatography (HPLC) technique and circulate sample and mobile phase solutions throughout the IC instrument. The IC instrument as a whole also consists of one chemical suppressor, one analytical anion separation column, one sorbent column, a mobile phase degassing system, one conductivity detector, one pressurized argon tank, a 6-port electronic-actuated control valve, an autosampler and a fraction collector. The IC instrument is coupled with a microprocessor and PeakSimple (SRI) chromatography data system software to control instrumentation via a contact closure relay board.

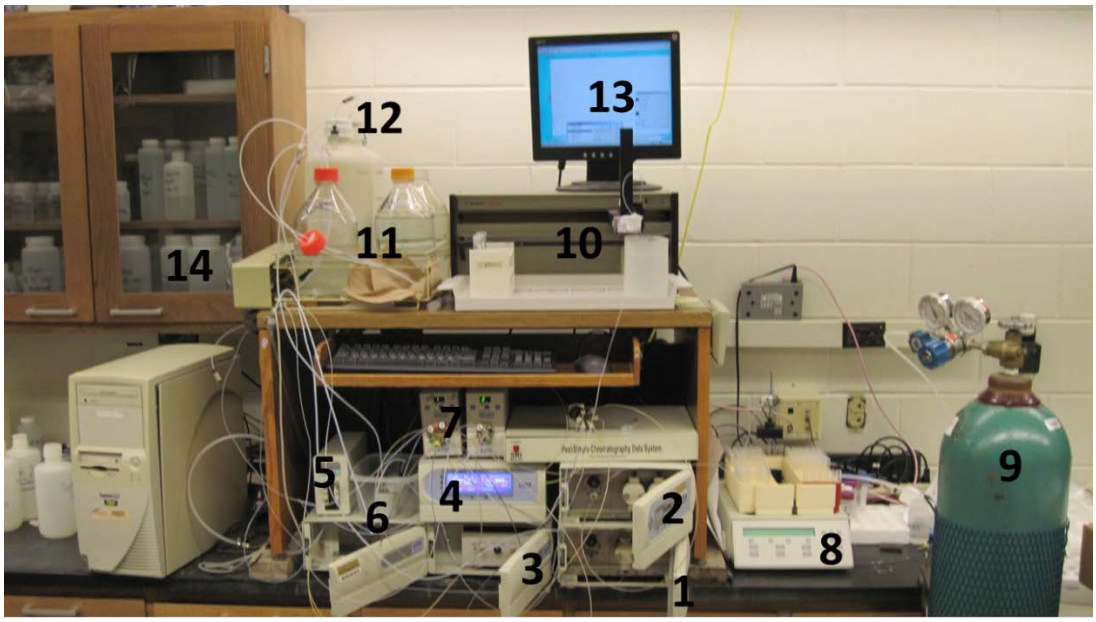

Figure 20 PSI HPLC instrumentation. Composed of: 1) sample pump, 2) mobile phase pump, 3) housing for analytical and sorbent columns, 4) conductivity detector, 5) mobile phase degassing system, 6) suppressor 7) 6-port control valve, 9) fraction collector, 9) argon tank, 10) autosampler, 11) mobile phase, 12) reagent, 13) PeakSimple (SRI) chromatography software, and 14) known anion standards.

The autosampler (Gilson, 222) is capable of holding 176, 15 mL centrifuge tubes containing aerosol samples held into place by sample racks (Gilson Rack 23). The sample pump is a single head pump (Alltech 426) with a pumping rate of 1 mL/min. Each aerosol sample solution is pumped through a SPE sorbent C18 (Omnifit) chromatographic tube to trap and remove organic particulate matter. The sample solution is then pumped onto the analytical column (4mm Dionex IonPac AS14). The analytical column is designed to separate inorganic anions such as: fluoride, chloride, nitrite, bromide, nitrate, phosphate, and sulfate based on their affinity for the column resin.

The mobile phase pump is a dual-head pump (Alltech 626) with a pumping rate of 2 mL/min. The mobile phase or eluent is a 3.5 mM/1.0 mM, 2 L solution of sodium bicarbonate/sodium carbonate ($NaHCO_3/Na_2CO_3$), respectively. The mobile phase is directed into a degassing system (Alltech Micro) to remove dissolved gases. Inside the degassing system the mobile phase flows through a short length Teflon tubing held inside a vacuum chamber where the dissolved gases are then expelled. The degassing system removes any bubbles that may exist in the mobile phase that could potentially cause poor pump performance and interfere with conductivity detection.

The mobile phase is then pumped to a 6-port electronic-actuated control valve (SelectPro Fluid Processor) which directs flow into the analytical column to allow the mobile phase to elute the anions at 2mL/min into a chemical suppressor (4mm Dionex AMMS300), where a reagent, a 50 mN, 4L solution (two, 2 L tanks) of sulfuric acid (H_2SO_4) suppresses the mobile phase's contribution to conductivity. The suppressor is regenerated by H_2SO_4 that flows into the suppressor at 3 mL/min from two pressurized 2 L tanks. The suppressor decreases mobile phase conductivity without removing any sample from the solution by using a micro-membrane to exchange H^+ in the reagent for Na^+ in the eluent, where the $NaHCO_3/Na_2CO_3$ is converted into H_2O and CO_2 (Figure 21). The micro-membrane suppressor reduces the background conductivity of the mobile phase down to -22 microseimens (μS), so that only the electric conductance of each sample is measured by the conductivity detector.

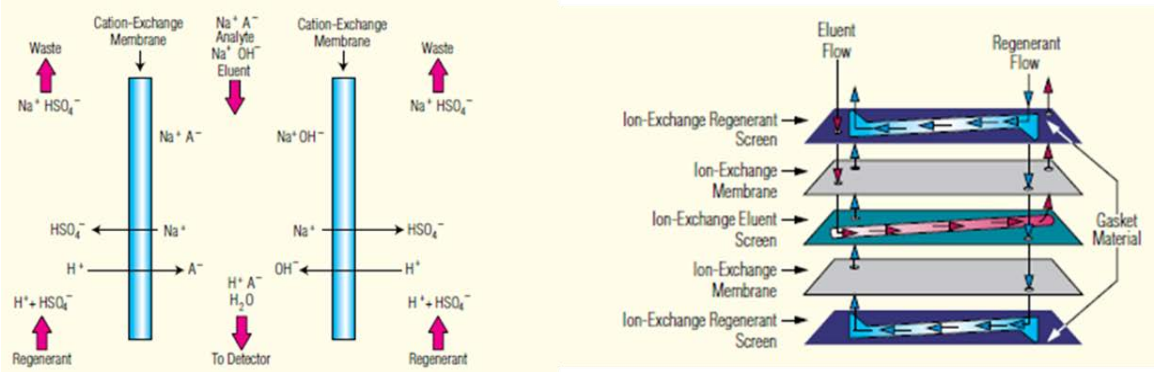

Figure 21 Internal construction of the micro-membrane (MMS 300) suppressor (Dionex, 2010).

After suppression, the conductivity detector measures the electric conductance of each anion which is displayed on the detector's front panel in microseimens (µS) and integrated by the PeakSimple chromatograph software as a conductivity intensity curve versus time (µS min^{-1}), also known as peak area. PeakSimple software is also instrumental to the execution of programmable events as it initiates the contact closure relay board to allow instrument control and the completion of analytical and preparative analysis. Detailed instructions on how to use the IC in both the analytical and preparative modes is discussed in Appendix B.

2.5.1.1 Analytical Mode

In the analytical mode, the sample volume loop (100 µL) was removed and the entire sample volume analyzed. Therefore, each 15 mL aerosol sample was placed in a Steriflip tube base and weighed before and after analysis using an analytical balance. The initial (V_i) and final (V_f) volumes are recorded in lab logbook to determine the

sample volume ($\Delta V = V_i - V_f$) pumped through the IC instrument. Due to autosampler instrumentation, typically the volume ranged between 11.00-11.02 mL, with an error of ~2%.

Figure 22 Analytical balance and 15 mL centrifuge tube with tube base.

Each 15 mL centrifuge tube containing sample solutions are then loaded into sample racks and placed on the autosampler. The sample solutions are individually pumped into the sorbent column and onto the analytical column using a single head sample pump. The 6-port valve controls the flow of the sample and mobile phase solutions and operates in two positions: Position 1 and Position 2. The pump pressures in Position 1 are as follows: mobile phase ~90 psi and sample ~1195 psi. The pump pressures in Position 2 are as follows: mobile phase ~1230 psi and sample ~341 psi.

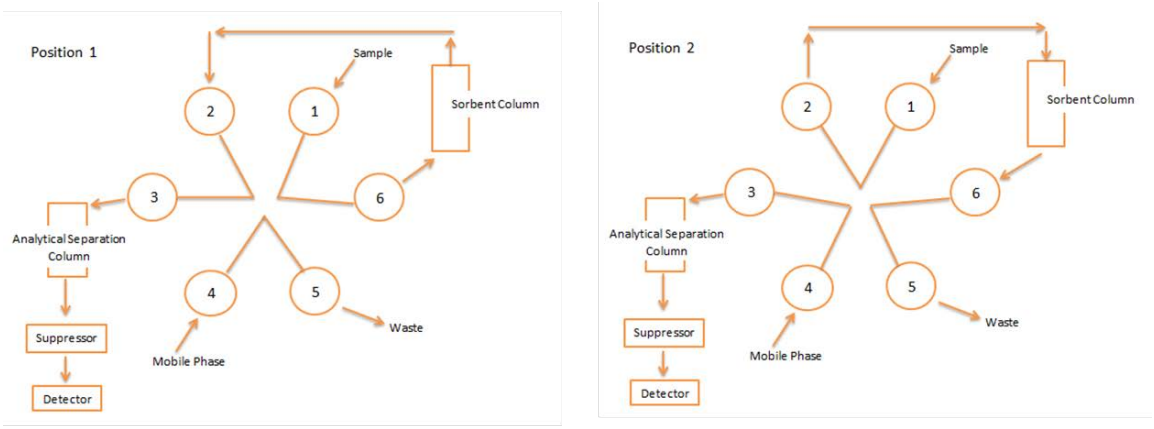

Figure 23 Schematic of the HPLC 6-port control valve positions.

In Position 1, the sample solution is directed onto the two columns for separation while the mobile phase goes to waste container. PeakSimple software regulates the 6-port control valve in position 1 until nearly all of the sample volume is pumped onto the analytical column before switching valves. In Position 2, the mobile phase bypasses the sorbent column and is directed into the analytical column to elute the anions. While in Position 2, the sample is eluted to the chemical suppressor and onto the conductivity detector where each anion is detected by conductivity. The PeakSimple software integrates and records peak areas for each detected anion and peak areas are displayed on the PeakSimple chromatograph. The PeakSimple software also allows users to manually integrate peak areas, which was applied consistently during the analysis of $PM_{2.5}$ aerosol samples.

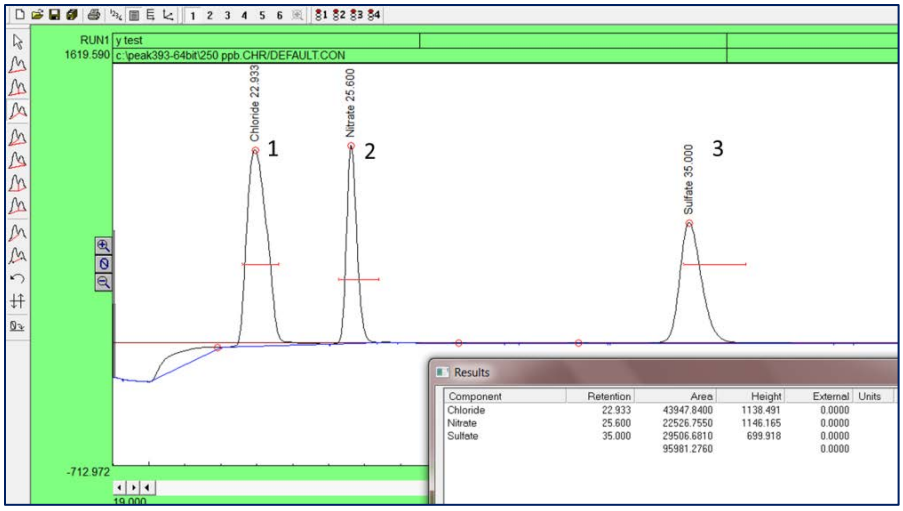

Figure 24 Integrated anion peak areas and peak retention times: 1) chloride, 2) nitrate, and 3) sulfate (PeakSimple version 3.93, 2010).

After detection the sample is then sent to the fraction collector where individual anions are collected as a function of retention time. Since the peak area is a function of concentration and volume, each measured volume pumped onto the IC is normalized to peak area intensity for each anion using the following expression:

$$P_f = \left[\left(\frac{(\Delta V - Vmax)}{Vmax}\right) + 1\right] \text{ x } P_i \qquad \text{Eq. 2.4}$$

where V_{max} is the maximum sample volume pumped (mL) onto the IC, ΔV is the sample volume (mL) pumped onto the IC, and P_i is the corresponding sample's initial peak area intensity. The final peak area intensity, P_f, is the normalized peak area. The change in sample volume pumped onto IC for three replicate standards of 50 ppb, 100 ppb, 200 ppb, 300 ppb, 400 ppb, and 1ppm was plotted against peak intensity to observe for change in conductivity intensity with change in volume.

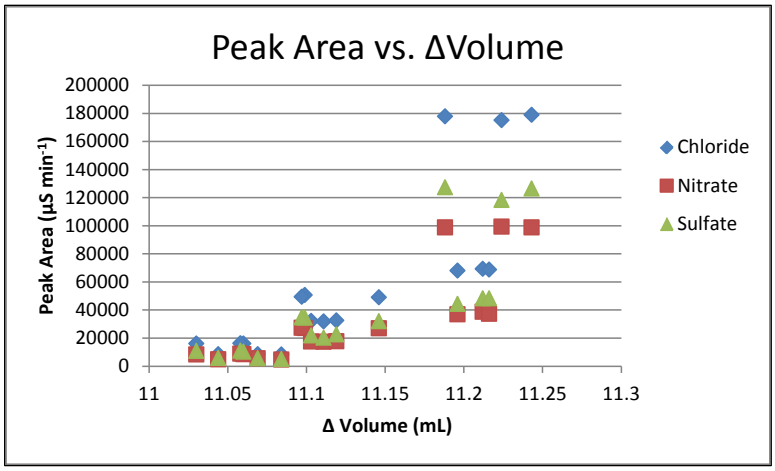

Figure 25 Peak area intensity vs. Δ volume. A 2% error in volume pumped onto the IC allowed for minimal change in peak area intensity.

Calibration standards are placed before and after samples and analyzed by the IC to determine anion concentrations. The standards produce calibration linearity curves which bracket each division (High, Medium, and Low) of estimated nitrate composition. The standard concentrations used to bracket filters containing nitrate in the High division included: 600 ppb, 800 ppb, 900 ppb, 1ppm, 2ppm and 3ppm. The standards for the Medium division included: 100 ppb, 200 ppb, 300 ppb, and 400 ppb. The standards for the Low division included: 50 ppb, 100 ppb, 150 ppb, and 200 ppb. The overall concentrations correspond to ~12-725 nMol of nitrate across the range of standards. Concentrations in samples are then determined from the linear equation by substituting the peak area for y and solving for x (Figure 26). A single $PM_{2.5}$ filter from each division was selected for aerosol extraction and each aerosol solution was ran through the IC to confirm calibration ranges. In addition, replicates of known standards (Cl^-, NO_3^-, SO_4^{2-}) ranging between 50 ppb to 1 ppm were measured on the IC to determine the overall

range of uncertainty (detection limit) and % error of the IC instrument. The IC yielded a 5% error with a ±14 ppb (± 0.014 µg/mL) range of uncertainty (detection limit) for the measured anions. The divisions of aerosol filter solutions based on estimated nitrate composition and the bracketing of these divisions with calibration standards allows for proper conductivity detection of anions at low concentrations and at high concentrations. This bracketing technique also allows for the column to properly separate anions and prevents saturation. Running a single sample in analytical mode takes ~45 minutes.

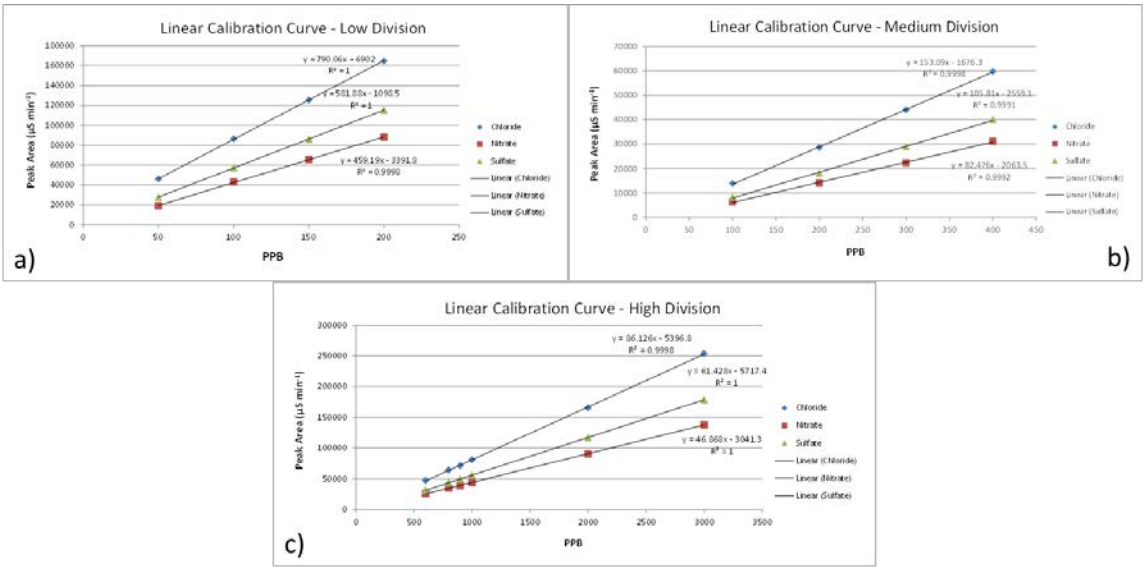

Figure 26 Linear calibration curves for $PM_{2.5}$ filter divisions. a) Low division, b) Medium division and c) High division.

The concentrations produced from the linear calibration curves are reported in ppb and multiplied by 1000 to convert into ppm. The ppm values are equivalent to µg/mL and converted to µg/m^3 using air sampler parameters in the following expression:

$$[B] = [A] \times V_i \times 1/Q_{avg} \times 1/T \qquad \text{Eq. 2.5}$$

Where [A] is the concentration of anion in µg/mL, V_i is the initial aerosol solution volume (mL), Q_{avg} is the average flow rate of air sampler (m^3/min), and T is the sample duration and [B] is then the concentration of the measured anion expressed in µg/m^3. For $PM_{2.5}$ filters the initial aerosol solution is constant at 15 mL.

2.5.1.2 Preparative Mode

The preparative mode of IC operation requires the entire sample volume to be pumped onto the analytical column. Due to autosampler instrumentation the sample volume pumped onto the column typically ranged between 11.00-11.02 mL. The preparative mode of IC operation is exactly the same as the analytical mode where chloride, nitrate, nitrite and sulfate are separated based on their affinity for the column resin. The mobile phase conductance is suppressed and the anions are eluded from the column to the conductivity detector for detection. In the preparative mode, the main difference is the addition of the fraction collector. Instead of anions going to waste after detection in Position 2 (Figure 27), the anions are sent to a fraction collector to collect and isolate individual anions.

The fraction collector (Spectrum Chromatography, CF-1) is interfaced with the PeakSimple software to direct the sample anions into individual collection vials. The sample travels from the conductivity detector to the fraction collector via 36'' x 1/6'' OD Teflon tubing. The fraction collector is design to collect 174 individual sample fractions in 5 mL (VWR polypropylene) vials. The fraction collector operates using timed collection

windows based on the retention time (peak) of the anions or the time it takes for anions to elude from the column and undergo complete detection.

A fraction collection window for each anion retention time is programmed into the collector's interface or is initiated by anion conductance through its peak detection capability. The windows are programmed using two collection modes: collect and skip. The collect mode actuates a 3-way control valve to direct sample flow from waste into collection vials to separate and collect respective anion peaks. Whenever the fraction collector is not in collect mode it remains idle in skip mode. The skip mode actuates the 3-way control valve to direct sample flow to the waste container.

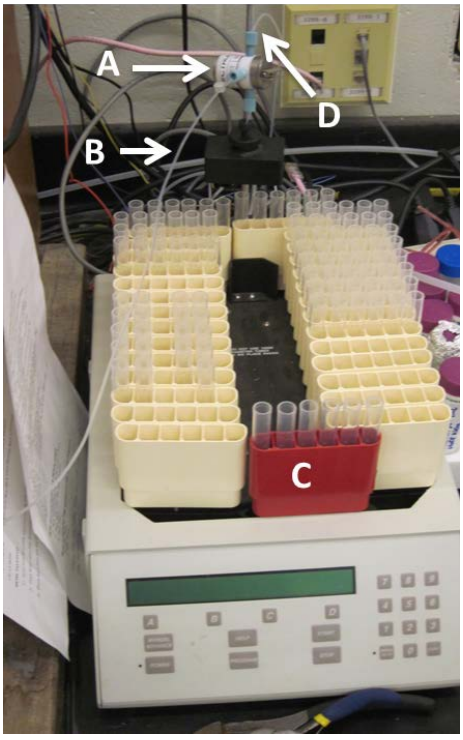

Figure 27 The Spectrum Chromatography CF-1 fraction collector. A) 3-port control valve, B) Teflon tube sample inlet, C) vial cartridge and vials, and D) Teflon tube waste outlet.

The fraction collector was operated using time-based collection windows, programmed through the fraction collector interface. Known standards of Cl^-, NO_3^-, and SO_4^{2-} bracketing the (High, Medium, and Low) filter divisions (Figure 26) were ran through the IC to determine retention times and the time based windows were programmed accordingly. For example, the nitrate peak has a collection window between 24 minutes and 26 minutes which corresponds to its retention time. The fraction collector will initiate collect mode during this time and after collection advance the collection cartridge to the next vial.

The fraction collector also includes a delay time that is programmed into the interface. The delay time is the time it takes for the anion solution to flow from the conductivity detector to the 3-way control valve via Teflon tubing. The fraction collector delay time is set before each anion collection window to ensure efficient peak separation and is determined using the following expression:

$$\text{Time}_{(\text{delay})} = 5.07 \times ID^2 \times (L/f) \qquad \text{Eq. 2.6}$$

Where the constant 5.07 is a conversion factor converting inches to cm, ID is the tubing inner diameter (in.), L is the tube length (cm) and f is the mobile phase pump flow rate (mL/min).

The fraction collector has the capacity to hold 174 vials but the collection window size may limit the number of samples that can be separated and anions isolated. Each collection cartridge has the capacity to hold 6 (5 mL) vials in case the collection windows may exceed the time it takes to fill a 5 mL fraction. Therefore, the fraction size is programmed to 250 drops per vial to prevent loss of anion fractions. For example, the

collection window for sulfate lasts 3 minutes, subsequently consuming two 5 mL vials at 250 drop per vial. The sulfate anion is also eluded late from the column causing an empty vial after collection of the nitrate fraction. As a result, only 27 samples can be placed on the IC for preparative analysis. In addition, when running samples there is always a risk of missed fractions due to closely spaced collection windows.

Despite these potential drawbacks, the sample pump and mobile phase pump rates remain constant over several days of analysis so that the anion elution times also remain consistent unless another column is introduced or significant contamination of the analytical column occurs. Therefore, the preparation mode is reliable across multiple sample runs over several days and provides a relatively convenient and efficient method to collect and isolate anions from aerosol solutions.

Table 4 PeakSimple Analytical and Preparative Timed Events

Event	**Time (minutes)**	**Purpose**
6-Port Control Valve Switch	0.01	Position 1 – sample directed onto column
Fraction Collector On	0.01	Power on fraction collector
Sample Pump On	0.05	Begin pumping sample onto column
Fraction Collector Off	0.08	Close relay contact closure. Fraction collector remains on
Sample Pump Off	12.333	Stop pumping sample onto column
Autosampler On	12.433	Move autosampler needle from sample to rinse container
Autosampler Off	12.453	Turn off autosampler and needle stays in rinse container
Sample Pump On	12.543	Begin pumping from rinse container
Sample Pump Off	17.043	Stop pumping from rinse container
Autosampler On	17.143	Move autosampler needle from rinse container to sample
Autosampler Off	17.163	Turn off autsampler and needle stays in next sample
6-Port Control Valve Switch	17.543	Position 2 – mobile phase elutes column to detector
ZERO	41.00	Conductivity detection set to zero

2.5.1.3 Collection Efficiency and Isotopic Integrity

The analytical and preparative IC operations were tested to ensure isotopic integrity and fraction collection efficiency from the aerosol solution. The fraction collection efficiency test is conducted to determine if the measured anions were properly separated and eluded off the analytical column and collected in the fraction collector. The isotopic integrity test is conducted to determine if isotopic fractionation

occurred during the separation and collection processes. To determine the collection efficiency and isotopic integrity, a lab calibrated isotopic working standard of Hoffman nitrate (Hi-Yield Nitrate of Soda Chilean fertilizer) was mixed into solution and ran through the IC in both the analytical and preparative modes. A bulk Hoffman solution was mixed containing 50 ppm of Hoffman nitrate in 1 L and serial diluted ($M_1V_1=M_2V_2$) to make 1 ppm of Hoffman nitrate in 1 L..

Twelve aliquots of 15 mL Hoffman solution were pipetted from the 1 ppm Hoffman into 15 mL sterile centrifuge tubes to mimic sample solutions and ran through the IC. The ppm value is equivalent to µg/mL, so the nMol of nitrate [NO_3^-] collected in each 5 mL fraction vial was determined by using the following expression:

$$[NO_3^-] = [A] * 1/MW * \Delta V \qquad \text{Eq. 2.5}$$

Where [A] is the concentration of nitrate in µg/mL, MW is the molecular weight of nitrate (µg/nMol), and ΔV is the sample volume (mL) pumped onto the IC. From Eq. 2.5 it was determined that each 5 mL vial contained 177 nMol of nitrate, roughly twice the estimated average nitrate composition for tribal $PM_{2.5}$ filters.

The isolated nitrate fractions were then collected and every 3 fractions decanted into a sterile 15 mL centrifuge tube to yield four, 531 nMol nitrate composites, enough for isotopic analysis using the bacterial denitrifier technique. Since ($PM_{2.5}$) aerosol sample solutions are estimated to have very low amounts of nitrate, the 4 nitrate composites were also used to mimic the decanting method to produce monthly composites of nitrate. The nitrate composites were placed into a Savant centrifugal evaporator (SpeedVac SC200) connected to an external Labconco freeze dryer system

(Freeze dryer 4.5) and freeze dried. The freeze dryer system operates at -40°C with a vacuum pressure of <100 microns Hg (13.33 kPa). The centrifuge operates at 1000 rpm to concentrate the nitrate which was then rehydrated to 1mL for isotopic analysis.

The recovered composites of Hoffman nitrate were analyzed using the denitrifier method (Sigman et al., 2001; Casciotti et al., 2002) for $\delta^{15}N$, $\delta^{18}O$, and $\Delta^{17}O$ values. The average isotope values for the (4) collected NO_3^- composites were compared to the average isotope values from (4) replicates of the Hoffman isotopic working standard calibrated to VSMOW and atmospheric air N_2. (Table 5).

Table 5 Hoffman standard compared to collected NO_3^- (n = 4)

	Standard Isotope Measurement			Value from NO_3^- Fraction		
	^{15}N	^{18}O	$\Delta^{17}O$	^{15}N	^{18}O	$\Delta^{17}O$
Mean:	1.7	61.2	21.9	1.2	60.6	21.1
St. Dev:	0.3	0.2	0.5	0.6	1.2	0.4

The four replicates of the Hoffman standard each contained 500 nMol of nitrate and showed an average value of 1.7‰ for $\delta^{15}N$, 61.2‰ for $\delta^{18}O$, and 21.9‰ for $\Delta^{17}O$. The nitrate composites showed an average value of 1.2‰ for $\delta^{15}N$, 60.6‰ for $\delta^{18}O$, and 21.1‰ for $\Delta^{17}O$. There is good agreement between the bulk Hoffman standard and that of the collected nitrate fraction. Therefore, the test indicates no significant fractionation occurring during the separation and collection processes. Furthermore, the test indicates the column effectively eluded the anions and the fraction collector successfully isolated the nitrate anion.

2.5.2 PM_{10} Ion Chromatography Instrumentation

The PM_{10} aerosol solutions were analyzed using a standard analytical IC instrument (Dionex-Thermo Scientific Inc.) located in Purdue's Civil Engineering laboratory. The analytical IC operation employs the HPLC technique and uses only a portion of the aerosol sample to determine anion concentrations. Preparative analysis was not conducted on the PM_{10} aerosol solutions since NO_2^- anions were not detected and each sample solution contained adequate amounts of nitrate for isotopic analysis. The analytical IC is composed of: one mobile phase pump, one anion self-regenerating suppressor coupled with a detection stabilizer, one analytical separation column, one guard column, one conductivity detector, one pressurized nitrogen tank, a 6-port control valve, and an autosampler. The IC instrument is coupled with a microprocessor and PeakNet chromatography software to remotely control instrumentation.

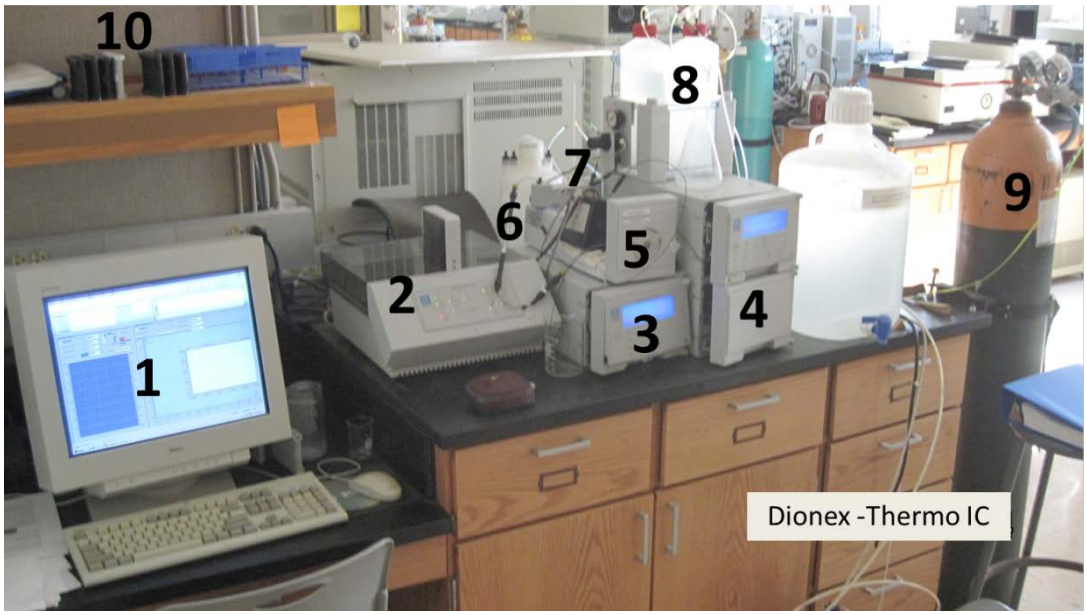

Figure 28 Purdue Civil Engineering Lab HPLC instrumentation. The IC is composed of: 1) PeakNet chromatography software, 2) autosampler, 3) conductivity detector, 4) mobile phase pump , 5) 6-port control valve, 6) analytical and guard column, 7) suppressor and detection stabilizer, 9) nitrogen tank, 9) sample vial cartridges.

The autosampler (Dionex AS40) currently has the capacity to hold forty two, 5 mL sample vials or eighty, 0.5 mL sample vials (Thermo Scientific Polyvials). For PM_{10} anion analysis, 0.5 mL of the 50 mL aerosol solutions were pipetted (Fisherbrand Finnpippette® II, 100-1000 µL) into 0.5 mL sample vials which were cleaned using an aseptic technique. The sample vials were then filter capped (Thermo Scientific 0.20 µm filter caps) and placed into sample vial cartridges and loaded onto the autosampler. The autosampler is equipped with a positive displacement piston which plunges into each sample vial against a backpressure of up to 600 kPa (100 psi) to deliver and load the sample into a 25 µL analytical loop without the need of an external sample pump. The PeakNet software actuates the 6-port valve from load position into detect position and

the 25 µL sample is injected into the mobile phase and sent into a single guard column (4mm Dionex IonPac AG11) to remove organic particulate matter. The sample is then pumped onto the analytical column (4mm Dionex IonPac AS11), where the anions are separated based on their affinity for the column resin.

The mobile phase pump is a dual-head pump (Dionex GP40 Gradient Pump) with a flow rate of 1 mL/min and the mobile phase solution is a 2.5 mM of $NaHCO_3$ and Na_2CO_3 in 2 L. The mobile phase elutes the anions off the column into an anion self-regenerating suppressor (Dionex 4mm ASRS 300) and detection stabilizer (Dionex DS3-1), where electrolysis is applied to suppress mobile phase conductivity. The suppressor's micro-membrane then exchanges the H^+ created during electrolysis for Na^+ in the eluent, where the $NaHCO_3/Na_2CO_3$ is converted into H_2O and CO_2. The micro-membrane suppressor reduces the background conductivity of the mobile phase down to <0 microseimens (µS), so that only the electric conductance of each anion is measured by the conductivity detector (Dionex CD20 Conductivity Detector).

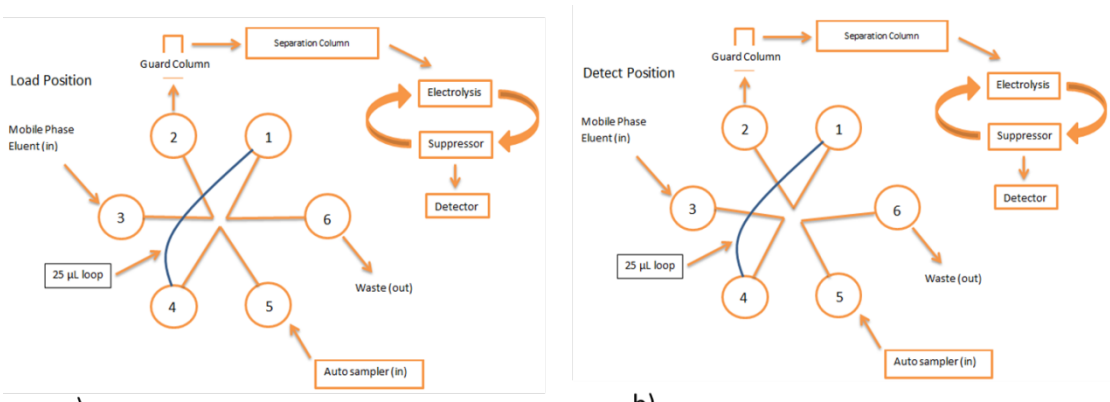

Figure 29 Schematic of the 6-port control valve positions and IC instrumentation

The conductivity detector measures the conductivity of each anion and conductance is displayed on the detector's front panel in microseimens (µS) and integrated by the PeakNet chromatograph software as a peak area. The very same analytical IC method used to determine anion concentrations in $PM_{2.5}$ aerosol solutions was applied to PM_{10} IC analysis (Reference Chapter 2, Section 2.5.1). Except, the only major difference between the two methods is in regards to the sample volume pumped into the IC. Since the sample volume loop remained constant at 25 µL, there was no need to record sample volumes in order to normalize peak areas.

PM_{10} filters were separated into two divisions (High and Low) based on estimated nitrate composition (Eq. 2.1-2.3). Calibration standards were mixed to produce calibration linearity curves to bracket each (High and Low) division of estimated nitrate composition in order to determine anion concentrations.

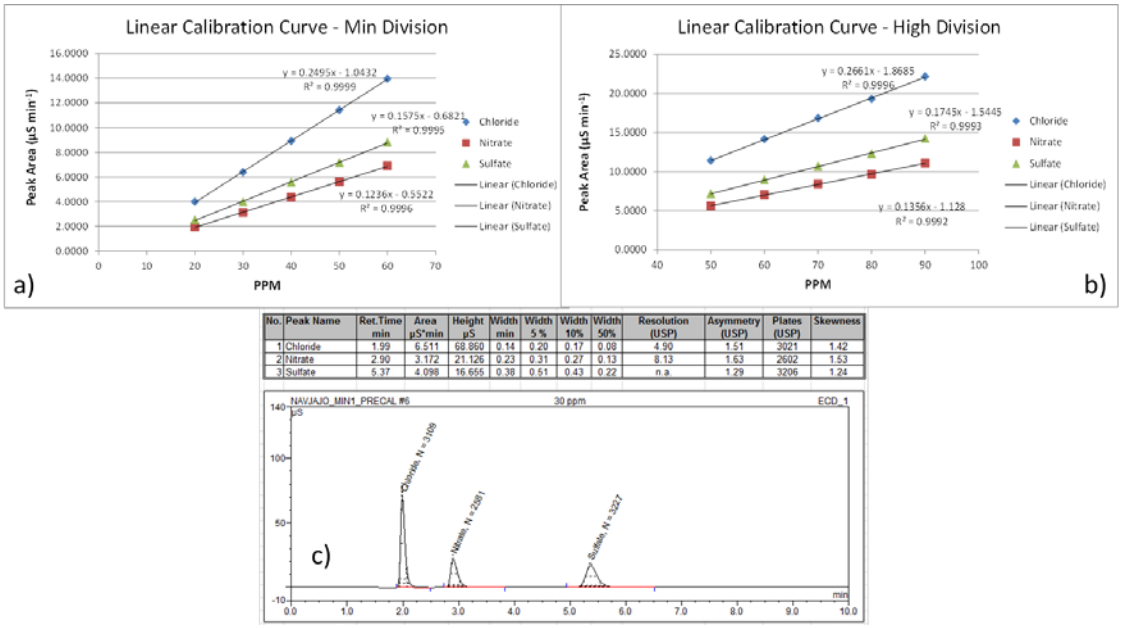

Figure 30 Linear calibration curves for $PM_{2.5}$ filter divisions. a) Low division, b) High division and c) PeakNet anion chromatograph

Replicates of known standards (Cl^-, NO_3^-, SO_4^{2-}) ranging between 1 ppb to 70 ppm were measured on the IC to determine the overall range of uncertainty (detection limit) and % error of the IC instrument. The IC yielded a 1.6% error with a ±1 ppm (±1 µg/mL) range of uncertainty (detection limit) for the measured anions.

The measured anion concentrations were then scaled back into µg/m^3 using air sampler parameters and applying Eq. 2.5. The nitrate concentration is used to determine the volume (mL) needed from each 50 mL aerosol solution to produce 500 nMol NO_3^- for isotopic analysis using the following expressions:

$$B = [A] * 1/MW \qquad \text{Eq. 2.5}$$

$$V = 500\ nMol * 1/B \qquad \text{Eq. 2.6}$$

Where [A] is the concentration of nitrate in µg/mL, MW is the molecular weight of nitrate (µg/nMol), B is nMol NO_3^-/mL and V is the volume (mL) needed to make 500 nMol NO_3^-. Each volume (V) of aerosol solution was then placed into a Savant centrifugal evaporator connected to an external Labconco freeze dryer system and freeze dried. The centrifugal evaporator and freeze drier system concentrate the nitrate which was then rehydrated to 1mL for isotopic analysis. The main drawback in preparing nitrate for isotopic analysis using this technique is the possible introduction of nitrite into the bacterial reduction method. This nitrate preparation technique was applicable since nitrite was not observed in any of the chromatographs for tribal PM_{10} aerosol solutions. As mentioned, depending on the analytical method, oxygen isotope analysis of nitrate in the presence of nitrite or sulfate can interfere with oxygen isotope values.

The analytical IC instrument is a fast and effective way of determining anion concentrations in aerosol solutions. Running a single sample through the IC takes 10 minutes.

CHAPTER 3. OBSERVATIONS OF ^{15}N, ^{18}O, AND $\Delta^{17}O$ IN ATMOSPHERIC NITRATE

3.1 Technical Note

Due to unforeseen freeze dryer system malfunction, $PM_{2.5}$ nitrate did not undergo isotopic analysis. Particulate matter anions in both the coarse and fine aerosol filters were measured using the analytical and preparative IC methods described in Chapter 2. The aerosol anions and measured $\delta^{15}N$, $\delta^{18}O$, and $\Delta^{17}O$ of nitrate in PM_{10} collected from the Navajo Nation and Southern Ute Indian Reservation will be discussed in this chapter.

3.2 Isotope Analysis of NO_3^- using the Denitrifier Technique

The δ total isotopic composition of nitrate in PM_{10} was carried out using the "denitrifier technique" (Sigman et al., 2001; Kaiser et al., 2007). The nitrate was added to a solution containing *Pseudomonas aureofaciens*, a denitrifying bacteria that converts NO_3^- into gaseous N_2O (Casciotti et al., 2002). Bacteria solutions were placed in 12 mL glass screw top septum vials (LabCo) and purged with helium at 40 mL/min prior to introduction of nitrate sample. Each sample contained ~500 nMol of nitrate and were incubated in bacteria solution for 2 hours. The N_2O was collected using a headspace extraction device and gas chromatography before being passed over a gold reaction tube where the N_2O was converted into N_2 and O_2. After thermal decomposition, the

product N_2 and O_2 was then directed into a continuous flow isotope ratio mass spectrometer (Thermo Delta V) to determine the $\delta^{15}N$, $\delta^{18}O$, and $\Delta^{17}O$ values of the original nitrate with a precision of ±0.7, 0.4, and 0.6 ‰, respectively. Lab calibrated isotopic working standards (Hoffman-20, NC32, Hoffman-10, and Antarctic) were used to obtain linear calibrations which were then used to correct sample peak areas and determined measured results

3.3 Results

3.3.1 Navajo Nation – Nazlini Study Area

Particulate matter ($PM_{2.5}$ and PM_{10}) were collected from the Nazlini monitoring site on the Navajo reservation (Apache County, AZ). Nazlini is a semi-arid region of the Colorado Plateau located in northwestern Arizona (35.88 °W, -109.43 °N). The Nazlini site elevation is 1,902 m ASL and is located near the Nazlini community (pop: 489; US Census 2010), on the Defiance Plateau and sited by NNAQCP to represent air quality conditions at a general/background location. Prevailing winds at Nazlini blow from the south to the north, with 30.8% of the wind speeds between 3 – 6 m/s (Figure 31).

Over the coarse of a year, daily mean temperatures range from -13°C – 28°C, with a daily mean summer temperature of 21.4°C and winter temperature of -1.9°C. $PM_{2.5}$ concentrations have been 10% of the NAAQS (35 $\mu g/m^3$) with no violations since monitoring began in 2008. $PM_{2.5}$ was collected for a 1-year period beginning June 2009 and ending June 2010. PM_{10} was collected for a 1-year period beginning January 2006

and ending December 2006. Only PM and meteorological parameters are monitored at the Nazlini site, therefore trace gas monitoring was not observed for the Nazlini site.

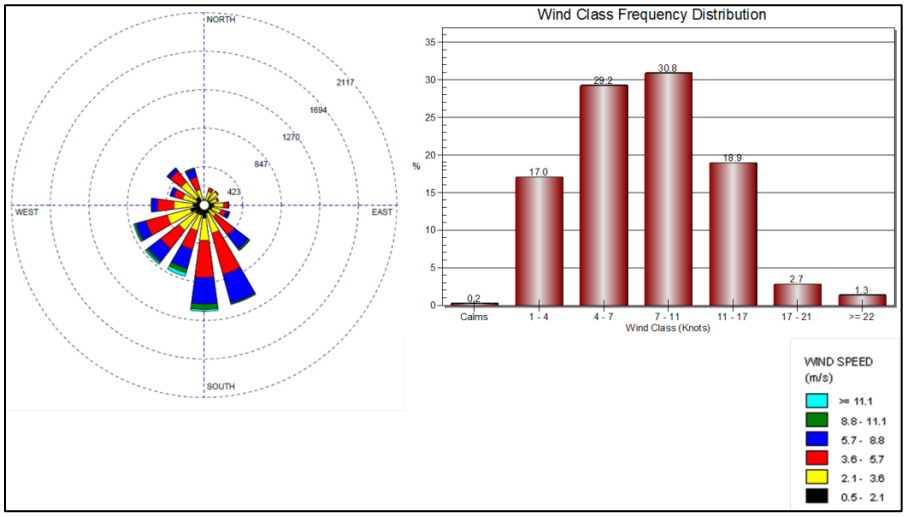

Figure 31 Navajo Nation – Nazlini annual wind rose. The wind rose depicts frequency of occurrence of winds using wind direction sectors (blowing to site) and wind speed classes measured at 10 m.

3.3.1.1 Navajo Nation Seasonal Particulate Matter and Nitrate

Both coarse and fine particulate matter mass exhibited a seasonal trend. The measured $PM_{2.5}$ mass concentration (hereafter denoted $PM_{2.5\ [mass]}$) at the Nazlini site had a mean of 3.5 µg/m^3 for the year with seasonal mean concentrations higher in the summer and fall ($PM_{2.5}$ = 4.1 µg/m^3) compared to spring and winter ($PM_{2.5}$ = 2.8 µg/m^3). $PM_{10\ [mass]}$ had an annual mean of 15 µg/m^3 with higher seasonal mean concentrations in the fall and winter (PM_{10} = 17.6 µg/m^3) compared to spring and summer (PM_{10} = 13 µg/m^3). Both $PM_{2.5\ [mass]}$ and $PM_{10\ [mass]}$ displayed a bimodal distribution (Figure 32 and 34) with profound $PM_{2.5\ [mass]}$ peak in April (15.4 µg/m^3) and two high $PM_{10\ [mass]}$ peaks in April (46.8 µg/m^3) and November (58.1 µg/m^3).

Measured $PM_{2.5}$ nitrate concentrations (hereafter denoted $PM_{2.5\ [NO3]}$) had a mean of 0.12 μg/m^3. $PM_{2.5\ [NO3]}$ had higher seasonal mean concentrations in the spring and summer ($PM_{2.5}$ = 0.14 μg/m^3) compared to fall and winter ($PM_{2.5}$ = 0.10 μg/m^3) (Figure 33). Profound $PM_{2.5\ [NO3]}$ peaks were observed in January (0.59 μg/m^3), April (0.37 μg/m^3) and May (0.38 μg/m^3). Nitrate in PM_{10} (hereafter denoted $PM_{10\ [NO3]}$) had a mean concentration of 0.70 μg/m^3 with higher concentrations in the fall and summer (0.9 μg/m^3) compared to spring and winter (0.5 μg/m^3) (Figure 34). The fraction of Nazlini $PM_{2.5\ [NO3]}/PM_{2.5\ [mass]}$ ranged from 1.1% – 18% with a mean of 3.8% and the fraction of $PM_{10\ [NO3]}/PM_{10\ [mass]}$ ranged from 0.9% – 22% with a mean of 6.8%.

Table 6 Navajo Nation, Nazlini – Seasonal Mean PM Nitrate

	*$PM_{2.5\ [NO3]}$ (μg/m^3)	**$PM_{10\ [NO3]}$ (μg/m^3)
Winter	0.09	0.4
Spring	**0.15**	0.6
Summer	**0.13**	**1.0**
Fall	0.10	**0.8**

*$PM_{2.5}$ collected June 2009 thru June 2010
**PM_{10} collected January 2007 thru December 2007
Bold = elevated seasonal mean concentrations

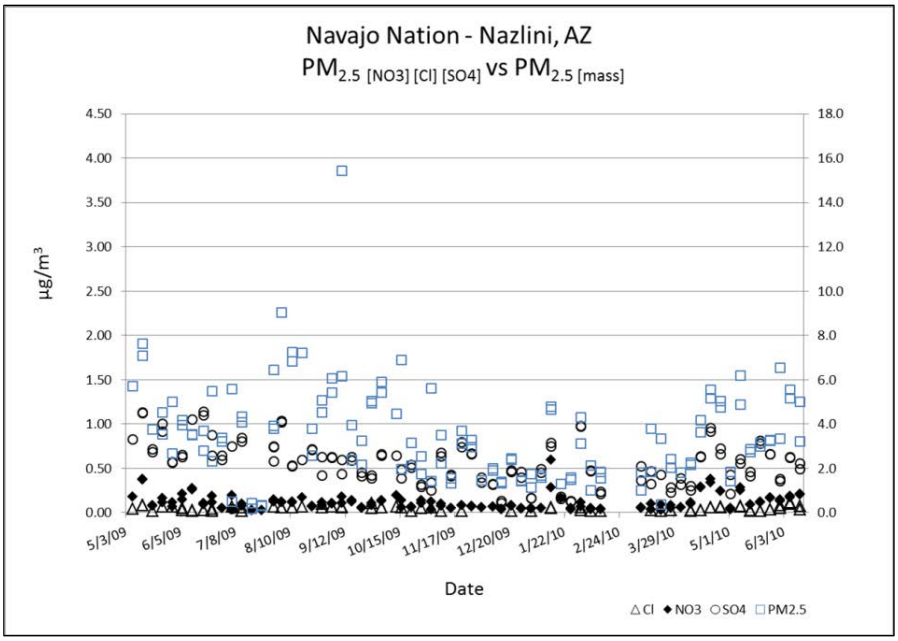

Figure 32 Navajo Nation – Nazlini $PM_{2.5}$ versus anion concentrations. The $PM_{2.5}$ mass (blue rectangles) corresponds to the secondary y-axis.

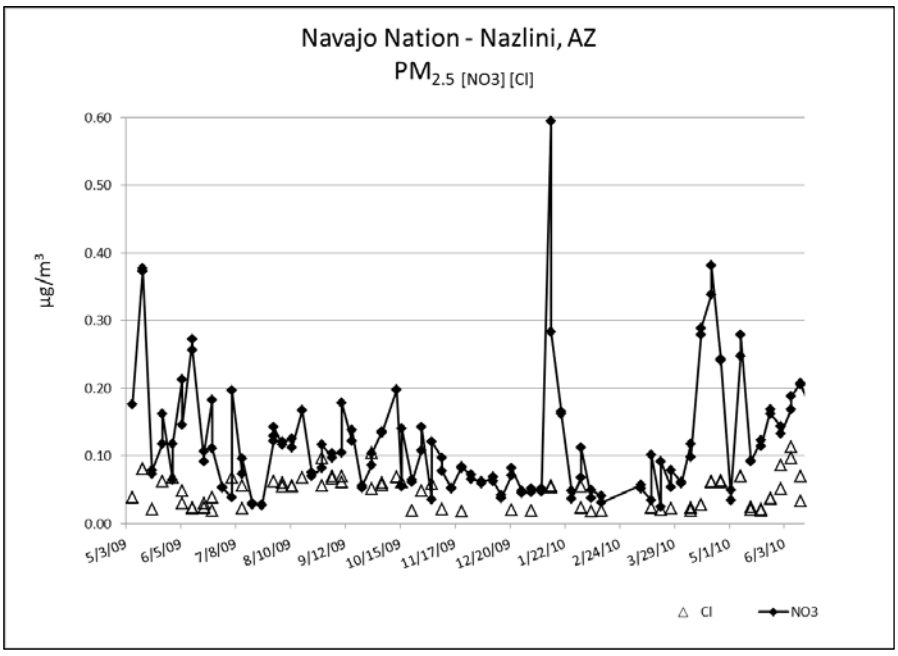

Figure 33 Navajo Nation – Nazlini $PM_{2.5\ [NO3]}$ and $PM_{2.5\ [Cl]}$.

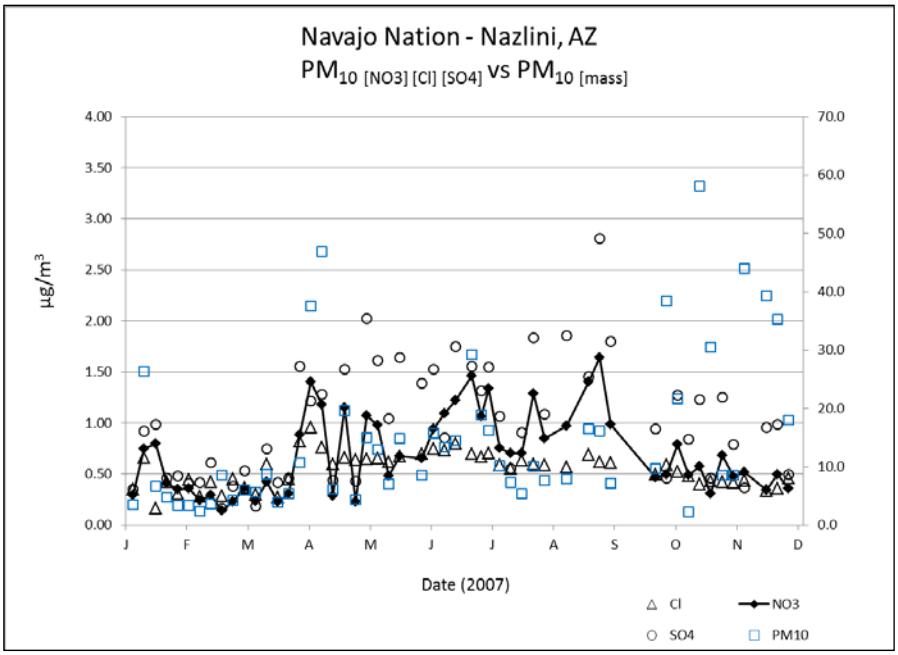

Figure 34 Navajo Nation – Nazlini PM_{10} versus anion concentrations. The $PM_{2.5}$ mass (blue rectangles) corresponds to the secondary y-axis.

3.3.1.2 Navajo Nation $\delta^{15}N$ values of Nitrate in PM_{10}

The $\delta^{15}N$ values of coarse particulate nitrate (PM_{10} nitrate) exhibited a seasonal trend (Figure 35) similar to observed $\delta^{15}N$ values in coarse particulate nitrate collected in Germany and France as well as in rain water collected from the Midwestern and Northeastern United States (Freyer, 1991; Elliot et al., 2007). The measured $\delta^{15}N$ values at Nazlini had a mean of -0.15‰ for the year and indicated elevated values during the winter (-2 – 9.8‰) relative to summer (-4.2 – 1.7‰). The maximum $\delta^{15}N$ values occurred in fall and winter (9.3‰ and 9.8‰) with minimums occurring during the spring and summer (-4.8‰ and -4.2‰), respectively.

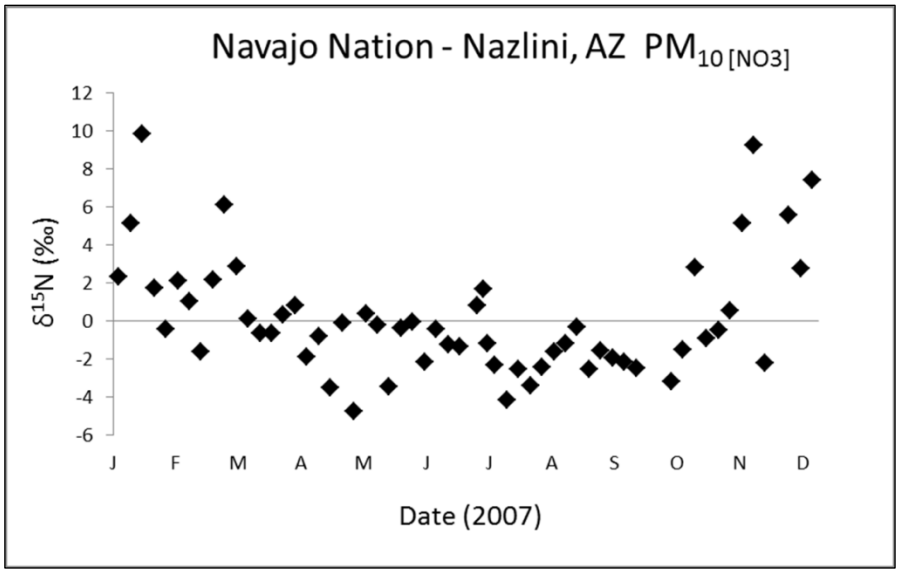

Figure 35 Navajo Nation – Nazlini $\delta^{15}N$ of $PM_{10\ [NO3]}$

Table 7 Navajo Nation, Nazlini – Seasonal Mean of $\delta^{15}N$

Nazlini *$PM_{10\ [NO3]}$	$\delta^{15}N$ (‰)
Winter	**2.8**
Spring	-0.4
Summer	-1.5
Fall	0.1

*PM_{10} collected January 2007 thru December 2007
Bold = elevated seasonal mean concentration

3.3.1.3 Navajo Nation $\delta^{18}O$ and $\Delta^{17}O$ values of Nitrate in PM_{10}

The observed $\delta^{18}O$ values and $\Delta^{17}O$ values measured in of PM_{10} nitrate both exhibited a seasonal trend (Figure 36) similar to observed values in particulate nitrate collected in La Jolla, CA (Michalski et al., 2003). The measured $\delta^{18}O$ values at Nazlini had a mean of 76.4‰ for the year with a large isotopic enrichment relative to VSMOW (57 –

86‰). The $\delta^{18}O$ values were elevated during the summer and spring ($\delta^{18}O$ = 78.1‰) compared to fall and winter ($\delta^{18}O$ = 74.4‰) (Figure 36). The maximum $\delta^{18}O$ values occurred in spring and fall (86‰ and 86.4‰) with minimums occurring during the winter and summer (57.4‰ and 61.7‰), respectively. The measured $\Delta^{17}O$ values at Nazlini had a mean of 29‰ for the year with large ^{17}O excess ranging from 20 to 35‰. Elevated $\Delta^{17}O$ values were observed during the spring and winter ($\Delta^{17}O$ = 30.2‰) compared to summer and fall ($\Delta^{17}O$ = 28‰) (Figure 36). The maximum $\Delta^{17}O$ values occurred in spring and winter (32.8‰ and 34.7‰) with minimums occurring during the winter and summer (20.2‰ and 20.6‰), respectively. The observed $\delta^{18}O$ and $\Delta^{17}O$ of PM_{10} nitrate indicated a mixing line between the isotopic composition of O_2 and H_2O (intercept is $\delta^{18}O$ = 33.3‰, $\Delta^{17}O$ = 0‰), as these two species take part in atmospheric nitrate formation (via NO_x oxidation by HO_2 (RO_2) and N_2O_5 hydrolysis) (Figure 37).

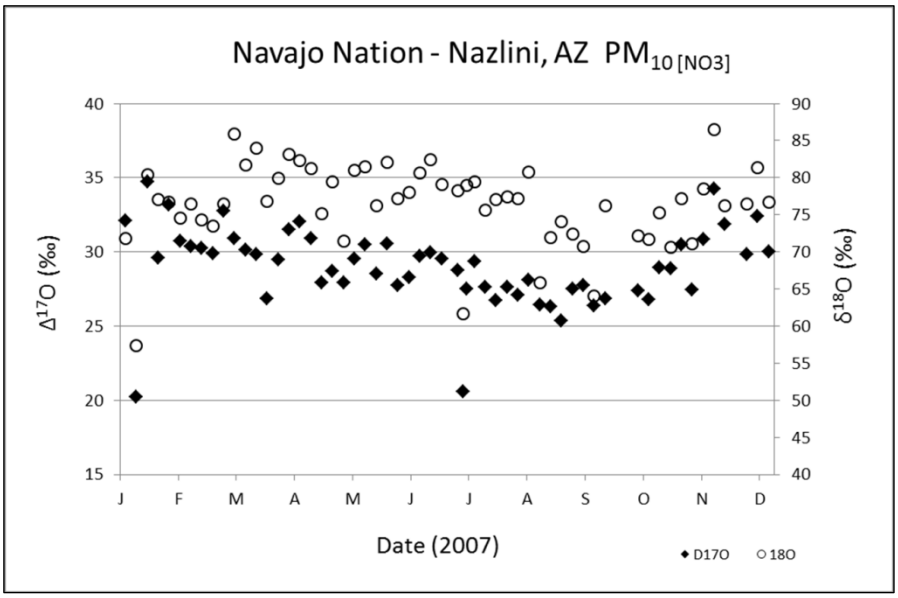

Figure 36 Navajo Nation – Nazlini $\delta^{18}O$ and $\Delta^{17}O$ of $PM_{10\,[NO3]}$

Table 8 Navajo Nation, Nazlini – Seasonal Mean of $\delta^{18}O$ and $\Delta^{17}O$

*$PM_{10\ [NO3]}$	$\delta^{18}O$ (‰)	$\Delta^{17}O$ (‰)
Winter	74.8	**30.4**
Spring	**79.9**	**29.9**
Summer	**76.3**	27.6
Fall	73.9	28.4

*PM_{10} collected January 2007 thru December 2007
Bold = elevated seasonal mean concentrations

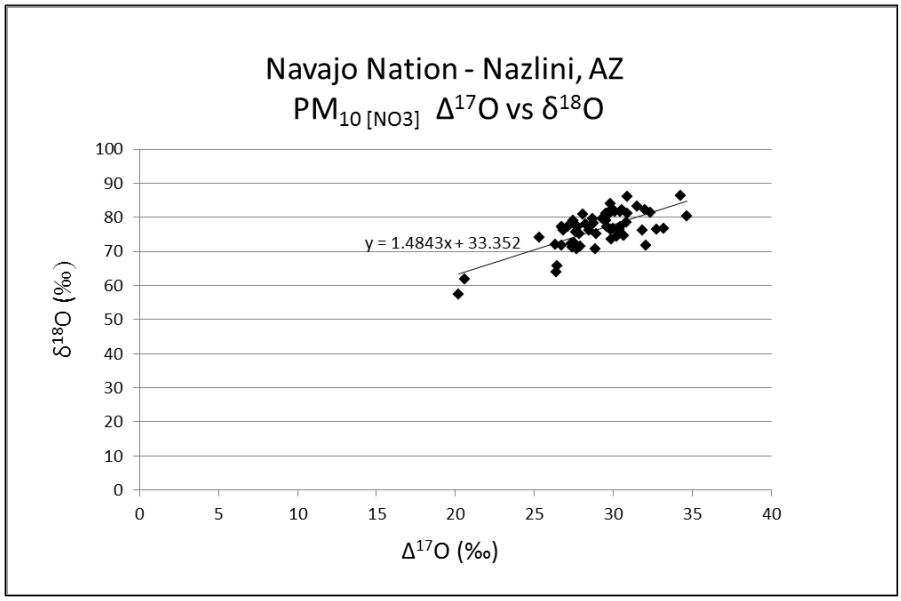

Figure 37 Navajo Nation – Nazlini $PM_{10\ [NO3]}$ $\delta^{18}O$ versus $\Delta^{17}O$ (intercept is $\delta^{18}O$ = 33.3‰, $\Delta^{17}O$ = 0‰).

3.3.2 Southern Ute Indian Tribe – Ute 1 and Ute 3 Study Area

Particulate matter ($PM_{2.5}$ and PM_{10}) were collected from the Ute 3 monitoring station on the Southern Ute Indian Reservation near Bondad, CO (La Plata County), atop the eastern rim of the Animas River Valley (37.10 °N, -107.63 °W). The Ute 3 site is at an elevation of 1,966 m ASL and is located off State Highway 550 and stationed on the Southern Ute Indian Reservation approximately 11 miles south of Durango, CO (pop. 17,200; US Census, 2010) and 25 miles northwest of Farmington, NM (pop. 45,900; US Census, 2010). The Ute 3 area is characterized as primarily an agricultural area, with various surrounding stationary, area, and mobile sources. Two megawatt coal fired power plants are located in northern New Mexico approximately 35 miles to the southwest of Ute 3. Population density and land use maps indicate the Ute 3 area is more densely populated than originally thought, however, the housing is rural with the presence of some oil and gas development. Over the coarse of a year, daily mean temperatures at Ute 3 range from -9.5°C – 25.8°C, with a daily mean summer and daily mean winter temperature of 20.9°C and -1.9°C, respectively. Prevailing winds at Ute 3 blow to the site from NE, with 44.8% of the wind speeds between 0.5 – 2 m/s (Figure 38). Higher velocity winds blow from the SW to the NE.

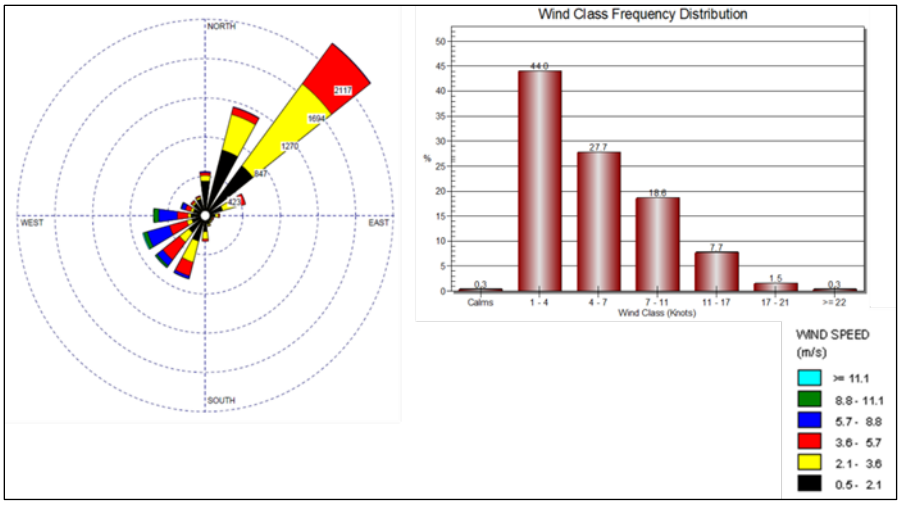

Figure 38 Southern Ute Indian Tribe, Ute 3 annual wind rose. The wind rose depicts frequency of occurrence of winds using wind direction sectors (blowing to site) and wind speed classes measured at 10 m.

Additional $PM_{2.5}$ was collected from the Ute 1 monitoring station, approximately 20 miles east of the Ute 3 site, and located near the population and commercial center of the reservation in Ignacio, CO (pop. 708; US Census 2010). The Ute 1 area is made of the Pine River Valley with the La Plata Mountains and San Juan National Forest to the north. The Ute 1 site is dominated by low-velocity drainage flow winds blowing from the NE to the SW with higher velocity winds blowing to the site from SW (Figure 39). Both Ute 1 and Ute 3 $PM_{2.5\,[mass]}$ have been 12% of the NAAQS (35 µg/m^3) with no violations since monitoring commenced in June of 2009. Currently, the reservation is classified as attainment/ unclassifiable for all criteria pollutants. $PM_{2.5}$ was collected for a 1-year period at Ute 1 and Ute 3 beginning June 2009 and ending June 2010. PM_{10} was collected at the Ute 3 site for a 9 month period beginning January 2006 and ending in

September of 2006. In addition to PM and meteorological monitoring, Ute 1 and Ute 3 stations also monitor the following gaseous parameters: O_3, NO, NO_2, NO_x, and CO. Isotopic analysis was conducted only on PM_{10} filters collected at Ute 3.

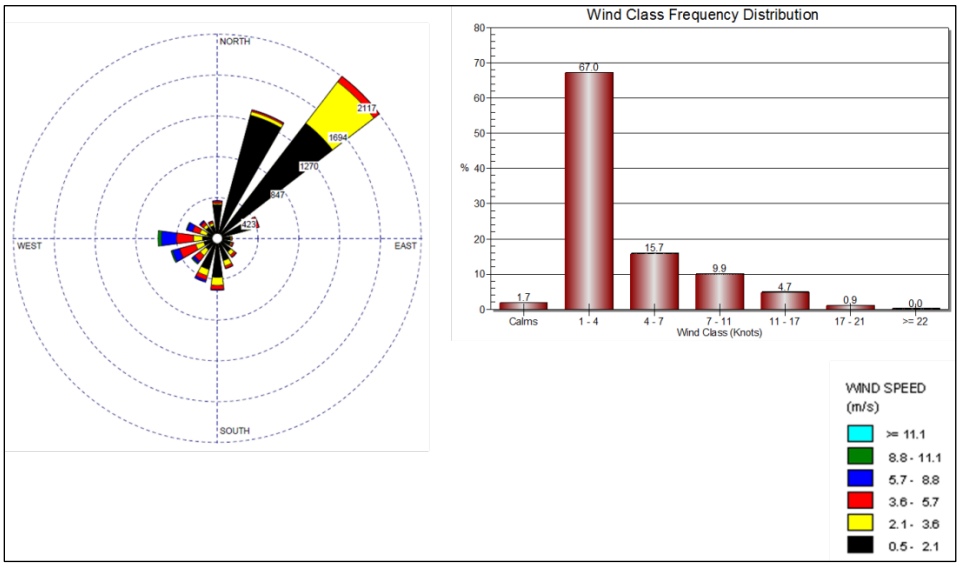

Figure 39 Southern Ute Indian Tribe, Ute 1 annual wind rose. The wind rose depicts frequency of occurrence of winds using wind direction sectors (blowing to site) and wind speed classes measured at 10 m

3.3.2.1 Southern Ute Indian Reservation Seasonal Particulate Matter and Nitrate

The measured $PM_{2.5\ [mass]}$ at the Ute 3 site exhibited a seasonal trend. The $PM_{2.5\ [mass]}$ had a mean of 4.5 µg/m^3 for the year with seasonal mean concentrations higher in the summer and winter ($PM_{2.5}$ = 5.2 µg/m^3) compared to spring and fall ($PM_{2.5}$ = 3.9 µg/m^3). $PM_{2.5\ [mass]}$ displayed a bimodal distribution (Figure 40) with $PM_{2.5\ [mass]}$ peaks in August (11.8 µg/m^3), January (11.1 µg/m^3), and May (11.4 µg/m^3). $PM_{10\ [mass]}$ had a 9 month mean of 10.2 µg/m^3 with high seasonal mean concentrations in the summer and

spring (PM_{10} = 10.6 μg/m^3) compared to the fall and winter (PM_{10} = 9.4 μg/m^3). $PM_{10\ [mass]}$ displayed peaks in April (24 μg/m^3) and May (19 μg/m^3).

$PM_{2.5\ [NO3]}$ had a mean of 0.33 μg/m^3 for the year with seasonal mean concentrations higher in the spring and winter (0.63 μg/m^3) compared to summer and fall (0.069 μg/m^3). Profound $PM_{2.5\ [NO3]}$ peaks were observed beginning in December and ending in March (Figure 40) with maximums occurring in January (3.7 μg/m^3) and February (2 μg/m^3). $PM_{10\ [NO3]}$ had a mean of 0.22 μg/m^3 with higher concentrations in spring and winter (0.27 μg/m^3) compared to summer and fall (0.16 μg/m^3) (Figure 41). The fraction of Ute 3 $PM_{2.5\ [NO3]}/PM_{2.5\ [mass]}$ ranged from 0.7% – 33% with a mean of 5.8% and the fraction of $PM_{10\ [NO3]}/PM_{10\ [mass]}$ ranged from 0.8% – 10.6% with a 9 month mean of 2.5%. Measured NO_x concentrations (year 2006) exhibited seasonal trends at the Ute 3 site with daily average maximums for NO, NO_2 and NO_x occurring during the winter (0.0097 ± 0.002, 0.0214 ± 0.004, 0.0304 ± 0.006 ppmv, respectively).

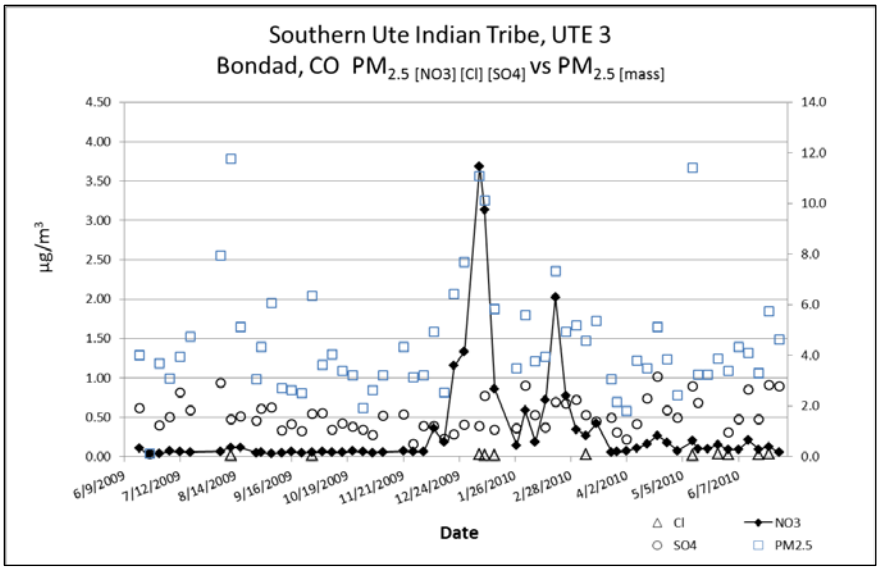

Figure 40 Southern Ute Indian Tribe, Ute 3 $PM_{2.5}$ versus anion concentrations. The $PM_{2.5}$ mass (blue rectangles) corresponds to the secondary y-axis.

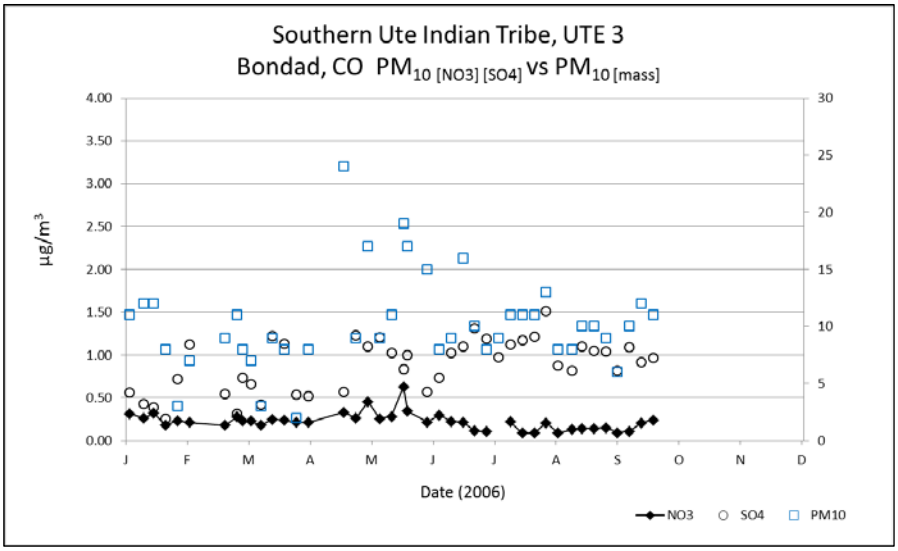

Figure 41 Southern Ute Indian Tribe, Ute 3 PM_{10} versus anion concentrations. The $PM_{2.5}$ mass (blue rectangles) corresponds to the secondary y-axis. Chloride not reported due to detection limit of IC instrument.

Table 9 Southern Ute Indian Tribe – Seasonal Mean PM Nitrate

	Ute 1	Ute 3	
	*$PM_{2.5\ [NO3]}$ ($\mu g/m^3$)	*$PM_{2.5\ [NO3]}$ ($\mu g/m^3$)	**$PM_{10\ [NO3]}$ ($\mu g/m^3$)
Winter	**1.01**	**1.08**	**0.25**
Spring	**0.16**	**0.17**	**0.29**
Summer	0.07	0.08	0.16
Fall	0.06	0.05	0.16

*$PM_{2.5}$ collected June 2009 thru June 2010
**PM_{10} collected January 2006 thru September 2006
Bold = elevated seasonal mean concentrations

The Ute 1 site also exhibited a seasonal trend in $PM_{2.5\ [mass]}$. The $PM_{2.5\ [mass]}$ had a mean of 4.4 $\mu g/m^3$ with higher mean seasonal concentration in the summer and winter ($PM_{2.5}$ = 5.0 $\mu g/m^3$) compared to spring and fall (3.6 $\mu g/m^3$). The Ute 1 site exhibited high $PM_{2.5\ [mass]}$ peaks in August (8.5 $\mu g/m^3$), January (9.7 $\mu g/m^3$), and February (7.8 $\mu g/m^3$). The Ute 1 site $PM_{2.5\ [NO3]}$ had a mean of 0.33 $\mu g/m^3$ with higher concentrations in spring and winter (0.59 $\mu g/m^3$) compared to summer and fall (0.13 $\mu g/m^3$). Similar to Ute 3, profound $PM_{2.5\ [NO3]}$ peaks were observed for Ute 1 beginning in December and ending in March with maximums occurring in January (4.1 $\mu g/m^3$) and February (2 $\mu g/m^3$) (Figure 42). The fraction of Ute 1 $PM_{2.5\ [NO3]}/PM_{2.5\ [mass]}$ ranged from 0.7% – 33% with a mean of 6%. Measured NO_x concentrations had noticeable trends at Ute 1 with daily average maximums for NO, NO_2, and NO_x occurring during the winter (0.01 ± 0.001, 0.023 ± 0.004, 0.042 ± 0.006 ppmv, respectively).

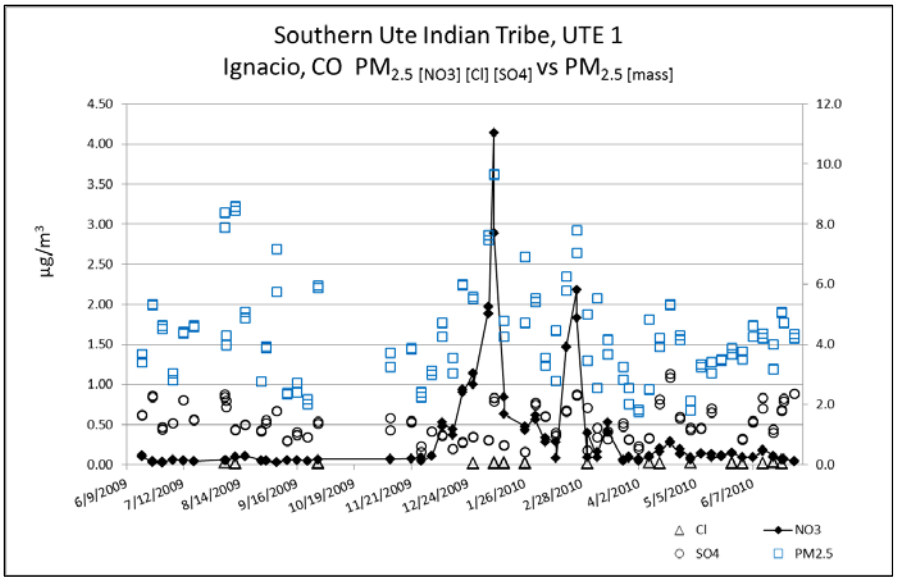

Figure 42 Southern Ute Indian Tribe, Ute 3 $PM_{2.5}$ versus anion concentrations. The $PM_{2.5}$ mass (blue rectangles) corresponds to the secondary y-axis.

3.3.2.2 Southern Ute Indian Tribe $\delta^{15}N$ values of Nitrate in PM_{10}

The $\delta^{15}N$ values in coarse particulate nitrate (PM_{10} nitrate) was not representative of a complete yearly data set as the tribal AQP stopped PM_{10} monitoring in September of 2006. The $\delta^{15}N$ values in PM_{10} nitrate did exhibit a similar trend (Figure 43) to observed $\delta^{15}N$ values in coarse particulate nitrate collected on the Navajo Nation, Germany and rain water collected from the Midwestern and Northeastern United States (Freyer, 1991; Elliot et al., 2007). The measured $\delta^{15}N$ values at Ute 3 had a 9 month mean of 9.4‰ for the year and indicated elevated values during the winter (8.4 – 23.2‰) relative to summer (2.6 – 8.6‰). The maximum $\delta^{15}N$ values occurred in fall and spring (16.1‰ and 23.2‰) with minimums occurring during the summer and spring (2.6‰ and 6.1‰), respectively.

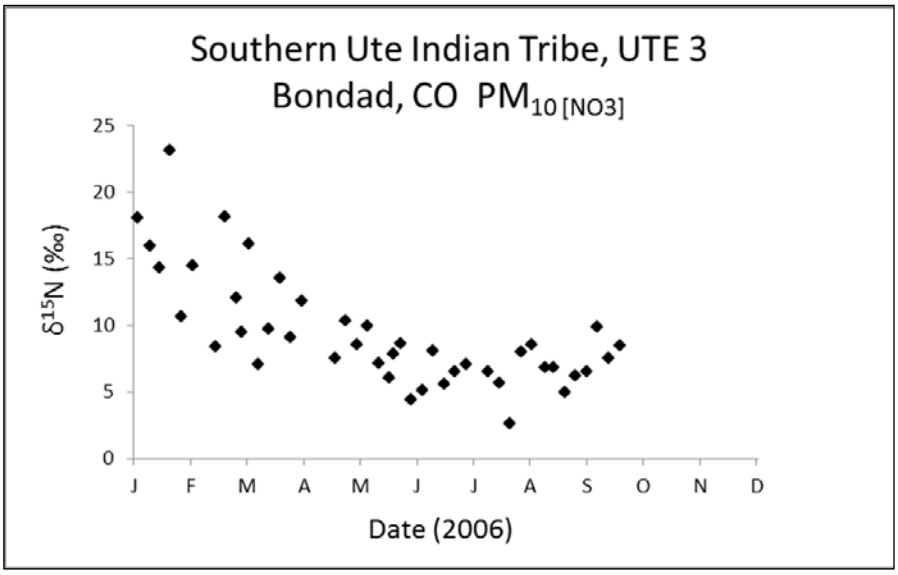

Figure 43 Southern Ute Indian Tribe, Ute 3 $\delta^{15}N$ of $PM_{10\ [NO3]}$

Table 10 Southern Ute Indian Tribe, Ute 3 – Seasonal Mean of $\delta^{15}N$

Ute 3 *$PM_{10\ [NO3]}$	$\delta^{15}N$ (‰)
Winter	**15**
Spring	9.5
Summer	6.2
Fall	7.7

*PM_{10} collected January 2006 thru September 2006
Bold = elevated seasonal mean concentration

3.3.2.3 Southern Ute Indian Tribe $\delta^{18}O$ and $\Delta^{17}O$ values of Nitrate in PM_{10}

The observed $\delta^{18}O$ values and $\Delta^{17}O$ values measured in of PM_{10} nitrate both exhibited a seasonal trend (Figure 44) similar to observed values in particulate nitrate collected in La Jolla, CA (Michalski et al., 2003). The measured $\delta^{18}O$ values at Ute 3 had a 9 month mean of 62.5‰ with a large isotopic enrichment relative to VSMOW (36 – 86‰). The $\delta^{18}O$ values were elevated during the winter and spring ($\delta^{18}O$ = 68.8‰) compared to summer and fall ($\delta^{18}O$ = 55.4‰) (Figure 44). The maximum $\delta^{18}O$ values occurred in spring and winter (72.8‰ and 86.2‰) with minimums occurring during the summer and fall (36.6‰ and 46.3‰), respectively. The observed $\delta^{18}O$ and $\Delta^{17}O$ of PM_{10} nitrate indicated a mixing line between the isotopic composition of O_2 and H_2O (intercept is $\delta^{18}O$ = 9‰, $\Delta^{17}O$ = 0‰), as these two species take part in particulate nitrate formation (via NO_x oxidation by HO_2 (RO_2) and N_2O_5 hydrolysis) (Figure 45).

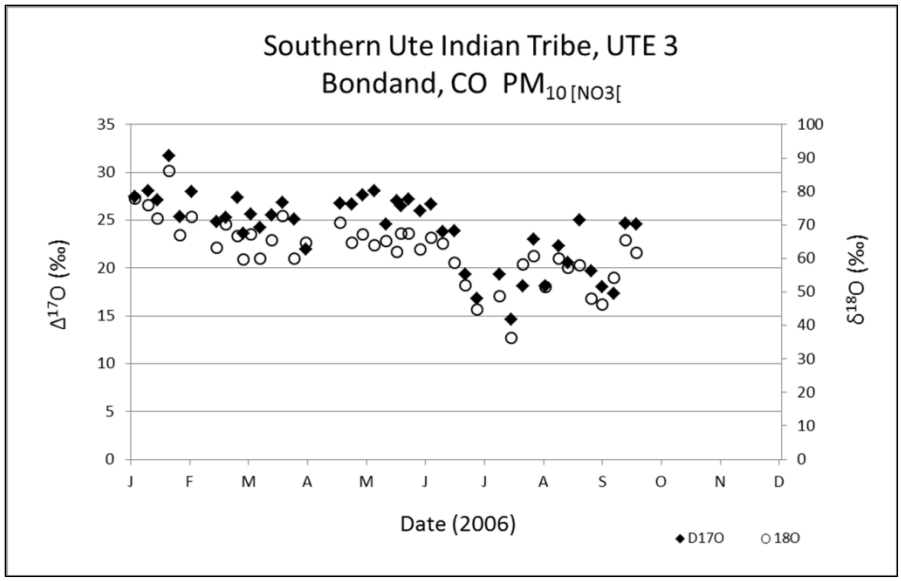

Figure 44 Southern Ute Indian Tribe, Ute 3 $\delta^{18}O$ and $\Delta^{17}O$ of $PM_{10\ [NO3]}$

Table 11 Southern Ute Indian Tribe, Ute 3 – Seasonal Mean of $\delta^{18}O$ and $\Delta^{17}O$

*$PM_{10\ [NO3]}$	$\delta^{18}O$ (‰)	$\Delta^{17}O$ (‰)
Winter	**72.3**	**27.2**
Spring	**65.2**	**25.8**
Summer	55.7	21.3
Fall	46.3	20.8

*PM_{10} collected January 2006 thru September 2006
Bold = elevated seasonal mean concentrations

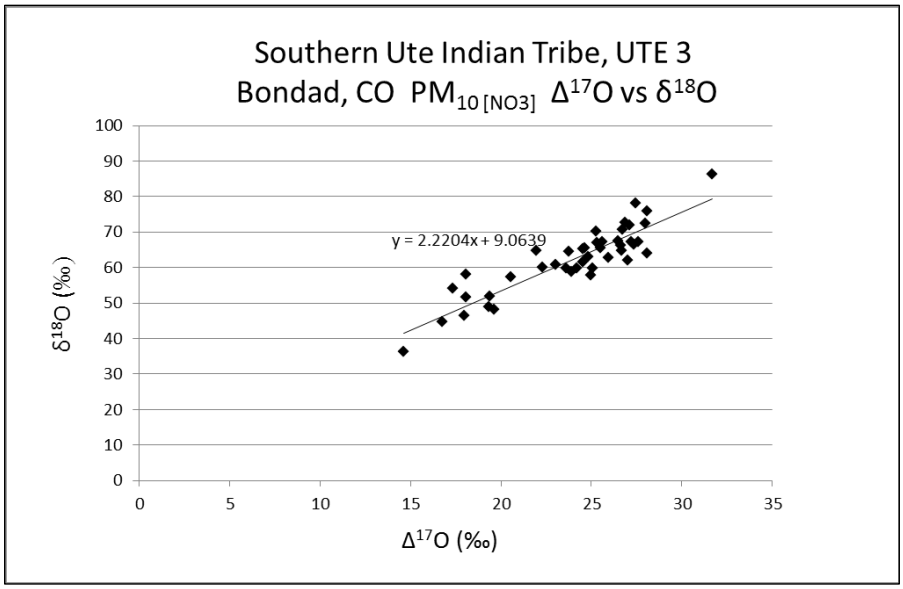

Figure 45 Southern Ute Indian Tribe, Ute 3 $PM_{10\ [NO3]}$ $\delta^{18}O$ versus $\Delta^{17}O$

3.4 Discussion

3.4.1 Comparison of Seasonal Nitrate Concentrations in PM on Tribal Lands

The bimodal distribution of PM mass concentrations and peaks in nitrate concentrations on the Navajo Nation and Southern Ute Indian Reservation are likely linked to seasonal changes in boundary layer height (BLH), NO_x sources, meteorology, photochemistry as well as increases in windblown crustal material. The observed aerosol composition of $PM_{2.5}$ collected from the Colorado Plateau has shown to have large fractions of fine soils and organics relative to other measured species (NARSTO, 2004). These observations are applicable to tribal lands as they encompass the Colorado Plateau and are subject to fugitive dust emissions from agricultural and mining activities. Furthermore, tribal emissions inventories also indicate other impacting sources such as

residential wood burning, prescribed burns, wildland fires, vehicle emissions, oil and gas development and electrical generating units (EGU).

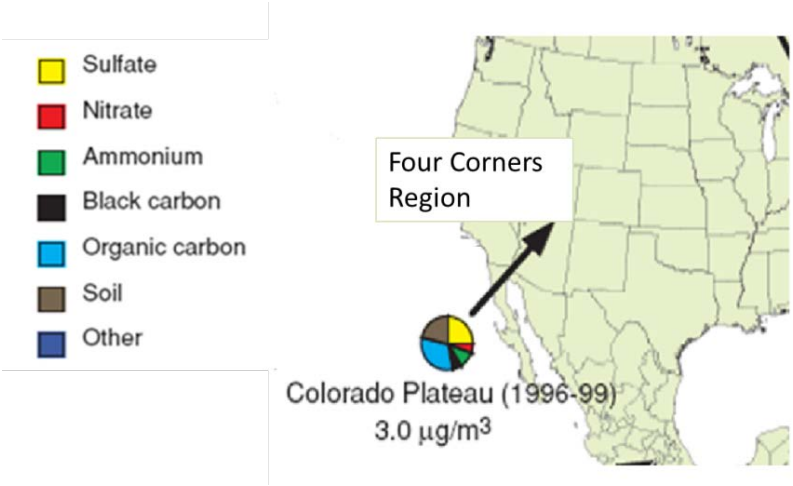

Figure 46 Colorado Plateau $PM_{2.5}$ concentration and chemical composition (NARSTO, 2004).

Elevated concentrations and spikes in fine particulate nitrate concentrations ($PM_{2.5\,[NO3]}$) were observed in the winter and spring months on Southern Ute Indian Reservation. These observed concentrations are likely associated with the nitric acid reaction with ammonia to form sub-micron ammonium nitrate (R1.11). When ammonia neutralizes the acidic components of aerosols it is transferred into the particulate phase and therefore increases in nitrates and sulfates are typically observed (Seinfeld and Pandis, 2006). The elevated $PM_{2.5\,[NO3]}$ during the winter and spring is highly likely since the dynamic equilibrium with ammonia and nitric acid is thermally unstable in which formation favors high RH and low temperature.

Electrical Generating Units or power plant emissions attributing to the observed spikes in $PM_{2.5\,[NO3]}$ seemed insignificant as there were no corresponding observed

spikes in fine particulate sulfate ($PM_{2.5\ [SO4]}$). $PM_{2.5\ [SO4]}$ at Ute 1 and Ute 3 remained constant throughout the year with mean concentrations of 0.52 µg/m^3, respectively. Furthermore, atmospheric mixing heights tend to be lower during the nighttime (Seinfeld and Pandis, 2006), yielding a much smaller boundary layer volume during the winter. A lower BLH combined with winter inversions allows local NO_x emission sources to have a greater impact on nitrate concentrations. In addition, winter wind roses for Ute 1 and Ute 3 indicate a higher frequency of low velocity winds blowing in from the northeast, opposite of major NO_x emission sources in the Four Corners.

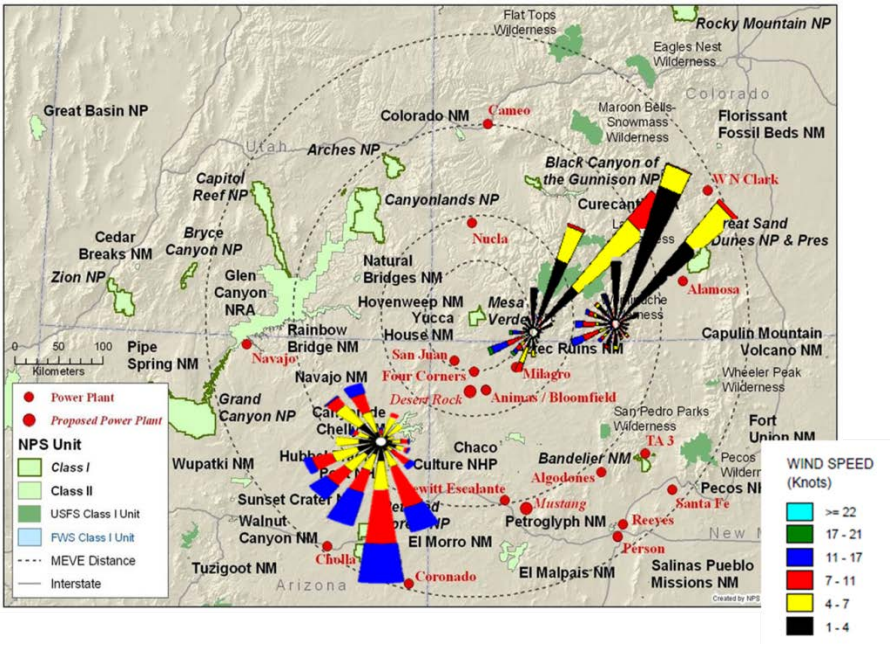

Figure 47 Winter wind roses for Ute 1 and Ute 3 (CO) and Nazlini (AZ). Map depicts proximity to power plants and protected CAA Class I and Class II air sheds.

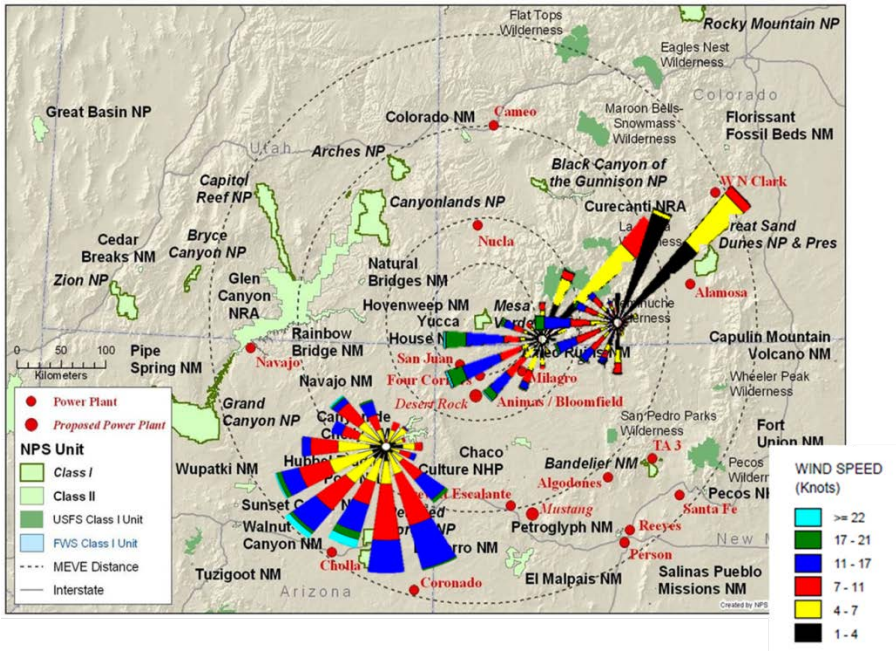

Figure 48 Spring wind roses for Ute 1 and Ute 3 (CO) and Nazlini (AZ).

Increases in carbon monoxide and nitrogen dioxide concentrations were also observed during the winter months on the Southern Ute Indian Reservation (Figure 49). Therefore it was determined that the spikes in winter $PM_{2.5\ [NO3]}$ were affected by seasonal changes in BLH and contributions from local activity such as automobile traffic and residential wood burning. These sources are likely contributors to winter and spring $PM_{2.5\ [NO3]}$ measured at the Ute 1 and Ute 3 monitoring sites.

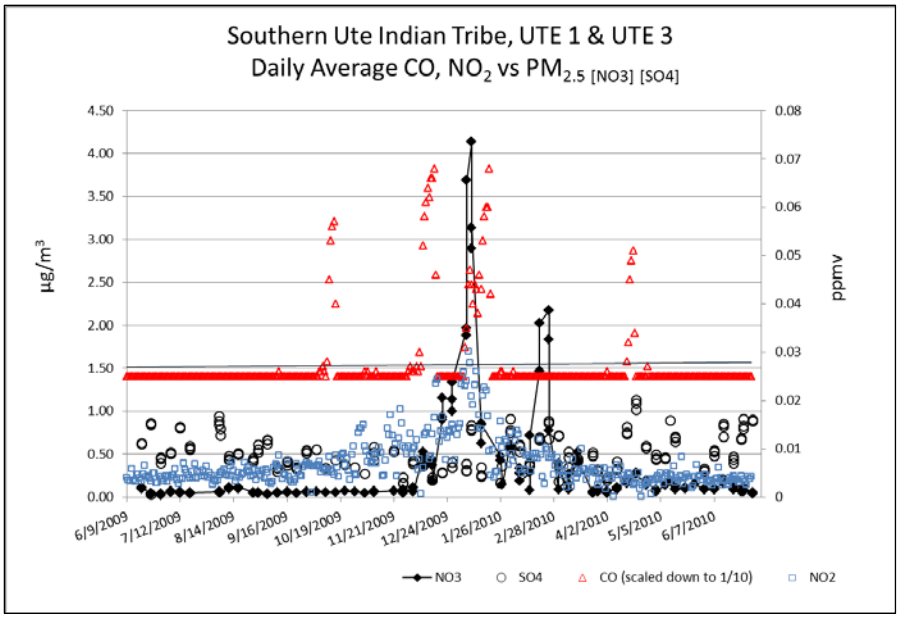

Figure 49 Southern Ute Indian Tribe CO, NO_2 and $PM_{2.5}$ anion concentrations.

The Navajo Nation Nazlini site also indicated profound $PM_{2.5\ [NO3]}$ spikes in winter and spring. No trace gas data was reported for the Nazlini area during these seasons but similar inferences can be applied regarding nitric acid reactions with ammonia to form ammonium nitrates. On the other hand, Nazlini indicated somewhat opposing seasonal $PM_{2.5\ [NO3]}$ when compared to those observed at Ute 1 and Ute 3. Nazlini reported elevated concentrations in the spring and summer rather than the winter and spring which may suggest seasonal changes in BLH and increase photochemistry resulting in higher concentrations.

To the contrary, the Nazlini site is characterized as a rural pristine area and therefore predicted to be less impacted by anthropogenic sources in comparison to the Southern Ute sites (Hobbs et al., 1985). Since combustion of fossil fuels and industrial processes are linked to $PM_{2.5}$ formation; the $PM_{2.5\ [NO3]}$ is likely to reflect observed

seasonal NO_x concentrations (Figure 50). Therefore, the fraction of Nazlini $PM_{2.5\ [NO3]}/PM_{2.5\ [mass]}$ was compared to those on the Southern Ute Indian Reservation in order to estimate anthropogenic contributions. The mean fraction of Southern Ute $PM_{2.5\ [NO3]}/PM_{2.5\ [mass]}$ was ~6%, whereas the mean fraction of Nazlini $PM_{2.5\ [NO3]}/PM_{2.5\ [mass]}$ was 3.8%. Therefore, it was determined the Nazlini area had lower anthropogenic contributions to $PM_{2.5\ [NO3]}$ which then can influence $PM_{2.5\ [NO3]}$.

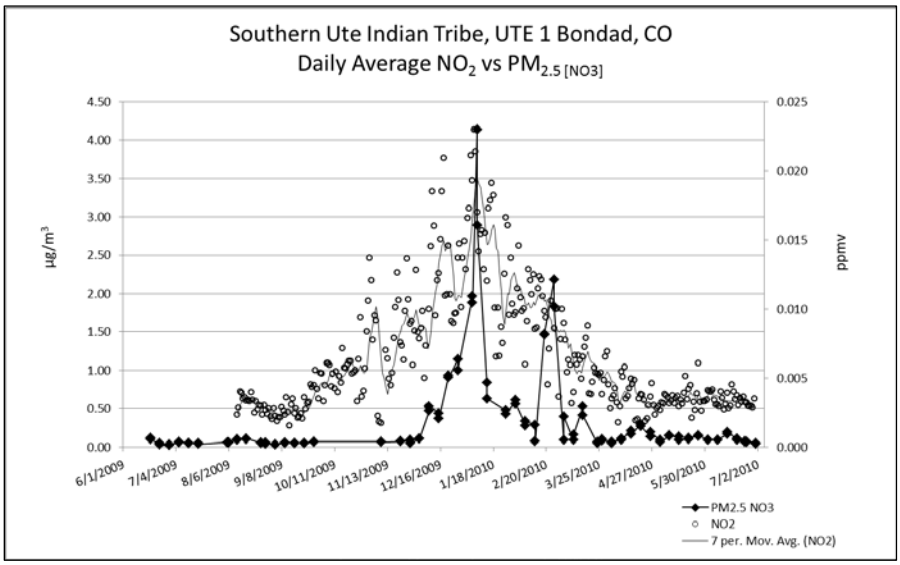

Figure 50 Southern Ute Indian Tribe, Ute 3 O_3, NO_2 versus $PM_{2.5\ [NO3]}$

The Nazlini site also exhibited PM_{10} nitrate concentrations ($PM_{10\ [NO3]}$) opposite of that observed at the Ute 3 site. Nazlini reported elevated $PM_{10\ [NO3]}$ during the summer and fall whereas Ute 3 reported elevated $PM_{10\ [NO3]}$ during the spring and winter. The Nazlini annual mean $PM_{10\ [NO3]}$ was 0.70 µg/m^3 which is over 3 times of that reported at Ute 3 (0.22 µg/m^3). Rural aerosols have been reported to contain large fractions of windblown crustal material (dust), pollen, and plant waxes (Deepak and Gali,

1991). Therefore, both dust and pollen may account for the high peaks observed in $PM_{10\ [mass]}$ in April at both Nazlini (15.4 µg/m^3, Figure 34) and Ute 3 (24 µg/m^3, Figure 41).

While fine particulate nitrate is the result of nitric acid/ammonia reactions forming ammonium nitrate, coarse particulate nitrate is the product of nitric acid and sodium chloride or crustal material reactions. More than half of aerosol nitrate is found in the coarse mode (Seinfeld and Pandis, 2006). Elevated concentrations of nitric acid vapor typically occur during the summer due to increase photochemistry and high summertime temperatures (Seinfeld and Pandis, 2006). At this time, the Nazlini area is impacted by higher wind velocities compared to Ute 1 and Ute 3 sites. The summer prevailing winds blow from the south to the NE and NW with dominate wind speeds between 3.6 – 5.7 m/s. These high wind velocities can increase as well as transport windblown alkaline dust and other air pollutants into the Nazlini area, thus enhancing the nitric acid and crustal material reactions and consequently leading to elevated PM_{10} nitrate concentrations.

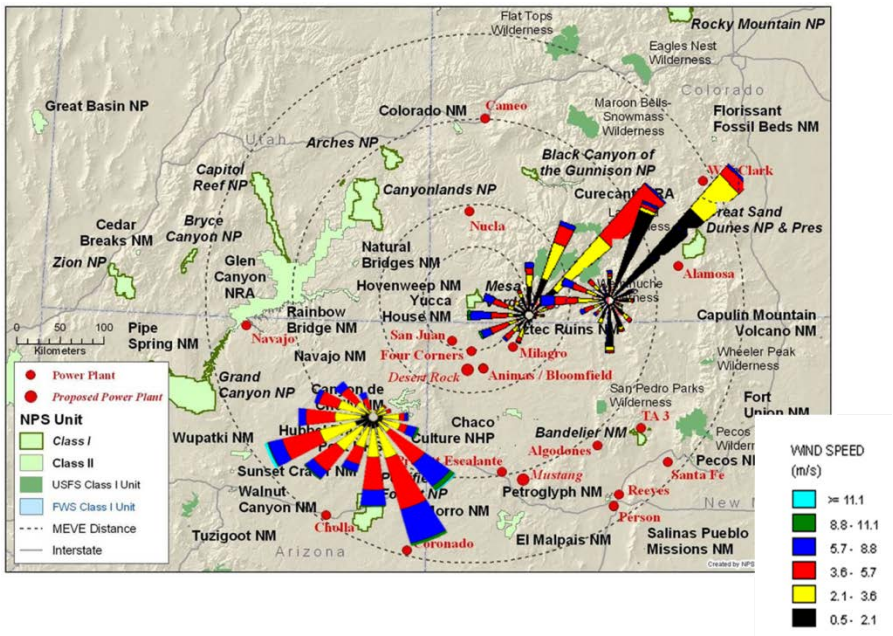

Figure 51 Summer wind roses for Ute 1 and Ute 3 (CO) and Nazlini (AZ).

On the other hand, summer increases in BLH would allow pollutants to mix higher in the atmosphere which may dilute both surface aerosol concentrations and $PM_{10\ [NO3]}$, as this may be the case for the Ute 3 site. The July maximum of 0.04 in of precipitation recorded at Ute 3 indicates the summer monsoon (July – August) season in the Four Corners region. Coarse particulates are highly soluble and more efficiently removed by cloud and rain drops, thus monsoon events can lead to PM wash out as well as shallow mixing heights consequently impacting surface aerosol concentrations and $PM_{10\ [NO3]}$.

3.4.2 Comparison of Seasonal $\delta^{15}N$ of Nitrate in PM_{10} on Tribal Lands

Although both Nazlini and Ute 3 indicate similar seasonal trends in observed $\delta^{15}N$ values of PM_{10} nitrate, a stark contrast is the 9.7 ‰ mean difference between the two sites, with Ute 3 exhibiting higher values relative to Nazlini. The Nazlini site had a mean $\delta^{15}N$ of 0.15‰ for the year, while Ute 3 revealed a 9 month mean of 9.4‰. Both tribal sites show different ranges of $\delta^{15}N$ values and this may indicate nitrate sources from different origins. Recent studies have suggested that the seasonal variations in the $\delta^{15}N$ values in nitrate aerosols are "fingerprints" of different NO_x sources (Elliot et al., 2007; Elliot et al. 2009, Felix et al., 2012).

If this is the case, then the higher $\delta^{15}N$ values at the Ute 3 site is likely associated with higher NO_x inputs from anthropogenic sources relative to the Nazlini site. For example, the $\delta^{15}N$ values of NO_x emitted from power plants (+6 to +13‰), vehicle exhaust (+3.7 to +5.7‰) and biomass burning (+14‰) are significantly higher than biogenic emissions (-49 to -20‰). As a result, the higher $\delta^{15}N$ values in PM_{10} nitrate at Ute 3 suggest a greater anthropogenic influence. On the other hand, variations in observed seasonal $\delta^{15}N$ have also been suggested to reflect seasonal shifts in NO_x chemistry that form aerosol nitrate rather than differences in emission sources (Freyer, 1991). Freyer, 1991, suggests kinetic and equilibrium nitrogen isotope fractionation effects occur during chemical formation mechanisms; therefore, impacting observed $\delta^{15}N$ values in atmospheric nitrate.

To address the questions whether seasonal $\delta^{15}N$ values of atmospheric nitrate provide insight into the sources of NO_x or reflect shifts in seasonal NO_x chemistry, an

emission model and an isotopic exchange equilibrium model was applied and compared to the observed $\delta^{15}N$ values in PM_{10} nitrate. A mass balance model using mean observed $\delta^{15}N$ values from NO_x sources (Table 3) coupled with a NO_x emission inventory for the Four Corners region was used to determine the fraction of NO_x from each source and calculate the $\delta^{15}N$ of NO_x on tribal land. The model approach assumes the $\delta^{15}N$ of NO_x mirrors that of atmospheric nitrate. Model results and observed $\delta^{15}N$ values were also supplemented with seasonal wind roses to estimate air mass trajectories.

Table 12 Four Corners Region NO_x Emission Inventory (tons/year) (ARS, 2010)

	*Environ 2005 Four Corners Emission Inventory		% of Four Corners Region NO_x Due to Source
	NO_x	VOC	NO_x
Biogenic	8,447	213,050	3.7
Oil & Gas (area & point)	68,831	122,273	30.1
EGU	72,668	281	31.8
Other **	78,532	70,607	34.4
Total Emissions	228,478	406,211	100

*Emission inventory encompasses state, federal, and tribal inventories.
**Includes on and off road, aircraft, forest and prescribed fire, wood burning, cooking, solvents, surface coating, fuel combustion, structure fires, other point sources.

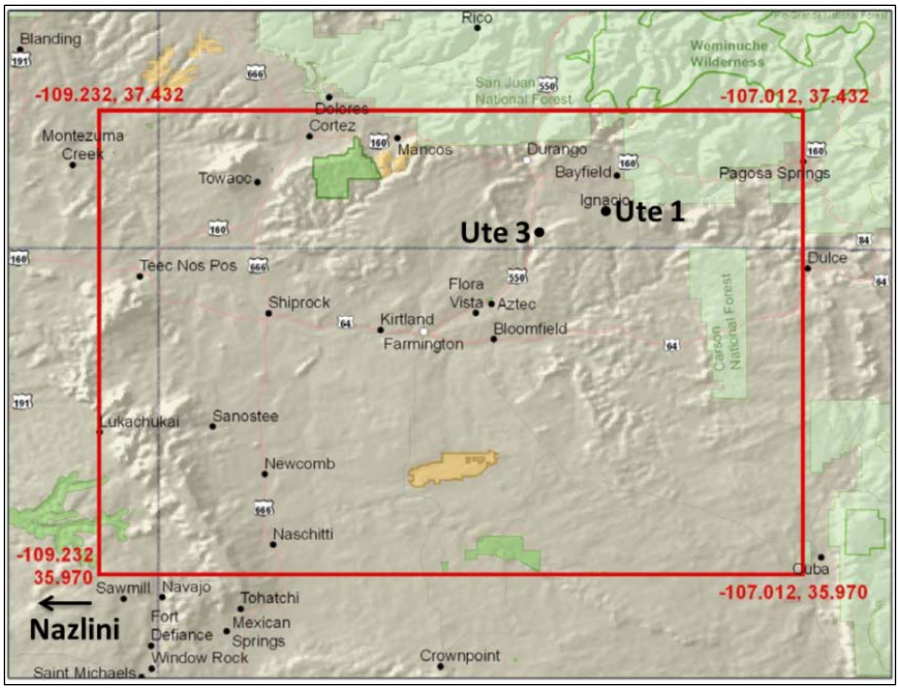

Figure 52 Four Corners Enivron emission inventory area (FCAQTF, 2007).

The 2005 Environ NO_x emission inventory for the Four Corners region (150 x 156 km area) was used to determine the fraction of NO_x emissions by source which was then applied to the following isotopic mass balance equation to determine the $\delta^{15}N$ of NO_x:

$$\delta^{15}N_{NOx} = f_{EGU}(\delta^{15}N_{EGU}) + f_{non\text{-}road}(\delta^{15}N_{non\text{-}road}) + f_{road}(\delta^{15}N_{road}) + f_{biogenic}(\delta^{15}N_{biogenic})$$

Eq. 3.1

where f is the fraction of NO_x by source and $\delta^{15}N$ is the mean value for each NO_x source (Table 3). The mass balance equation yielded a $\delta^{15}N_{NOx}$ value of 4.5‰. The NNAQCP did not report NO_x emissions for the Chinle Agency (location of Nazlini site) and neither tribe reported seasonal emissions (Table 1). For this reason, the USEPA National

Emission Inventory (NEI) data base was used to gauge whether the calculated $\delta^{15}N_{NOx}$ would potentially change with seasonal emissions.

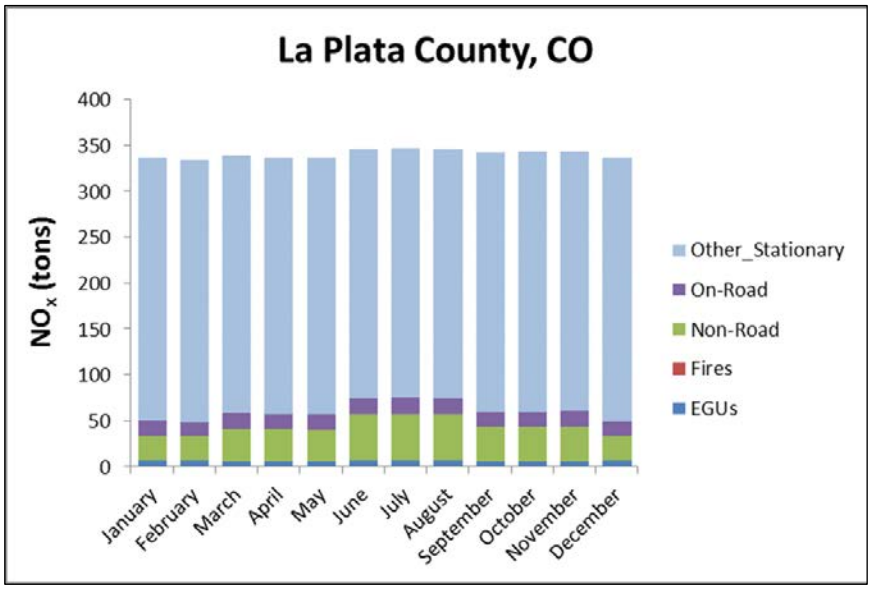

Figure 53 La Plata County, Colorado 2005 Emission Inventory (US EPA NEI, 2005)

The La Plata County (location of Ute 3) emissions and sources remain relatively constant through the course of a year (Figure 53). Therefore, the observed seasonal variations of the $\delta^{15}N$ isotope were not supported by the emission model. Furthermore, the summer wind roses for the Nazlini and Ute 3 site indicates higher velocity winds blowing from the south and southwest to the north and northeast during spring and summer (Figure 48 and Figure 51). Since power plants and large cities (Flagstaff, Holbrook, Winslow, Phoenix, Farmington) are located downwind of both the Nazlini and Ute 3 sites, one would suspect higher $\delta^{15}N$ values at this time, but rather the opposite is observed, yielding a summer $\delta^{15}N$ mean values of -1.5‰ and 6.2‰, respectively. The spring $\delta^{15}N$ mean value for Nazlini and Ute 3 PM_{10} nitrate is slightly more enriched

relative to the summer but lower than the winter values of 2.8‰ and 15‰, respectively (Table 7 and Table 8).

The alternate hypothesis in determining variations in atmospheric nitrate $\delta^{15}N$ values on tribal lands is shifts in seasonal NO_x chemistry. For example, the gas-particle phase dissociation equilibrium of ammonium nitrate would prefer the lighter ^{14}N isotopes in $HNO_{3\ (g)}$ during the summer months leading to an enrichment of ^{15}N in the residual fine particulate nitrate. Unfortunately, isotopic analysis of $PM_{2.5}$ was not conducted to observe this fractionation effect but one would suspect higher values in the summer, yet studies have shown this not to be the case (Freyer, 1991).

Secondly, the nighttime exchange reaction between NO_2, NO_3, and N_2O_5 are in thermal equilibrium (R1.7a, b) and subject to equilibrium isotope fractionation and this can lead to the enrichment of ^{15}N in the more oxidize species. This enrichment is then carried onto atmospheric nitrate via nighttime heterogeneous formation mechanisms (R1.7a, b, R1.10) which dominate during the winter, due to low temperatures and decrease sunlight. As a result, this enrichment of $\delta^{15}N$ values in PM_{10} nitrate on tribal lands would shift $\delta^{15}N$ values higher in the winter.

Thirdly, the isotope exchange equilibrium between gaseous NO and NO_2 can occur (R3.1, R3.2) if the exchange timescale happens faster than the daytime and nighttime NO_x removal mechanisms (R1.12, R1.13, R1.14).

$$^{15}NO + {}^{14}NO_2 \rightarrow {}^{14}NO + {}^{15}NO_2 \qquad \text{R3.1}$$

$$^{14}NO + {}^{15}NO_2 \rightarrow {}^{15}NO + {}^{14}NO_2 \qquad \text{R3.2}$$

The daytime NO_x removal pathway NO_2+OH forming nitric acid occurs on a similar scale as that of the nighttime removal by N_2O_5 heterogeneous hydrolysis. Therefore a ratio between the isotopic exchange reaction and the NO_2+OH removal reaction can be determined using the equilibrium constant for the two reactions, observed NO and NO_2 concentrations, and the estimated OH concentration (Sharma et al., 1970; Prinn et al., 1992). The equilibrium constant is derived from experimentally determined rate constants and expressed as:

$$K_{eq} = k_1/k_3 \qquad \text{Eq. 3.2}$$

Where K_1 is the rate constant for reaction R3.1 ($K_1 = 8.13x10_{-}^{14}$ molecules/sec at 296 K) and K_3 is the rate constant for the removal reaction ($K_3 = 1x10^{-11}$ molecules/sec at 298 K), yielding the equilibrium constant, $K_{eq} = 8.13x10^{-3}$ (Sharma et al., 1970). It was determine that complete isotope exchange between NO and NO_2 does occur in environments where NO concentrations are in parts per billion rather than parts per trillion (Riha and Michalski, 2013 in review).

Since the Nazlini site does not monitor for NO_x, it was assumed that NO_x isotope exchange does occur on both the Navajo Nation and Southern Ute Indian Reservation based on observed daily averages (ppmv) of NO_x at Ute 1 and nearby state and federal NO_x monitoring networks. Thus, the $\delta^{15}N$ of NO_2 was determined for the Ute 3 site by applying the following isotopic mass balance and equilibrium enrichment expressions:

$$\delta^{15}N_{NOx} = f_{NO}(\delta^{15}N_{NO}) + f_{NO2}(\delta^{15}N_{NO2}) \qquad \text{Eq. 3.3}$$

$$\delta^{15}N_{NO} = -\varepsilon(T) + \delta^{15}N_{NO2} \qquad \text{Eq. 3.4}$$

where *f* is the fraction of NO_x as NO or NO_2 observed at Ute 3 and ε(T) is the enrichment factor which is temperature dependent and calculated using the NO-NO_2 isotopic equilibrium constant (K_{eq}) derived from reduced partition functions (Richet et al., 1977; Michalski et al., 2004; Teffo et al., 1980; Henry et al., 1978).

The enrichment factor for NO-NO_2 isotopic exchange ranges linearly from 37‰ to 45.8‰ when plotted against a temperature range of 46°C to 7°C, yielding a slope of 0.233 (‰/°C) (Riha and Michalski, 2013 in review). The enrichment factor can then be determined from the linear equation and by applying observed ambient air temperatures into the following expression:

$$\varepsilon(T) = (\Delta T * 0.233) + 37]/-1 \qquad \text{Eq. 3.5}$$

Where ΔT is the change in temperature (46°C – observed) and 37‰ is the y-intercept. Using the calculated enrichment factor, the $\delta^{15}N$ of NO_2 can then be determined by substituting Eq. 3.4 into Eq. 3.3 and solving for $\delta^{15}N$ of NO_2 as shown in the following expressions:

$$\delta^{15}N_{NOx} = f_{NO}\,(-\varepsilon(T) + \delta^{15}N_{NO2}) + f_{NO2}\,(\delta^{15}N_{NO2}) \qquad \text{Eq. 3.6}$$

$$\delta^{15}N_{NO2} = [f_{NO}\,(\varepsilon(T)] + \delta^{15}N_{NOx} \qquad \text{Eq. 3.7}$$

The $\delta^{15}N$ of NO_x in the Four Corners was estimated at 4.5‰ (Eq. 3.1) and using Eq. 3.3 thru Eq. 3.7, the calculated $\delta^{15}N$ of precursor NO_x was found to exhibit a similar seasonal trend to the observed $\delta^{15}N$ of PM_{10} nitrate with a weak ($r^2 = 0.41$) but significant correlation. Other fractionation processes occurring during NO_x oxidation reactions may contribute to the deviations between the observed and calculated.

Overall, the calculated $\delta^{15}N$ of PM_{10} nitrate suggests the isotope exchange equilibrium between NO and NO_2 in the Four Corners region is playing a key role in the observed seasonal trends. On the other hand, the significant 9.7‰ offset in the ranges of $\delta^{15}N$ values observed on tribal lands is likely attributed to nitrate sources from different origins. The elevated $\delta^{15}N$ values observed at Ute 3 site in comparison to the Nazlini site indicate the tribal air shed on the Southern Ute Indian Reservation is influenced more by anthropogenic sources relative to the Nazlini site. Therefore it can be determined that both seasonal changes in NO_x chemistry and sources are the two main processes controlling the observed $\delta^{15}N$ of PM_{10} nitrate on both the Southern Ute Indian Reservation and Navajo Nation.

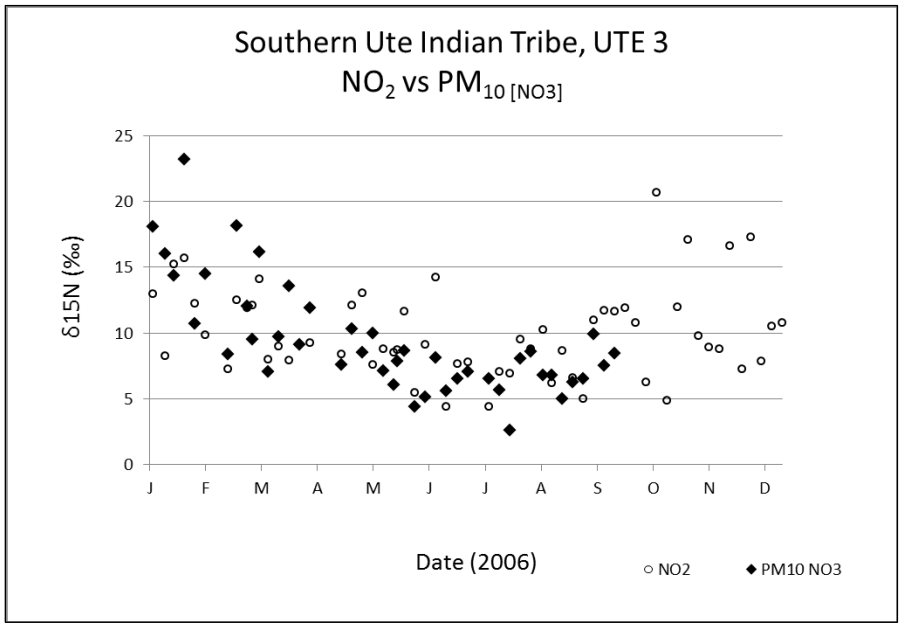

Figure 54 Southern Ute Indian Tribe, Ute 3 $\delta^{15}N$ in PM_{10} nitrate concentrations versus calculated $\delta^{15}N$ of precursor NO_2. The calculated $\delta^{15}N$ values were reported in accordance with the EPA 1 in 6 day PM sampling schedule.

3.4.3 Comparison of Seasonal $\delta^{18}O$ and $\Delta^{17}O$ of Nitrate in PM_{10} on Tribal Lands

Both Nazlini and Ute 3 indicate similar seasonal trends in observed $\Delta^{17}O$ values of PM_{10} nitrate, with higher values in spring and winter compared to summer and fall. This observation is in agreement with observed $\Delta^{17}O$ values for atmospheric nitrate collected at mid-latitudes with seasonal trends showing maximum $\Delta^{17}O$ values occurring during midwinter (Michalski et al., 2003). A profound contrast is the range of excess ^{17}O at Ute 3 versus Nazlini, with Ute 3 exhibiting a larger range (14 – 32‰) relative to Nazlini (20-35‰). Observed mid-latitude $\Delta^{17}O$ values typically range from 20-30‰, where seasonal variations in the $\Delta^{17}O$ values are attributed to shifts in the cycling and oxidation pathways of NO_x to form HNO_3. Therefore, a qualitative approach can be used to provide insight into NOx oxidation pathways by evaluating the $\Delta^{17}O$ values in atmospheric nitrate.

Observed $\Delta^{17}O$ seasonal trends compared to model observations found shifts in NO_x oxidation pathways to be a result of temperature dependences, NO_x concentrations and hours of sunlight (Michalski et al., 2003). Therefore, qualitatively observed increases in particulate nitrate $\Delta^{17}O$ values would suggest an increase in N_2O_5 hydrolysis during the winter, whereas lowered values would suggest an increase in daytime NO_2+OH reactions during the summer. Furthermore, since NO_2 is also influenced by peroxy radical oxidation, the mass transfer of O atoms from ozone to NO_2 become diluted by peroxy radical ($\Delta^{17}O$ <1‰) oxidation; subsequently modifying the amount of ^{17}O excess found in atmospheric nitrate (Rockmann et al., 2001). As a result, lower $\Delta^{17}O$ values observed during the summer and spring at the Ute 3 site can be

caused by increases in peroxy radical oxidation, further suggesting that the Southern Ute Indian Reservation is influenced by greater anthropogenic inputs in comparison to Nazlini.

Due to the low observed $\Delta^{17}O$ values in PM_{10} nitrate at the Ute 3 site, a dual isotope approach was applied using both the observed $\delta^{18}O$ and $\delta^{15}N$ from Ute 3 and Nazlini to gauge whether values were representative of published isotope measurements using the denitrifier method (black box, Figure 55). Since atmospheric nitrate is enriched in $\delta^{18}O$ compared to other sources, the dual isotope approach has gained acceptance as a tracer of atmospheric nitrate (Kendall et al., 2008).

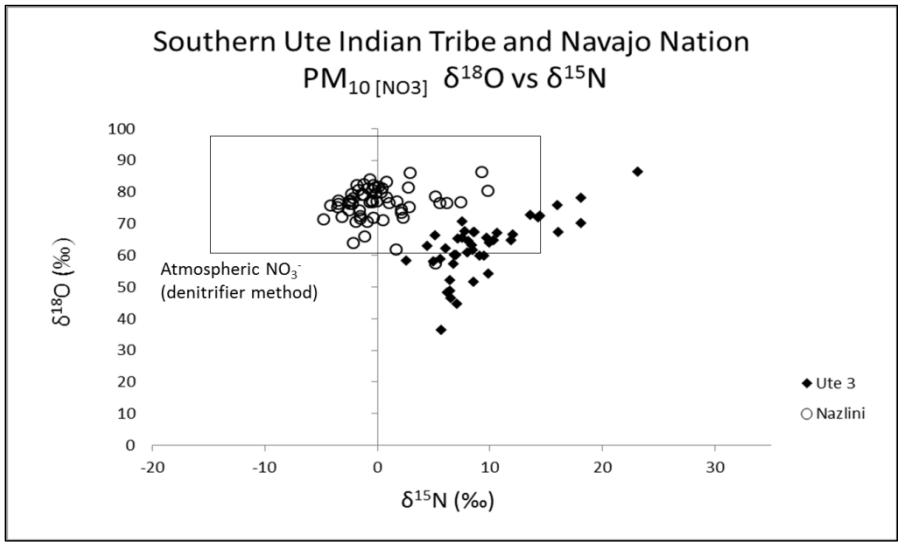

Figure 55 Dual isotope ^{18}O and ^{15}N plot of tribal PM_{10} nitrate

The dual isotope approach determined that PM_{10} nitrate collected at the Nazlini site exhibited good agreement with observed $\delta^{18}O$ and $\delta^{15}N$ values of atmospheric nitrate processed using the denitrifier method. The $\delta^{18}O$ values at the Ute 3 site were in between the range of observed $\delta^{18}O$ values in atmospheric nitrate derived from the

denitrifier method and values obtained using the silver nitrate method (Figure 14). The dual isotope plot suggests the Ute 3 measured $\delta^{18}O$ values are adequate to provide insight into NO_x oxidation.

Lastly, it has been suggested the nighttime heterogeneous removal pathway of NO_x forming nitric acid is more variable and can be quite rapid on aerosol surfaces that contain water to produce nitric acid (Detener and Crutzen, 1993). Furthermore, measurements of N_2O_5 uptake coefficients were shown to be highly variable and are influenced by relative humidity, aerosol acidity, and aerosol composition, such as sulfate mass or sulfate to organic ratio (Brown, et al., 2006). Therefore, the observed $\Delta^{17}O$ values at Nazlini were compared to measured anions to qualitatively assess the N_2O_5 uptake with aerosol composition.

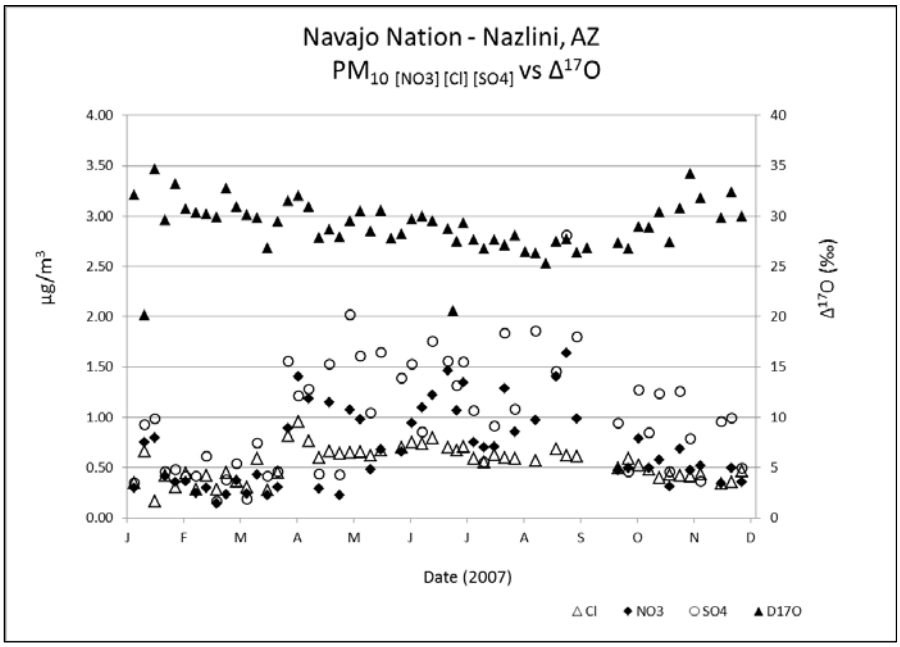

Figure 56 Navajo Nation – Nazlini PM10 anion concentrations versus $\Delta^{17}O$

The N_2O_5 heterogeneous hydrolysis mechanism is dominant during the winter months since the dissociation equilibrium between NO_2, NO_3 and N_2O_5 favors N_2O_5 formation under cool temperatures (Brown et. al., 2006; Chang et. al., 2011). On the other hand, anion concentrations at Nazlini increase during the summer due to increase photochemistry and decrease during the winter, whereas the $\Delta^{17}O$ is elevated during the winter. One would suspect N_2O_5 hydrolysis to increase with sulfate concentrations, but sulfate elevates in the summer and fall (1.3 $\mu g/m^3$) whereas $\Delta^{17}O$ decreases indicating a shift toward the daytime NO_x oxidation mechanism.

Particulate nitrate also inhibits N_2O_5 uptake, suggesting a relatively small N_2O_5 uptake occurring when elevated concentrations are observed (Brown et. al., 2006). Changes to relative humidity and the addition of organic coatings to particles can also inhibit N_2O_5 uptake (Brown et al., 2006). As a result, observations of $\Delta^{17}O$ can be used both qualitatively and quantitatively to constrain the N_2O_5 uptake coefficient and NO_x oxidation pathways. A qualitative approach based on a mixing line between the daytime ($\Delta^{17}O$ ~20‰) reaction and nighttime ($\Delta^{17}O$ ~32‰) reaction versus temperature can estimate the seasonal occurrence of these two NO_x removal pathways to nitrate formation (Figure 57).

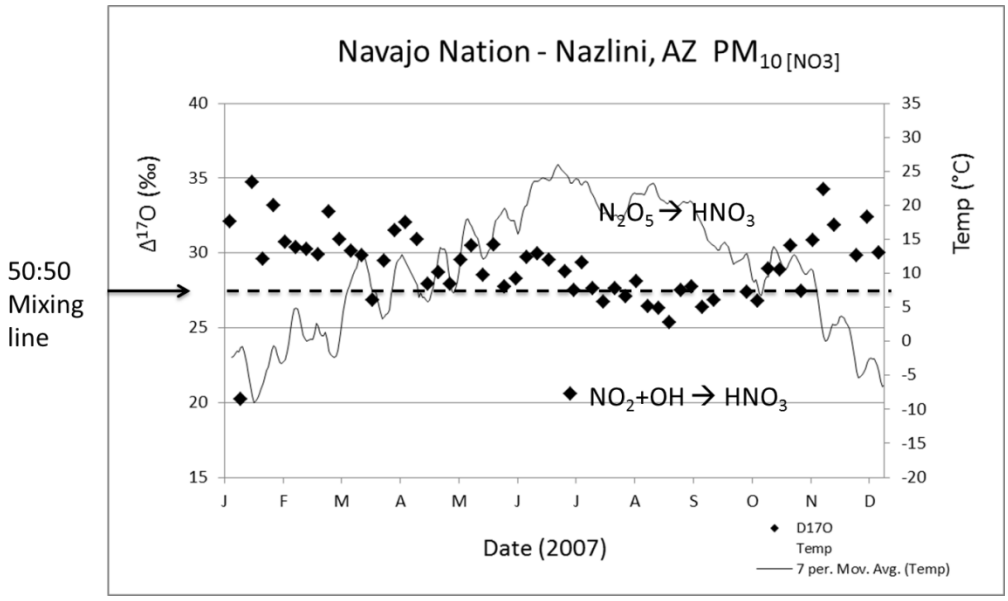

Figure 57 Navajo Nation – Nazlini, AZ $\Delta^{17}O$ versus temperature (°C) with mixing line (dash line) indicating NO_x removal by N_2O_5 hydrolysis dominate in winter months.

Another qualitative approach involves observing the $\delta^{18}O$ and $\Delta^{17}O$ composition of PM_{10} nitrate to derive the mixing line between O_2 ($\delta^{18}O$ = 23‰, $\Delta^{17}O$ = 0‰) and H_2O ($\delta^{18}O$ = -10‰, $\Delta^{17}O$ = 0‰, Bowen and Ravenaugh, 2003), which then gives qualitative insight into NO_x removal pathways and formation mechanisms of nitrate. Both O_2 and H_2O influence NO_x removal via NO_x oxidation by HO_2 (RO_2) and N_2O_5 hydrolysis, respectively (Figure 58). The y-intercept ($\delta^{18}O$ = 9.6‰) of the observed mixing line between O_2 and H_2O from tribal PM_{10} nitrate would suggest a shift favoring daytime NO_x removal pathway to nitrate formation (Figure 58). Low relative humidity and increase photochemistry indicative of the southwestern U.S. may be contributing factors to this shift toward daytime NO_x removal.

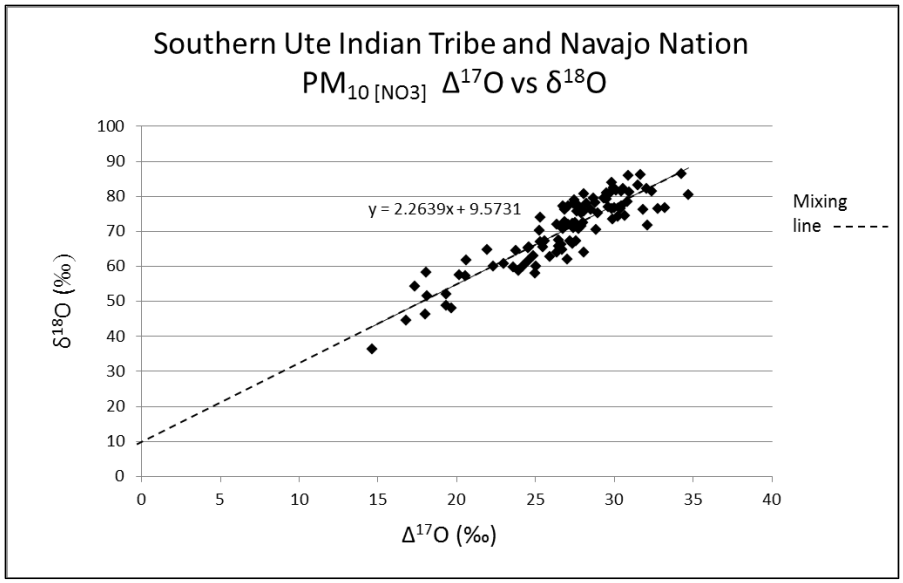

Figure 58 Navajo Nation – Nazlini, AZ $\delta^{18}O$ vs $\Delta^{17}O$ vs temperature (°C) with mixing line (dash line). The intercept at $\delta^{18}O$ = 9.6‰ indicates roughly two-third O_2 contributions to PM_{10} nitrate formation relative to H_2O.

On the other hand, a mass balance approach can be applied to quantitatively determine the $\Delta^{17}O$ signature of each NO_x removal pathway leading to nitrate formation as seen in Chapter 1. Constraining NO_x oxidation pathways would then involve the coupling of this mass balance approach with the photochemical model, ISO-RACM. The model can then determine seasonal changes in the branching ratios for each NO_x removal pathway as well as the corresponding $\Delta^{17}O$ value of the nitric acid product. The model output $\Delta^{17}O$ values can then be adjusted to match observed $\Delta^{17}O$ values, therefore allowing for better parameterization of the N_2O_5 pathway which then leads to accurate predictions of trace gas concentrations (Detener and Crutzen, 1993). The ISO-RACM modeling results for the Ute 3 site is currently pending and the discussion of those results are outside the scope of this thesis project.

CHAPTER 4. CONCLUSION

4.1 Seasonal Nitrate Concentrations in PM on Tribal Lands

Both the Southern Ute Indian Tribe and Navajo Nation monitoring sites indicated spikes in $PM_{2.5\ [NO3]}$ and seasonal trends in $PM_{10\ [NO3]}$ throughout the respective sampling years. Estimated air mass trajectories, observed trace gas monitoring, and $PM_{2.5\ [NO3]}$ on tribal lands determined that the spikes in winter were affected by decreases in BLH and contributions from local activity such as automobile traffic and residential wood burning. It was also determined the Nazlini area had lower anthropogenic contributions to $PM_{2.5\ [NO3]}$ relative to the Southern Ute monitoring sites, thus influencing $PM_{2.5\ [NO3]}$.The ammonia and nitric acid reaction was also associated to fine particulate nitrate formation during winter months or when sulfate levels are low and ammonia and nitrogen oxide emissions are high (NOAA, 2005).

On the other hand, increases in BLH and photochemistry during the summer months can also result in higher seasonal $PM_{10\ [NO3]}$. Furthermore, estimated air mass trajectories indicate higher wind velocities during the summer which may increase windblown crustal material and contributing to an increase in $PM_{10\ [NO3]}$ via the nitric acid and sodium chloride or crustal material reactions. To the contrary, increases in BLH can cause pollutants to mix higher in the atmosphere which can lead to a dilution effect

therefore decreasing $PM_{10\ [NO3]}$ at Ute 3. The seasonal trend in PM nitrate concentrations on the Navajo Nation and Southern Ute Indian Reservation are likely linked to seasonal changes in boundary layer height (BLH), local sources, meteorology, photochemistry and increases in windblown crustal material.

4.2 Seasonal $\delta^{15}N$ of Nitrate in PM_{10} on Tribal Lands

The $\delta^{15}N$ seasonal variations in aerosol nitrate have been hypothesized to be a result of changing NO_x emission sources or reflection of changing NO_x chemistry (Elliot et al., 2007; Freyer, 1991). For example, the $\delta^{15}N$ values of NO_x emitted from power plants (+6 to +13‰), vehicle exhaust (+3.7 to +5.7‰) and biomass burning (+14‰) are significantly higher than biogenic emissions (-49 to -20‰). Therefore, variations in NO_x origins are hypothesized to lead to $\delta^{15}N$ variations in aerosol nitrate. On the other hand, $\delta^{15}N$ variations have also been suggested to reflect seasonal shifts in NO_x chemistry that form aerosol nitrate rather than differences in emission sources (Freyer, 1991). Freyer, 1991, suggests nitrogen isotope fractionation occurs during the gaseous NO and NO_2 equilibrium (R3.1, R3.2), leading to the enrichment of ^{15}N in the more oxidized species. It is assumed the exchange timescale happens faster than the daytime and nighttime NO_x removal mechanisms, and this enrichment is then carried onto atmospheric nitrate.

To test these two hypotheses, a mass balance approach was applied to an emission model and an isotopic exchange equilibrium model to determine the $\delta^{15}N$ of NO_x which was then compared to the observed $\delta^{15}N$ values in tribal PM_{10} nitrate. Both models assume the $\delta^{15}N$ of NO_x mirrors that of atmospheric nitrate. Model results and

observed $\delta^{15}N$ values were also supplemented with seasonal wind roses to estimate air mass trajectories. Even though both the Ute 3 site and Nazlini site exhibited a stark offset of 9.7 ‰ mean difference between the two sites, both had similar seasonal trends in $\delta^{15}N$ values. Therefore, it was determined the higher $\delta^{15}N$ offset observed at the Ute 3 site was likely associated with higher NO_x inputs from anthropogenic sources relative to the Nazlini site. The seasonal $\delta^{15}N$ trends correlated closely to the model results derived from the isotope exchange equilibrium, indicating the seasonal variations are driven by chemistry rather than sources. As a result, it was determined that both sources and chemistry influence $\delta^{15}N$ seasonal variations in tribal PM_{10} nitrate.

4.3 Seasonal $\Delta^{17}O$ of Nitrate in PM_{10} on Tribal Lands

Both Nazlini and Ute 3 indicated similar seasonal trends in observed $\Delta^{17}O$ values of PM_{10} nitrate, with higher values in spring and winter compared to summer and fall. This observation is in agreement with observed $\Delta^{17}O$ values for atmospheric nitrate collected at mid-latitudes, where seasonal variations in the $\Delta^{17}O$ values are attributed to shifts in the cycling and oxidation pathways of NO_x to form HNO_3 (Michalski et al, 2003). Therefore, a qualitative approach was used to provide insight into NO_x oxidation pathways over tribal lands by evaluating the $\Delta^{17}O$ values in PM_{10} nitrate.

Qualitative observations indicated increases in particulate nitrate $\Delta^{17}O$ values during the winter which suggested an increase in N_2O_5 hydrolysis, whereas lowered values observed during the summer suggested an increase in daytime NO_2+OH reactions. Furthermore, low $\Delta^{17}O$ values observed during the summer and spring at the

Ute 3 site were likely linked to increases in peroxy radical oxidation, which further suggests that the Southern Ute Indian Reservation is influenced by greater anthropogenic inputs in comparison to the Nazlini area.

The nighttime heterogeneous removal pathway of NO_x forming nitric acid is highly variable and measurements of N_2O_5 uptake coefficients were shown to be influenced by relative humidity and aerosol composition, such as sulfate mass or sulfate to organic ratio (Brown, et al., 2006). Furthermore, aerosol acidity and the addition of organic coatings to particles can inhibit N_2O_5 uptake (Brown et al., 2006). As a result, observations of $\Delta^{17}O$ can be used both qualitatively and quantitatively to constrain the N_2O_5 uptake coefficient and NO_x oxidation pathways

A mass balance approach coupled with a photochemical box model (ISO-RACM) can be applied to quantitatively determine $\Delta^{17}O$ values which can then be adjusted to match observed $\Delta^{17}O$ values in tribal PM_{10} nitrate. This quantitative approach can better parameterize the N_2O_5 pathway in chemical modeling schemes which then leads to accurate predictions of trace gas concentrations (Detener and Crutzen, 1993). The ISO-RACM modeling results for the Ute 3 site is currently pending and the discussion of those results are outside the scope of this thesis project.

4.4 Broader Impacts

This thesis utilized the chemical and stable isotopic composition of particulate nitrate to determine source contributions and chemical formation pathways of aerosol nitrate on tribal lands. This resolution can supplement Tribal Air Quality Programs (AQP)

and assist with their continual development of policies and regional planning efforts to improve air quality in several ways. First of all, it was determined increases in local NO_x emissions on reservation lands impacts fine particulate nitrate concentrations, with increases during the winter months. The winter increases were attributed to local residential wood burning combined with meteorological conditions. The tribal AQP's can use this baseline knowledge to gauge whether an EPA residential wood stove change out campaign may be implemented to improve air quality. After implementation a follow up study can also be conducted to monitor progression.

Secondly, the observed $\delta^{15}N$ values in PM nitrate can be used as an effective new tool for monitoring regulatory NO_x emission reductions from stationary sources. The observed $\delta^{15}N$ values can also help constrain the relative importance of source versus transport in the NO_x budget over tribal lands. For example, a follow up study after the removal of a major anthropogenic NO_x source should reveal a reduction in the enrichment of $\delta^{15}N$ values, whereas increases would suggest the transport of NO_x into the area or the addition of new NO_x sources.

Lastly, the $\Delta^{17}O$ signature of PM nitrate can help constrain NO_x oxidation pathways and predict regional air quality by adjusting photochemical (ISO-RACM) model outputs of $\Delta^{17}O$ values to observed values. This technique allows better parameterization of the regional N_2O_5 uptake coefficient to better predict NO_x oxidation, which then dictates the oxidation capacity of the atmosphere and regional air quality. In addition, the chemical model scheme is portable into widely used 1-D, 2-D, and 3-D chemical transport models. The photochemical model, ISO-RACM can be

parameterized using tribal $\Delta^{17}O$ values and air quality data to predict trace gas and particulate concentrations that are currently of high concern for tribal air quality managers. The ISO-RACM modeling results for tribal air quality monitoring stations can also be used to assist in future EPA criteria pollutant attainment/non-attainment designations.

REFERENCES

REFERENCES

Alexander, B., M. G. Hastings, D. J. Allman, J. Dachs, J. A. Thornton and S. A. Kunasek, Quantifying atmospheric nitrate formation pathways based on a global model of the oxygen isotopic composition ($\Delta^{17}O$) of atmospheric nitrate, *Atm. Chem. Phys.,9*(14), 5043-5056, 2009.

Ammann, M.; Siegwolf, R.; Pichlmayer, F.; Suter, M.; Brunold, C. Estimating the uptake of traffic-derived NO_2 from ^{15}N abundance in Norway spruce needles, *Oecologia*, 118 (2), 124−131, 1999.

Andreae, Meinrat O and Crutzen, Paul J. Atmospheric Aerosols: Biogeochemical Sources and Role in Atmospheric Chemistry, *Science.,* 276 (5315), 1052-1058, 1997.

Archer, David and Stefan Rahmstorf. *The Climate Crisis*. New York: Cambridge University Press, 2010.

Air Resource Specialist, Inc., Final report review of four corners air quality task force report of mitigation options, *ARS, Inc*. 2010.

Baars, D. L., *Navajo country: A geology and natural history of the Four Corners region*. University of New Mexico Press, Albuquerque, 1995.

Baars, Donald L., *The Colorado Plateau: A Geologic History*. Albuquerque: UNM Press, 2000.

Bauer, S.E., D. Koch, N. Unger, S.M. Metzger, D.T. Shindell, and D.G. Streets, Nitrate aerosols today and in 2030: Importance relative to other aerosol species and tropospheric ozone. *Atmos. Chem. Phys*., 7, 5043-5059, 2007.

Bobbink, R., K. Hicks, J. Galloway, T. Spranger, R. Alkemade, M. Ashmore, M. Bustamante, S. Cinderby, E. Davidson, F. Dentener, B. Emmett, J. W. Erisman, M. Fenn, F. Gilliam, A. Nordin, L. Pardo and W. De Vries, Global assessment of nitrogen deposition effects on terrestrial plant diversity: a synthesis, *Ecological Applications,20*(1), 30-59, 2010.

Brown, S. S., T. B. Ryerson, A. G. Wollny, C. A. Brock, R. Peltier, A. P. Sullivan, R. J. Weber, W. P. Dube, M. Trainer, J. F. Meagher, F. C. Fehsenfeld and A. R. Ravishankara, Variability in nocturnal nitrogen oxide processing and its role in regional air quality, *Science,311*(5757), 67-70, 2006.

Brown, S. S., H. Stark, T. B. Ryerson, E. J. Williams, D. K. Nicks, M. Trainer, F. C. Fehsenfeld and A. R. Ravishankara, Nitrogen oxides in the nocturnal boundary layer: Simultaneous in situ measurements of NO_3, N_2O_5, NO_2, NO, and O_3, *J. Geophys. Res.,108*(D9), 4299-DOI: 10.1029/2002JD002917, 2003.

Brown, S. S., R. K. Talukdar and A. R. Ravishankara, Rate constants for the reaction $OH+NO_2+M \rightarrow HNO_3+M$ under atmospheric conditions, *Chem. Phys. Lett.,299*(3,4), 277-284, 1999.

Bureau of Indian Affiars, and George A. Kiersch. *Mineral Resources, Navajo-Hopi Indian Reservations, Arizona-Utah: Geology, Evaluation, and Uses, Volumes 1–3, United States Bureau of Indian Affairs 1955-1956*. Vol. 1-3. Tuscon: University of Arizona, 1955.

Casciotti, K. L., D. M. Sigman, M. G. Hastings, J. K. Böhlke and A. Hilkert. Measurement of the oxygen isotopic composition of nitrate in seawater and freshwater using the denitrifier method, *Anal. Chem.,74*(19), 4905-4912, 2002.

Casciotti, K.L., Böhlke, J.K., Mellvin, M.R., Mroczkowski, S.J., and Hannon, J.E., Oxygen isotopes in nitrate: Analysis, calibration, and equilibration. *Analytical Chemistry*, 79, (6), 2427-2436, 2007.

Chang, W. L., P. V. Bhave, S. S. Brown, N. Riemer, J. Stutz and D. Dabdub, Heterogeneous Atmospheric Chemistry, Ambient Measurements, and Model Calculations of N_2O_5: A Review, *Aerosol Sci. Tech*., 45(6), 665-695, 2011.

Chuang, C. C., Penner, J. E., Taylor, K. E., Grossmann, A. S., and Walton, J. J., An assessment of the radiative effects of anthropogenic sulfate, *J. Geophys. Res*., 102, 3761–3778, 1997.

Dentener F.J., P.J. Crutzen, Reaction of N_2O_5 on Tropospheric Aerosols: Impact on the Global Distrubutions, *Journal of Geophysical Research*, Vol 98, 7149-7163, 1993.

Department of Information Technology, Navajo Nation. "History." *Welcome to the Navajo Nation Government*, 2011. Web. 04 June 2013. http://www.navajo-nsn.gov/history.htm

Dubey, M.K., R. Mohrschladt, N.M. Donahue and J.G. Anderson, Isotope-specific kinetics of hydroxyl radical (OH) with water (H_2O): Testing models of reactivity and atmospheric fractionation, *J. Phys. Chem. A.,* 101, 1494-1500, 1997.

Dionex Corporation and Thermo Scientific, Inc., *Documents and Manuel's*, Web acess, 2013. www.dionex.com.

Eastern Research Group, Inc., Emission Inventory Report for Sources on the Navajo Nation: Final Report-FY 2005, *ERG, Inc*., Morrisville, NC, 2005.

Eldred, R. A., T. A. Cahill and R. G. Flocchini, Composition of PM2.5 and PM10 aerosols in the IMPROVE network, pp. 194-203, 1997.

Electronic Code of Federal Regulations website."Part 58 Ambient Air Quality Surveillance."Appendix E, Probe & Monitoring Path Citing Criteria for Ambient Air Quality Monitoring. Access Oct, 2009. http://ecfr.gpoaccess.gov/cgi/t/text/text-idx?c=ecfr&tpl=%2Findex.tpl

Elliott, E. M., C. Kendall, E. W. Boyer, D. A. Burns, G. G. Lear, H. E. Golden, K. Harlin, A. Bytnerowicz, T. J. Butler and R. Glatz, Dual nitrate isotopes in dry deposition: Utility for partitioning NOx source contributions to landscape nitrogen deposition, *Journal of Geophysical Research-Biogeosciences,114*, 2009.

Elliott, E. M., C. Kendall, S. D. Wankel, D. A. Burns, E. W. Boyer, K. Harlin, D. J. Bain and T. J. Butler, Nitrogen isotopes as indicators of NOx source contributions to atmospheric nitrate deposition across the Midwestern and northeastern United States, *Envir. Sci. Tech.,41*(22), 7661-7667, 2007.

Felix, J. D.; Elliott, E. M.; Shaw, S. L. Nitrogen Isotopic Composition of Coal-Fired Power Plant NOx: Influence of Emission Controls and Implications for Global Emission Inventories. *Environ. Sci. Technol*. 46 3528-3535, 2012.

Feng, Y. and J.E. Penner, Global Modeling of Nitrate and Ammonium: Interaction of Aerosols and Tropospheric Chemistry, *J. Geophys. Res*., 112, D01304, doi:10.1029/2005JD006404, 2007.

Fenn, M. E., R. Haeuber, G. S. Tonnesen, J. S. Baron, S. Grossman-Clarke, D. Hope, D. A. Jaffe, S. Copeland, L. Geiser, H. M. Rueth and J. O. Sickman, Nitrogen emissions, deposition, and monitoring in the western United States., pp. 391-403, 2003.

Fenn, M. E., M. A. Poth, J. D. Aber, J. S. Baron, B. T. Bormann, D. W. Johnson, A. D. Lemly, S. G. McNulty, D. E. Ryan and R. Stottlemyer, Nitrogen excess in North American ecosystems: Predisposing factors, ecosystem responses, and management strategies, *Ecological Applications,8*(3), 706-733, 1998.

Finlayson-Pitts, B. J. and J. N. Pitts, Jr., Tropospheric air pollution: ozone, airborne toxics, polycyclic aromatic hydrocarbons, and particles, pp. 1045-1052, 1997.

Four Corners Air Quality Task Force (FCAQTF) website, Report of Mitigation Options, 2007. Web Access Oct. 2010. http://www.nmenv.state.nm.us/aqb/4C/

Four Corners Air Quality Task Force Report of Mitigation Options, November 1,2007, available at: http://www.nmenv.state.nm.us/aqb/4C/TaskForceReport.html

Freyer, H. D., Seasonal-Variation of N-15-N-14 Ratios in Atmospheric Nitrate Species, *Tellus Series B-Chemical and Physical Meteorology,43*(1), 30-44, 1991.

Galloway, J. N., Acid deposition: perspectives in time and space, *Water, Air, and Soil Pollution,85*(1), 15-24, 1995.

Galloway, J. N., Dentener, F., Capone, D., Boyer, E., Howarth R., Seitzinger, S., Asner, G., Cleveland, C., Green, P., Holland, E., Karl, D., Michaels, A., Porter, J., Townsend, A., Vorosmarty, C., Nitrogen cycles: Past, present, and future. *Biogeochemistry*, 70, 153-226, 2004.

Galloway, N., J., Townsend, R., A., Erisman, William, J., Bekunda, Mateete, Cai, Zucong, Freney, R., J., Martinelli, A., L., Seitzinger, P., S., Sutton, and A., M. Transformation of the nitrogen cycle: Recent trends, questions, an potential solutions, *Science*, 320, 889-892, doi: 10.1126/science.1136674, 2008.

Gao, Y.Q., and R.A. Marcus, Strange and unconventional isotope effects in ozone formation, *Science*, 293, 259-263, 2001.

Hansen, J., et al., Efficacy of climate forcings, *Journal Geophys. Res*., doi:10.1029/2005JD005776, in press. 2005.

Hallquist, M., D. J. Stewart, J. Baker and R. A. Cox, Hydrolysis of N_2O_5 on submicron sulfuric acid aerosols, *J. Phys. Chem A, 104*(17), 3984-3990, 2000.

Hastings, M. G.; Jarvis, J. C.; Steig, E. J. Anthropogenic impacts on nitrogen isotopes of ice-core nitrate. *Science*, 324, 1288. 2009.

Hastings, M. G., D. M. Sigman and F. Lipschultz, Isotopic evidence for source changes of nitrate in rain at Bermuda, *J. Geophys. Res.,108*, (4790), 2003.

Hanway, D., and Tao, F.-M. A Density Function Theory and Ab Initio Study of the Hydrolysis of Dinitrogen Pentoxide. *Chem. Phys*. Lett. 285:459–466, 1998.

Heaton, T. H. E., Isotopic studies of nitrogen pollution in the hydrosphere and atmosphere: A review, *Chem. Geol.,59*(1), 87-102, 1986.

Henry, A.; Le Moal, M. F.; Cardinet, Ph.; Valentin, A. Overtone Bands of 14N16O and Determination of Molecular Constants. *J. Mol. Spectrosc*. 70 18-26, 1978.

Hoering, T. The isotopic composition of ammonia and nitrate ion in rain. *Geochim. Cosmochim. Acta*, 12: 97-102, 1957.

Hwang J, Chan C. Effects of Air Pollution on Daily Clinic Visits for Lower Respiratory Tract Illness. *American Journal of Epidemiology* 155; 1-10, 2002.

"Indian Country Defined." Title 18 *U.S. Code* Sec. 1151 et seq. 2006 ed. Supp. IV, 2010. Web 21 May 2013. http://www.gpo.gov/

IPCC, 2007: Summary for Policymakers. In: *Climate Change 2007: The Physical Basis. Contribution of Working Group I to the Fourth Assessment Report of the Intergovernmental Panel on Climate Change* [Solomon, S., D. Qin, M. Manning, Z. Chen. M. Marquis, K.B. Averyt, M. Tignor and H.L. Miller (eds.)]. Cambridge, United Kingdom and New York, NY, USA.

Jaegle, L., Steinberger, L., Martin, R.V., Chance, K., Global partitioning of NOx sources using satellite observations: relative roles of fossil fuel comburstion, biomass burning, and soil emissions, *Faraday Discuss*., 130, 407-423, 2005.

Kaiser, J., M. G. Hastings, B. houllton, T. Rockmann and D. M. Sigman, Online Method for Oxygen Triple Isotope Analyses of Nitrate (abstract), *American Geophysical Union,H52B-05*, 2005.

Kaiser, J., M. G. Hastings, B. Z. Houlton, T. Rockmann and D. M. Sigman, Triple Oxygen Isotope Analysis of Nitrate Using the Denitrifier Method and Thermal Decomposition of N_2O, *Analytical Chemistry,79*, 599-607, 2007.

Kampa, M., Castanas, E., Human health effects of air pollution. *Environmental Pollution*, 151 (2), 362-367, 2008

Kendall, C., Elliot, E.M. and Wankel, S.D. Tracing anthropogenic inputs of nitrogen to ecosystems, *Stable Isotopes in Ecology and Environmental Sciences, Second Edition* (eds r. Michener and K. Lajtha), Blackwell Publishing Ltd, Oxford, UK. 2008.

Lakes Environmental, *WRPLOT View*, Wind Rose Plots for Meteorological Data, Web Access: 2013.

Lelieveld, J., T. M. Butler, J. N. Crowley, T. J. Dillon, H. Fischer, L. Ganzeveld, H. Harder, M. G. Lawrence, M. Martinez, D. Taraborrelli and J. Williams, Atmospheric oxidation capacity sustained by a tropical forest, *Nature, 452*(7188), 737-740, 2008.

Liao, H. and J. H. Seinfeld, Global impacts of gas-phase chemistry-aerosol interactions on direct radiative forcing by anthropogenic aerosols and ozone, *Journal of Geophysical Research-Atmospheres, 110*(D18), 2005.

Li, D.; Wang., X. Nitrogen isotopic signature of soil-released nitric oxide (NO) after fertilizer application. Atmos. Environ. 42, 4747−4754, 2008.

Likens, G.E., Driscoll, C.T., and Buso, D.C. Long-term effect of acid rain: Response and recovery of a forest ecosystem. *Science*, 272, 244-246, 1996.

Lippmann, M., Health effects of airborne particulate matter. *New England Journal of Medicine*, 357 (23), 2395-2397, 2007.

Lyons, J.R., Transfer of mass-independent fractionation in ozone to other oxygen-containing radicals in the atmosphere, *Geophys. Res. Lett., 28*, 3231-3234, 2001.

Mase, D.F. (2010 Master's Thesis) A coupled modeling and observational approach to understanding oxygen-18 in atmospheric nitrate. Purdue University.

Mayewski, P.A., Lyons, W.B., Spencer, M.J., Twickler, M.S., Buck, C.F. and Whitlow, S., An ice core record of atmospheric response to anthropogenic sulphate and nitrate, *Nature* 346(6284): 554-556, 1990.

Mayewski, P.A., Spencer, M.J., Twickler, M.S. and Whitlow, S., A glaciochemical survey of the Summit region, Greenland, *Annals of Glaciol*. 14, 186-190, 1990.

Myers, O., H. Flowers, K. Huining, E. Bedrich, B. Whorton, C. Xichun, S.A. Christine, The Association between Ambient Air Quality Ozone Levels and Medical Visits for Asthma in San Juan County, *Division of Epidemiology and Biostatistics, Department of Internal Medicine, University of New Mexico (UNM) School of Medicine, Division of Environmental Epidemiology, New Mexico Department of Health*, 2007.

Martineau, Jr., Robert and Novello, David P., *The Clean Air Act Handbook Second Edition*. ABA Publishing, Chicago, Il, 2004.

Matsuhisa, Y., J. R. Goldsmith and R. N. Clayton, Mechanisms of hydrothermal crystallization of quartz at 250.degree.C and 15 kbar, *Geochim. Cosmochim.Acta,42*(2), 173-182, 1978.

Max Planck Institute for Chemistry Atmospheric Chemistry Department, website.Accessed: Oct 2010.http://www.atmosphere.mpg.de/enid/2.html

McCabe, J. R., Thiemens, M. H., and Savarino, J.: A record of ozone variability in South Pole Antarctic snow: Role of nitrate oxygen isotopes, *J. Geophys. Res*., 112, D12303, doi:10.1029/2006JD007822, 2007.

Mentel, T. F., M. Sohn and A. Wahner, Nitrate effect in the heterogeneous hydrolysis of dinitrogenpentoxide on aqueous aerosols, *Phys. Chem. Chem. Phys.,1*(24), 5451-5457, 1999.

Middlecamp, K. M.; Elliott, E. M.; Isotopic investigation of reactive nitrogen deposition along a highway road gradient. *EOS Trans. AGU*, 90 (52) Fall Meet. Suppl., Abstract B11F-04, 2009.

Milford, J.B., "Tribal Authority Under the Clean Air Act: How Is It Working?," *Natural Resources Journal*, 44:213-242, 2004.

Milford, J.B., Pienciak, A. "After the Clean Air Mercury Rule: Prospects for Reducing Mercury Emissions from Coal-Fired Power Plants," *Environmental Science and Technology*, 43:2669-2673, 2009.

Michalski, G., T. Meixner, M. Fenn, L. Hernandez, A. Sirulnik, E. Allen and M. Thiemens, Tracing atmospheric nitrate deposition in a complex semiarid ecosystem using $\Delta^{17}O$, *Envir. Sci. Tech.,38*(7), 2175-2181, 2004.

Michalski, G., Z. Scott, M. Kabiling and M. Thiemens, First Measurements and Modeling of $\Delta^{17}O$ in Atmospheric Nitrate, *Geophys. Res. Lett.,30*(16), (1870), 2003.

Michalski, G. M.; Jost, R.; Sugny, D.; Joyeux, M.; Thiemens, M. Dissociation energies of six NO2 isotopologues by laser induced flourescence spectroscopy and zero point energy of some triatomic molecules. *J. Chem. Phys*. 121 (15), 7153-7161, 2004.

Michalski, G. and F. Xu, Isotope modeling of nitric acid formation in the atmosphere using ISO-RACM.: Testing the importance of nitric oxide oxidation, heterogeneous reactions, and trace gas chemistry., *Atm. Chem. Phys.,In press*, 2010.

Miller, M. F., Isotopic fractionation and the quantification of ^{17}O anomalies in the oxygen three-isotope system: an appraisal and geochemical significance, *Geochim. Cosmochim.Acta,66*(11), 1881-1889, 2002.

Moore, H. The isotopic composition of ammonia, nitrogen dioxide, and nitrate in the atmosphere. *Atmos. Environ*. 11, 1239−1243, 1977.

Morton, J., J. Barnes, B. Schueler and K. Mauersberger, Laboratory Studies of Heavy Ozone, *J. Geophys. Res.,95*(D1), 901-907, 1990.

Morin, S., Savarino, J., Bekki, S., Gong, S., and Bottenheim, J.W. Signature of arctic surface ozone depletion events in the isotope anomaly ($\Delta^{17}O$) of atmospheric nitrate, *Atmos. Chem. Phys*., 6, 6255-6297, 2007.

Morin, S., Savarino, J., Frey, M., M., Yan, N., Bekki, S., Bottenheim, J.W., and Martins, J.M.F. Tracing the Origin and Fate of NO_x in the Arctic Atmosphere Using Stable Isotopes in Nitrate, *Science,322*(5902), 730-732, 2008.

NARSTO. *Particulate Matter Science for Policy Makers: A NARSTO Assessment*. P. McMurry, M. Shepherd, and J. Vickery, eds. Cambridge University Press, Cambridge, England, 2004.

Navajo Tourism Department, Navajo Nation. "Welcome to the Navajo Nation." *Discover Navajo*, 2008. Web. 04 June 2013. http://discovernavajo.com/

Nydick, Koren. *How's the air out there? Outdoor air quality in the eastern Four Corners region: Southwest Colorado and northwestern New Mexico.* Mountain Studies Institute, Durango, CO, 2009.

Patris, N., Cliff, S. S., Quinn, P. K., Kasem, M., and Thiemens, M. H. Isotopic Analysis of Aerosol Sulfate and Nitrate during ITCT-2k2: Determination of Different Formation Pathways as a Function of Particle Size. J. *Geophys. Res*., 112: D23301, 2007.

PeakSimple (SRI) Software. PeakSimple Version 3.93, Downloaded. Web access: 2010.

Pearl, H.W., Dennis, R.L., Whitall, D.R., Atmospheric deposition of nitrogen: Implications for nutrient over-enrichment of coastal waters. *Estuaries*, 25, 677-693, 2002.

Pearson, J.; Wells, D.; Seller, K.; Bennett, A.; Soares, A.; Woodall, J.; Ingrouille, M. Traffic exposure increases natural 15N and heavy metal concentrations in mosses. *New Phytol*. 147, 317−326, 2000.

Prinn, R.; Cunnold, D.; Simmonds, P.; Alyea, F.; Boldi, R.; Crawford, A.; Fraser, P.; Gutzler, D.; Hartley, D.; Rosen, R.; Rasmussen, R. Global Average Concentration and Trend for Hydroxyl Radicals Deduced From ALE/GAGE Trichloroethane (Methyl Chloroform) Data for 1978-1990. *J. Geophys. Res*. 97 (D2), 2445-2461, 1992.

Ramanathan, V., P.J. Crutzen, J.T. Kiehl and D. Rosenfeld, Atmosphere - Aerosols, climate, and the hydrological cycle, *Science,* 294 (5549), 2119-2124, 2001.

Richet, P.; Bottinga, Y.; Javoy, M., A review of hydrogen, carbon, nitrogen, oxygen, sulphur, and chlorine stable isotope fractionation among gaseous molecules. *Annu. Rev. Earth Planet. Sci*. 5 65-110, 1977.

Riha, Krystin and Greg Michalski, Seasonal variations in NO3- δ15N of PM2.5 and PM10: Insights into isotope exchange during NOx chemistry, *Environmental Science & Technology, in review*, 2013.

Rodriquez, A.M., Barna MG, Moore T., Regional Impacts of Oil and Gas Development in the Western United States. *Journal of Air Waste Management Association*, 2009, Sep;59(9):1111-8.

Russell, A. G., McRae, G. J., and Cass, G. R. The Dynamics of Nitric Acid Production and the Fate of Nitrogen Oxides. *Atmos. Environ*. 19:893–903, 1985.

Russell, A. G., and Cass, G. R. Verification of a Mathematical Model for Aerosol Nitrate and Nitric Acid Formation and Its Use for Control Measure Evaluation. *Atmos. Environ*. 20:2011–2025, 1986.

Sathers, Mark, et. al., Baseline Ambient Gaseous Ammonia Concentrations in the Four Corners Area and Eastern Oklahoma, USA (Sept. 2008), *Journal of Environmental Monitoring*. RSC Publishing. June 23, 2009.

Sakizzie, B., 2005 Air Emissions Inventory Criteria and Hazardous Air Pollutants Inventory Southern Ute Indian Reservation, Colorado, *Southern Ute Indian Tribe*, 2007, Web access: 2013.

Samet, J. M., F. Dominici, F. C. Curriero, I. Coursac and S. L. Zeger, Fine particulate air pollution and mortality in 20 U.S. cities, 1987-1994, pp. 1742-1749, 2000.

Savarino, J., S. K. Bhattacharya, S. Morin, M. Baroni and J. F. Doussin, The $NO+O_3$ reaction: A triple oxygen isotope perspective on the reaction dynamics and atmospheric implications for the transfer of the ozone isotope anomaly, *J. Chem. Phys.,128*(19), 194303-DOI: 10.1063/1.2917581, 2008.

Savarino, J., Kaiser, J., Morin, S., Sigman, D.M., and Thiemens, M.H. Nitrogen and oxygen isotopic constraints on the origin of atmospheric nitrate in coastal Antarctica, *Atmos. Chem. Phys*., 7, 1925-1945, 2007.

Savarino, J., and Thiemens, M.H. Mass-independent oxygen isotope (^{16}O, ^{17}O, ^{18}O) fractionation found in H_x, O_x reactions, *J. Phys. Chem*., 103, 9221-9229, 1999.

Schwartz, J. and L. M. Neas, Fine particles are more strongly associated than coarse particles with acute respiratory health effects in school children, *Epidemiology,11*(1), 6-10, 2000.

Seinfeld, John H. and Pandis, Spyros N. *Atmospheric Chemistry and Physics: From Air Pollution to Climate Change (2nd Edition)*, New York, John Wiley & Sons, 2006.

Sharma, H. D.; Jervis, R. E.; Wong, K. Y. Isotopic Exchange Reactions in Nitrogen Oxides. *J. Phys. Chem.* 74 (4), 923-933, 1970.

Sigman, D.H., Casciotti, K.L., Andreani, M., Barford, C., Galanter, M., Böhlke, J.K., A bacterial method for the nitrogen isotopic analysis of nitrate in seawater and freshwater. *Analytical Chemistry*. 73 (17), 4145-4153, 2001.

Southern Ute Indian Tribe Air Quality Program, US EPA 2009 Network Review, 2009.

Southern Ute Indian Tribe, and La Plata County, CO. "Southern Ute Indian Tribe - Living in La Plata County." *Southern Ute Indian Tribe*, 2013. Web. 04 June 2013. http://www.southernute-nsn.gov/natural-resources/lands/living-in-la-plata-county

Stockwell, W.R., Middleton, P., Chang., J.S., and Tang, X. The second generation regional acid deposition model chemical mechanism for regional air quality modeling. *J. Geophys. Res*., v.95, no. D10, 16343-16367.

Stockwell, W.R., Kirchner, F., Kuhn, M., Seefeld, S. A new mechanism for regional atmospheric chemistry modeling. *J. Geophys. Res*., 102(D22), 25,847-25,879, doi: 10.1029/97JD00849, 1997.

Teffo, J. L.; Henry, A.; Cardinet, Ph.; Valentin, A. Determination of Molecular Constrants of Nitric Oxide from (1-0), (2-0), (3-0) Bands of the 15N16O and 15N18O Isotopic Species. *J. Mol. Spectrosc*. 82 348-363, 1980.

Temte, J.R., Lee, C., Sakizzie, B., Hinkley, E.W., Air Emission Inventory Development of Criteria and Hazardous Air Pollutants on the Southern Ute Indian Reservation for 2002, *Southern Ute Indian Tribe*, Ignacio, CO, 2002. Web Access: 2013.

Thiemens, M., and Jackson, T. Pressure dependency for heavy isotope enhancement of ozone. *Geophysical Research Letters*. 17 (6), 717-719. 1990.

Thiemens, M. H. and J. E. Heidenreich, III, The mass-independent fractionation of oxygen: a novel isotope effect and its possible cosmochemical implications, *Science,219*(4588), 1073-1075, 1983.

Thiemens, M. H., J. Savarino, J. Farquhar and H. Bao, Mass-Independent Isotopic Compositions in Terrestrial and Extraterrestrial Solids and Their Applications, *Acc. Chem. Res.,34*(8), 645-652, 2001.

"Tribal Clean Air Act Authority." Title 40 *Code of Federal Regulations*, Pt. 49.1(a). 2010 ed. Web 21 May 2013. http://www.gpo.gov/

US Environmental Protection Agency, Air Quality System Data Mart [internet database] available at: http://www.epa.gov/ttn/airs/aqsdatamart Accessed Oct. 2010.

US Environmental Protection Agency. National Ambient Air Quality Standards. Web access: 2013.

US Environmental Protection Agency. "Particulate Matter (PM)," *Basic Information*. Web access: 2013.

US Environmental Protection Agency. The National Emissions Inventory (2005). Web access: 2013.

US Environmental Protection Agency. *Quality Assurance Handbook for Air Pollution Measurements, Volume 2, Ambient Air Quality Monitoring Program*. Vol 2. Research Triangle Park: USEPA Office of Air Quality Planning and Standards, 2008.

US Environmental Protection Agency, "Quality Assurance Guidance Document 2.12, Monitoring PM-2.5 in Ambient Air Using Designated Reference or Class I Equivalent Methods, 1998." available at: http://www.epa.gov/ttn/amtic/files/ambient/pm25/qa/m212covd.pdf Accessed Oct. 2010.

US Environmental Protection Agency, US EPA Indian Policy for the Administration of Environmental Programs on Indian Reservations, 1984, available at: http://www.epa.gov/tribal/basicinfo/presidential-docs.html Accessed Oct. 2010.

Wahner, A., T. F. Mentel, M. Sohn and J. Stier, Heterogeneous reaction of N_2O_5 on sodium nitrate aerosol, *J. Geophys. Res.,103*(D23), 31103-31112, 1998.

Whitby K.T., Cantrell B.K., Proceedings of the International Conference on Environmental Sensing and Assessment (ICESA), Institute of Electrical and Electronic Engineers (IEEE). Atmospheric aerosols: characteristics and measurement. IEEE #75-CH 1004-1, ICESA paper 29-1, Washington, DC: IEEE. p. 6., 1976.

World Health Organization (WHO) Working Group, Air quality guidelines for Europe. Copenhagen, World Health Organization Regional Office for Europe, *WHO Regional Publications, European Series, No. 23*, 2007.

World Health Organization (WHO) Working Group, Health Aspects of Air Pollution with Particulate Matter, Ozone and Nitrogen Dioxide.World Health Organization Regional Office for Europe, *WHO Regional Publications, European Series,* 2003.

APPENDICES

Appendix A Tribal NO_x Emission Inventory Source Sector Descriptions

Table 13 Tribal NO_x Emission Inventory Source Sector Descriptions

Category	**Detail Category Names**
Point Sources	Title V Stationary Sources (>100 tons/yr)
	Electric Generating Units
	Natural Gas Compressor Stations
	Natural Gas Plants
Area Sources	Minor Sources (<100 tons/year)
	Oil and Gas Wells
	Well-Head Minor Source Compressors
	Fireplace and Wood Burning Stoves
	Propane Use
	Airports
	Wildland Fire and Prescribed Burning
Mobile Sources	On/Non-Road - Gasoline
	On/Non-Road - Diesel
Biogenic	Soils

Appendix B Ion Chromatography Single Column Separation Instructions

1) To make acid solution, use a clean 50 mL centrifuge tube and add 5.6 mL 18M H_2SO_4 to 25 mL Millipore water. Decant into 4 L reservoir and fill with Millipore water to the line set at 4 L (8000 mL) making a 50 mN H_2SO_4 solution.

2) To make mobile phase (eluent), use 20 mL of concentrated eluent stock solution to 2 L (2000 mL) Millipore water making a 3.5 mM/1.0 mM Na_2CO_3/$NaHCO_3$ solution.

3) Adjust the argon tank regulator to ~90psi (Figure 59, a) and release pressure by selecting the "relay F" on the relay switch icons located on PeakSimple monitor (Figure 59, b). Should here the gas enter the acid tanks.

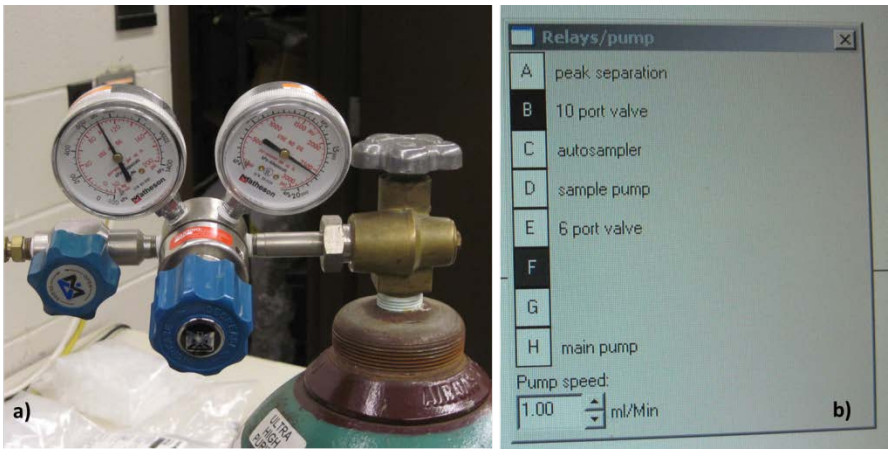

Figure 59 Argon tank (a) and PeakSimple (SRI) software relay selection (b)

4) Adjust the pressure system gauge found below the acid bottles to ~3 psi.

Figure 60 Acid pressure gauge

5) Let acid flow to suppressor for approximately 5 – 10 minutes. Observe acid flow by removing the large Teflon tubing which sends the acid to waste.

6) Turn on mobile phase pump by pressing the on/off button on the front panel of the eluent pump (should hear pump pistons engage).

7) Allow eluent to run for approximately 10 minutes. Be sure the 6-port valve is in position 2. Adjust the 6-port valve between position 1 and 2 by selecting the “E relay” icon. Position 2 directs the eluent into the analytical separation column to elude any remaining anions.

8) On the auto sampler controller (found on the right side of the IC) select “pause” and “home” to return the auto sampler needle to its home position if it’s not already there.

Figure 61 Auto sampler controller

9) Select the autosampler “C relay” switch icon twice to move auto sampler needle into the rinse reservoir.

10) While auto sampler needle is in the rinse reservoir, use 3 mL syringe to purge/prime the sample pump (Alltech 426). Unscrew purge/prime port and insert syringe and draw back on syringe very slowly to remove any air bubbles and allow water to be introduced to sample pump.

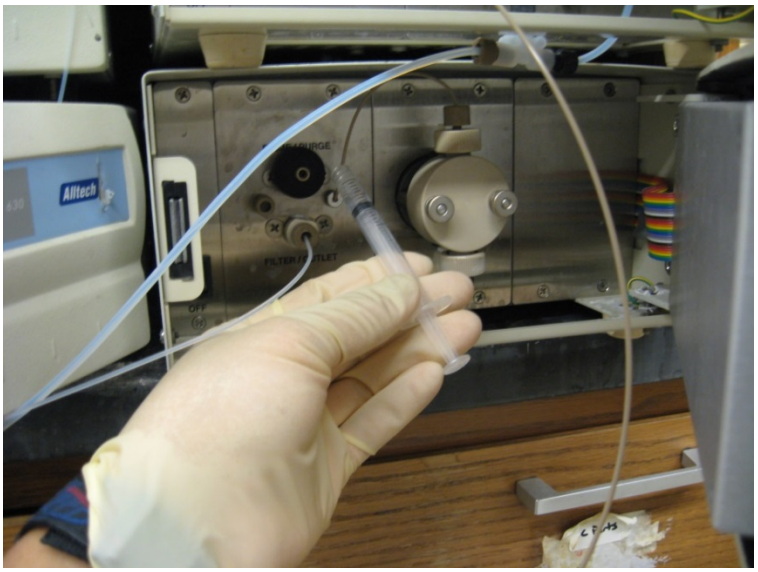

Figure 62 Sample pump purge/prime port

11) After purge is complete and no air bubbles present inside sample line, turn on sample pump and allow to run for 10 to 15 minutes. At this time switch the 6 port valve to position 1 so that Millipore water is pumped through the C-18 and analytical separation column for a thorough rinse.

12) Continue to switch between position 1 and position 2 by selecting the “E relay” to allow for thorough rinsing and elution of columns.

13) After rinsing is complete, return the auto sampler needle to its home position by pressing “pause” and “home” on the auto sampler controller.

14) Before actual auto sampling begins, be sure the 6-port valve is in position 2.

15) The IC is now prepared to analyze samples.

PeakSimple (SRI) Software Sample Run Setup

1) From the desktop open the folder named “Control File.”

2) Within the “Control File” open the “C18 Single Column Separation” folder.

3) Copy all files inside the “C18 Single Column Separation” folder. Do not alter any of the files (event files and .con files) inside this folder.

4) Make a new folder with your name and date of sample run. Place the copied files into this folder.

5) Open up PeakSimple software and under the “view” toolbar select “auto sampler.” This should open up the auto sampler que dialog box. While in the auto sampler que, select “add” and navigate to your folder you just made and add the “default.con” file (Figure 63, a). You should then be returned to the auto

sampler que and then select “edit all.” Another dialog box should then open up and there you want to select “add copies” (Figure 63, b). You will then be prompted to add files. Always add one less than your total number of 15 mL sample tubes.

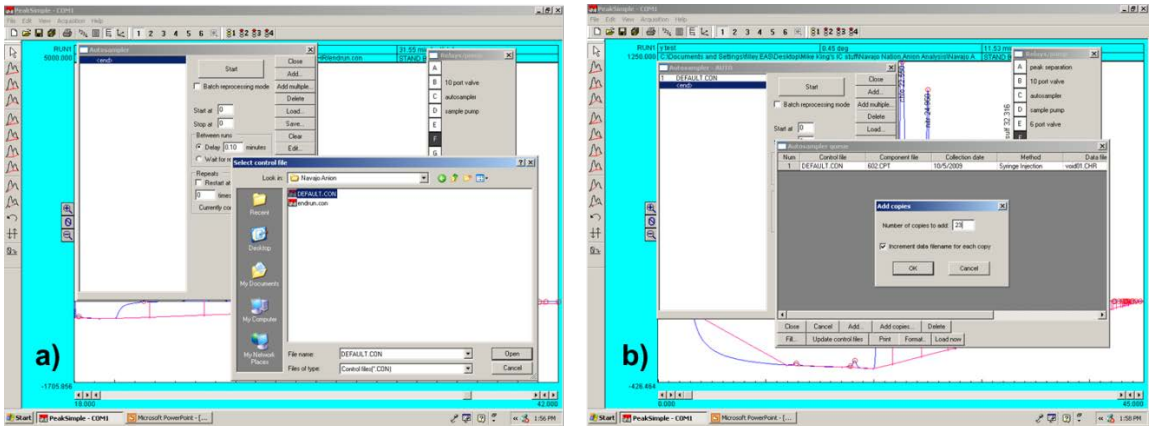

Figure 63 PeakSimple (SRI) software auto sampler que

6) Name the newly created .CHR files to correspond with the sample list or number of sample tubes set up on the auto sampler tray.

7) After .CHR files have been renamed appropriately, select “update control files.”

8) Then exit out of dialog box, returning back to the auto sampler que.

9) Once again select “edit all”, and this time just close out the dialog box that appears. You should return back to the auto sampler que. The number of files that you added should then appear as .con files

10) Add the “end.con” file by selecting “add “in the auto sampler que and navigating to your folder containing the “end.con” file.

11) Setup sample racks on auto sampler tray and go to auto sampler control panel and select “edit/file/save,” then select “enter” twice, then “start.” This should place the auto sampler needle into the first 15 mL tube, which should always be a water blank (to rinse the columns). Be sure each tube has 15 mL of sample solution and volumes recorded in log book. The event file is programmed to turn the sample pump on and pump a volume of 11 mL through the columns at 1 mL per minute.

12) Once the auto sampler needle is setup, turn on faction collector. Be sure the 6 port valve is in position 2 (select E-relay). Then select the “start” on the auto sampler que.

13) Be sure to adjust fraction collector windows to the anion peak retention times you want to collect by selecting “programs” and “fractions” on the collector’s program menu. Remember, the number of sample separations is limited by the fraction collector rack capacity.

Figure 64 Fraction collector main program menu

Appendix C Southern Ute Indian Tribe Agreement

A legal agreement was established with the Southern Ute Indian Tribe regarding research, writing, and publication on April 20, 2011 and March 20, 2013. Therefore, all correspondence shall only be obtained by written approval with consent of release from the Southern Ute Indian Tribe. All correspondence with the Navajo Nation will also be obtained by written approval with consent of release by the Navajo Tribe.

AGREEMENT REGARDING RESEARCH, WRITING, & PUBLICATION

THIS AGREEMENT is entered into the ___ day of _____, 2011, by and between the SOUTHERN UTE INDIAN TRIBE, P.O. Box 737, Ignacio, Colorado, 81137, hereinafter referred to as the "Tribe," and Michael King, Department of Earth and Atmospheric Sciences, Purdue Stable Isotope Lab, Purdue University, Civil Engineering Building, 550 Stadium Mall Drive West, Lafayette, IN, 47907-2051, hereinafter referred to as "Author."